The role of ATG16L1 in chronic inflammatory bowel disease

Dissertation

zur Erlangung des Doktorgrades

der Mathematisch-Naturwissenschaftlichen Fakultät

der Christian-Albrechts-Universität

zu Kiel

vorgelegt von:

Janne Böck

Kiel, 2012

Referent/in:	Prof. Dr. Rosenstiel
Korreferent/in:	Prof. Dr. Dr. Bosch
Tag der mündlichen Prüfung:	26.06.2012
Zum Druck genehmigt:	02.07.2012

gez. Prof. Dr. Lutz Kipp (Dekan)

Table of contents

1 INTRODUCTION

1.1 The role of autophagy in cell homeostasis and inflammation

Autophagy is a dynamic process for capturing cytosolic components like defective proteins or organelles and delivering them to lysosomes for hydrolytic degradation[1]. This multistep process is evolutionarily conserved and documented by the high conservation of the involved proteins which are encoded by AuTophaGy-related (ATG) genes, throughout the entire animal kingdom. The regulatory mechanisms are highly similar from yeast to mammals[2]. The term “autophagy” is derived from the Latin words for “self” and “eating” and the primary role of this mechanism is to protect cells under stress conditions, such as starvation. Degrading cytoplasmic material during periods of starvation provides the background to produce amino acids and fatty acids that can be used to synthesize new proteins or are oxidized by mitochondria to produce Adenosinetriphosphate (ATP) for cell survival. Defects in autophagy are associated with many diseases, including neurodegenerative diseases, tumorigenesis, diabetes and Crohn disease[3-5]. There are three different types of autophagy, including macroautophagy, chaperone-mediated autophagy and microautophagy. Macroautophagy (here referred to as ‘autophagy’) is essential for cell homeostasis and subject of this work. It uses specialized cytosolic vesicles that fuse with the lysosomes[6,7]. By contrast, microautophagy is the direct uptake of cytoplasm at the lysosome surface by invagination of the lysosomal membrane[8]. At last, chaperone-mediated autophagy takes place at the lysosome membrane, as well. It is a mechanism to translocate unfolded proteins across the membrane[9].

During autophagy, an expanding double-membrane structure termed the ‘phagophore’ or ‘isolation membrane’ engulfs portions of the cytoplasm. After completion to a closed autophagosome it fuses directly or indirectly with lysosomal vesicles for hydrolytic degradation of the enclosed material[10]. The way of autophagosome formation differs from vesicle formation in other membrane trafficking processes, such as endocytosis and the secretory pathway. In these pathways transport vesicles are generated by sprouting and scission from the membranes of donor organelles. In contrast, autophagosomes are described to be formed in the cytosol in a de novo process[11]. This formation depends on two protein conjugation systems, the ATG12-ATG5 and the ATG8-phosphatidyl ethanolamine

systems which both act as ubiquitin-like ligation systems[12]. The following steps are involved[2] (see Figure 1-1):

I) The formation of the phagophore (isolation membrane) is instituted by Beclin/VPS34 complex at the endoplasmic reticulum (ER) or other membrane systems and controlled by mTOR (target of Rapamycin) and class I PI3K (phosphatidylinositol-3-kinase 1) signaling pathway.

II) The formation of the ATG12-ATG5 conjugate depends on two enzymes, ATG7 (E1-like) and ATG10 (E2 like). Afterwards, in addition to the covalent interaction with ATG12, ATG5 interacts non-covalently with ATG16L1. Because ATG16L1 has a self-assembling character, the ATG12-ATG5 conjugate forms a multimeric complex with ATG16L1. The complex adheres to the phagophore, mediated by ATG5.

III) After processing the C terminus of LC3 by ATG4 to expose the glycine residue, the C-terminal glycine is attached to phosphatidyl ethanolamine (PE) by the E1-like activating enzyme ATG7 and the E2-like conjugation enzyme ATG3. The lipidated form of LC3 is associated with the autophagosomal membrane.

(During formation of the autophagosome, the ATG12-ATG5-ATG16L1 complex (named ATG16L1-complex) and the LC3-PE (LC3-II) cover the expanding phagophore. The ATG16L1-complex is situated mostly on the outer side, whereas LC3-II is found on both sides.)

IV) Selective or non-selective cargo is engulfed. When the autophagosome formation is completed, the ATG16L1-complex is released into the cytosol. Concurrently, a significant amount of LC3-II stays in the completed autophagosome.

V) The autophagosome fuses indirectly via fusion with late endosomes and formation of amphisomes or directly with the lysosomal compartment. The contents get hydrolyzed and monomers are recycled.

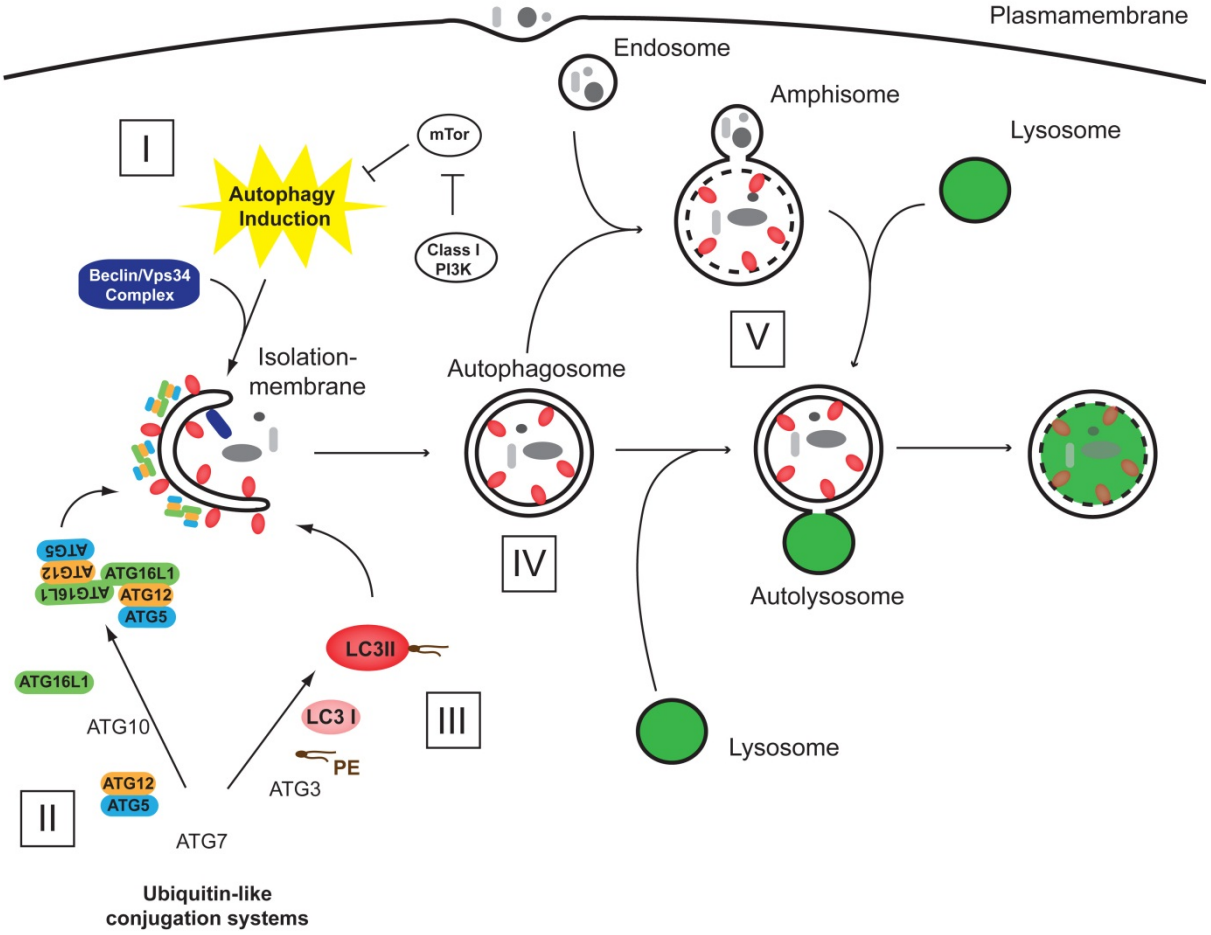

Figure 1-1: Steps of autophagosome formation.
I) Phagophore (isolation membrane) formation by Beclin/VPS34 complex at the endoplasmic reticulum (ER) or other membrane systems under the control of the inhibiting TOR (target of Rapamycin) and class I PI3K (phosphatidylinositol-3-kinase 1) signaling pathway; II) the ATG5-ATG12 complex assembles, supported by ATG16L1 and binds as a multimer to the phagophore; III) processing of LC3 (yeast Atg8) and insertion into the expanding phagophore membrane; IV) engulfment of random or selective cargo, closure of the autophagosome, partial recycling of LC3; V) fusion of the autophagosome with the lysosomal compartment (directly or indirectly via fusion with late endosomes and formation of amphisomes), hydrolysis of the cargo and recycling of monomers. Source: S.Billmann-Born et al. / European Journal of Cell Biology (2011)

Autophagy was originally described to be a non-selective mechanism, being characterized by autophagosomes primarily containing bulk cytoplasmic material. But it is now known that autophagosomes can engulf and degrade substrates in a selective manner[13]. During selective autophagy, only relevant cargoes are isolated into autophagosomes, which accordingly have contours that resemble those of the cargoes. The autophagosomes generated under these conditions contain little bulk cytosol between the cargo and the inner membrane. Examples of selective autophagy are Cvt vesicles (cytoplasm-to-vacuole transport vesicle in yeast), mitophagy (degradation of damaged mitochondria), pexophagy (degradation of peroxisomes), xenophagy (degradation of intracellular viruses and bacteria) and

reticulophagy (degradation of endplasmic reticulum)[14-17]. Cellular cargo is commonly targeted to autophagosomes by interactions between a molecular tag (such as polyubiqutitin), adaptor proteins such as p62/SQSTM1 or NBR1 and LC3. The adaptor proteins recognize the molecular tags and contain an LC3-interacting region (LIR). They enable autophagy to target cargo selectively to growing LC3-positive phagophores[13]. If autophagy-protein-dependent mechanisms fail in immunity, this may afford not only an increased susceptibility to infection, but also to chronic inflammatory diseases and autoimmune diseases like for example Crohn disease (CD). Beside these functions autophagy has important roles in protecting against cell death induced by ER stress. Blocking autophagy by chemical inhibition or deletion of an *ATG* gene (*ATG5, ATG6/Beclin1, ATG8/LC3*) in vitro, leads to an increased susceptibility to ER stress-mediated apoptotic cell death[18-20]. Conversely, induction of autophagy by treatment with the mTOR inhibitor rapamycin, leads to a higher resistance to endoplasmic reticulum (ER) stress in cells[18].

To sum up, in addition to stress management autophagy is involved in immunity, defense against microbial invasion[21], normal development[7], senescence[22] and lifespan extension[23]. Also in many human pathophysiologies it plays a role: for example cancer, myopathies, neurodegeneration, heart and liver disease, and gastrointestinal disorders[7,24].

1.2 The role of autophagy in endoplasmic reticulum stress

Protein synthesis and maturation (including correct folding) is not the only function of the endoplasmic reticulum (ER). It may also be a major source for building the autophagic isolation membrane by forming omegasomes[25,26]. ER stress is triggered when unfolded proteins accumulate in the ER due to advanced input of proteins (e.g. when protein synthesis is increased or the protein secretion from the ER is defective) or decreased capacity of the ER to fold proteins (e.g. upon changes in the Ca^{2+}, oxygen and glucose homeostasis). Notably, ER stress is also induced when unfolded proteins accumulate in the cytosol[27-29]. The unfolded protein resonse (UPR), the major ER stress pathway, is directly linked to autophagy[30-33] (see Figure 1-2). There are three branches of the UPR, mediated by three ER membrane-associated proteins, PERK (protein kinase RNA-like endoplasmic reticulum kinase), ATF6 (activating transcription factor) and IRE1 (inositol requiring enzyme 1).

PERK arranges the transcriptional activation of the autophagic proteins LC3 and ATG5 in hypoxic responses via the transcriptionsfactors ATF4 and CHOP[34]. Furthermore autophagosome formation is induced by the eukaryotic initiation factor 2α (eIF2 α) downstream of PERK under conditions of ER stress by inducing LC3 conversion and ATG12 upregulation[20]. An additional report of Kouroku et al. confirms this correlation by demonstrating that ER stress (PERK/eIF2α phospsorylation) enhances the ATG16L1 complex-dependent LC3 conversion from LC3I to LC3II. The group proposed that autophagy is a cellular defense mechanism against polyQ72-induced ER-stress-mediated cell death by degrading polyQ72 aggregates[20].

IRE1, a kinase and endoribonuclease directly upstream of XBP1 can induce activation of JNK signaling under conditions of ER stress, via its interaction with TRAF2[35]. JNK is directly able to induce autophagosome formation via LC3[36,37]. XBP1 deletion results in spontaneous enteritis and increased susceptibility to induced Colitis in addition to Paneth cell dysfunction. The hypomorphic XBP1 function is described to cause an overactivation of IRE1 along with increased JNK phosphorylation in small intestinal epithelium of *Xbp1*-deficient mice, leading to autophagome formation under conditions of ER stress[38] (see Figure 1-2).

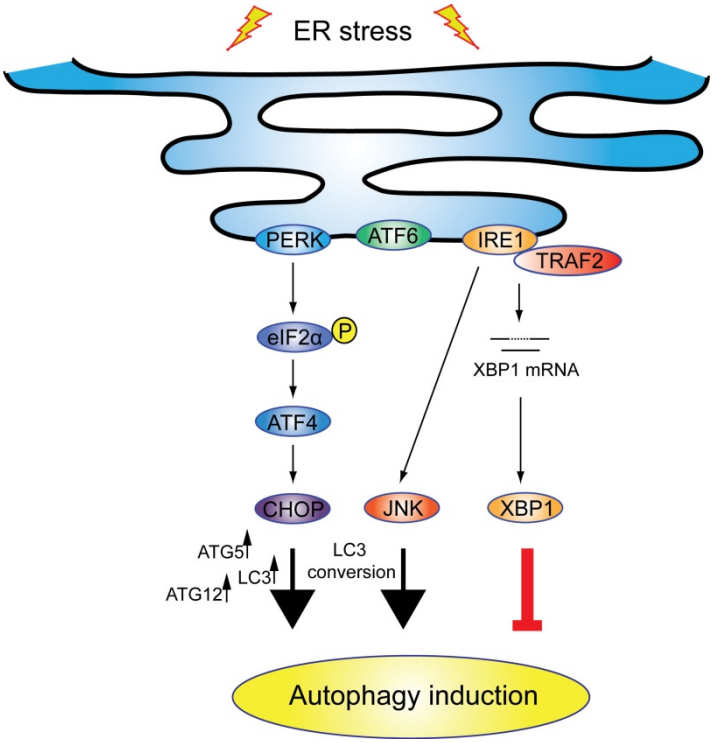

Figure 1-2: The link of UPR and autophagy
ER stress activates unfolded protein resonse (UPR) signaling mediated by three ER membrane-associated proteins, PERK (protein kinase RNA-like endoplasmic reticulum kinase), ATF6 (activating transcription factor) and IRE1 (inositol requiring enzyme 1). The responses are linked to the induction of autophagy via increasing the expression level of ATG5, ATG12 and LC3, further via leading to LC3 conversion or inhibition of the autophagy induction.

Another example demonstrating the linkage between ER stress and autophagy is given by studies of genetic *Atg7* deficiency in mice[39]. *Atg7* deficiency correlates with decreased autophagy and increased ER stress in liver[39]. As well, the *Atg7* deficiency results in impaired insulin signaling, which was previously reported as a consequence of pathological ER stress in obesity[40]. Further, the deletion of *ATG5, Beclin1* or *LC3* leads to an advanced susceptibility to apoptotic cell death during ER stress, as mentioned before.

At last, in a recent study Kimura et al. demonstrated that no protein delivery to vacuoles could be reported in the absence of autophagic activity in *Aspergillus oryzae*. Hence, they conclude that autophagy is responsible for the delivery of misfolded secretory proteins accumulated in the ER to vacuoles for degradation[41].

1.3 The autophagy protein ATG16L1

The *Atg16l1* gene (human: 3411base pairs (bp), RefSeq.NM_030803; mouse: 3149bp, RefSeq.NM_029846) is located on chromosome 2 on position 37.1 and encodes a protein involved in the formation of autophagosomes during autophagy. The autophagy protein ATG16L1 was identified in 2003 by Mizushima et al. and exhibits three isoforms: ATG16Lα, ATG16Lβ and ATG16Lγ. The human/mouse homology is defined by a protein identity of 94% and a DNA identity of 89.1% (generated with “HomoloGene”; human: gi|124256478|ref|NP_060444.3; mouse: gi|27777650|ref|NP_084122.2). It is named after the weak but significant homology in its N-terminal region (amino acid (aa) 106-208) with yeast APG16 (amino acid (aa) 28-145)[42]. ATG16L1 is an indispensable protein, whose deficiency, similar to the lethal phenotype of ATG5- and ATG7-deficient mice[43], leads to death within the 1st day of delivery[44]. This indicates that ATG16L1 is required for neonatal starvation[43,45]. It is ubiquitously expressed and consists of an N-terminal domain involved in ATG5 binding, a central coiled coil domain required for self oligomerization, and a C-terminal WD40 repeat domain whose role is entirely unknown in this protein (see Figure 1-3)[2]. In general, the WD-repeat domains are thought to have the common feature of folding into a beta propeller and forming a platform without any catalytic activity. Hence, it provides the opportunity for multiple protein complexes to assemble reversibly[46].

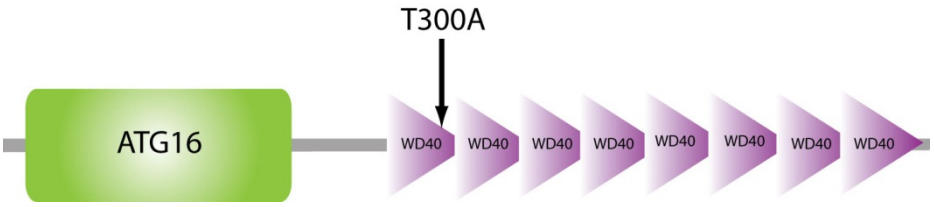

Figure 1-3: Domain structure of ATG16L1 displaying the allelic variant T300A
The N-terminal domain (ATG16) of the ATG16L1 protein is involved in ATG5 binding and the central coiled coil domain (CC) is required for self oligomerization. The C-terminal eight WD repeats are of unknown function and exhibit the Crohn disease associated coding SNP (T300A). Source: S.Billmann Born et al. / European Journal of Cell Biology (2011)

ATG16L1 forms a complex with the ATG12-ATG5 conjugate resulting in the ATG16L-ATG5-ATG12 complex, commonly named ATG16L complex. This complex has the capacity of a new type of E3-like enzyme and functions as a scaffold for LC3 lipidation by dynamically localizing to the putative source membranes for autophagosome formation.[47] These findings were supported by results of Saitoh et al. who illustrate that an ATG16L1-deficiency in mouse embryonic fibroblasts (MEFs) hinders the recruitment of the ATG12-ATG5 conjugate to the isolation membrane thus resulting in the loss of LC3 conjugation to phosphatidyl ethanolamine (PE) and the complete inhibition of the basal autophagy-machinery.[44] But it is shown that the truncation of the whole C-terminal WD40 domain had no effect on dimerization with ATG5[48]. Further, the autophagic machinery was implicated in the NLR system by Travassos et al. via demonstrating that in case of pathogen invasion the intracellular sensors NOD1 and NOD2 recruit ATG16L1 to the plasma membrane at the bacterial entry site.[49]

1.3.1 The role of ATG16L1 in Paneth cell vesicle export

1.3.1.1 Paneth cells

Paneth cells are part of the intestinal barrier, which is critical for health and disease. A layer of mucus, produced by specialized goblet cells, is the first line of defense of this barrier. Various bactericidal and bacteriostatic proteins that act together as a primary barrier are included in the mucus. The epithelial monolayer of the gastrointestinal tract provides a physical barrier between the external environment and the circulation. Resident microflora colonizes the lumen, hence being in contact with the apical brush borders, where nutrient absorption occurs. In this setting, epithelial transport must be balanced by keeping most microbial cell populations in check. It is suggested that innate immune mechanisms exist to counter microbial

colonization because of the low bacterial numbers in the small intestine relative to the distal ileum, cecum, and colon. Mediating this activity is the major role of Paneth cells, which secrete gene-encoded antimicrobial peptides and additional host defense proteins into the lumen[50,51]. These cells are 1 of 4 lineages that are produced by stem cells localized in the crypts of Lieberkühn. Paneth cells are unusual in comparison with the other intestinal epithelial lineages (absorptive enterocytes, mucus secreting goblet cells and hormone secreting enteroendocrine cells). At the base of the crypts, Paneth cells live >30 days. Their main function is to produce, package, and export a wide variety of antimicrobial proteins including an array of α-defensins (cryptdins), lysozyme, angiogenin-4, and secretory phospholipase A2[50,52]. To produce these proteins, mature Paneth cells contain an abundant endocytoplasmic reticulum, golgi apparatus, as well as distinct cytoplasmic granules, which are the hallmark of Paneth cells. The content of these cells is secreted into the gut lumen whereby the membrane of an individual granule fuses with the apical cell surface membrane. Lysozyme for example degrades the bacterial cell wall by its muramidase activity, but it is also capable of lysing bacterial membranes in a non-enzymatic manner[53]. Cryptdins have been demonstrated also to play a role in the clearance of potential pathogens. In 1 example, mice overexpressing 1 member of the cryptdin family of proteins were much less susceptible to oral infection by *Salmonella typhimurium*[54]. Further, Paneth cells have also been described to produce inflammatory cytokines in both a constitutive (TNF-α[55]) and inducible manner during injury (interleukin-17[56]).

1.3.1.2 ATG16L1 and Paneth cell vesicle export

Paneth cells came in the center of attention of Crohn disease, as CD patients with the *ATG16L1* risk variant T300A show abnormal secretion of their granula[57]. Consequently, Cadwell et al. generated and characterized mice that were hypomorphic for ATG16L1 to analyze the Paneth cell morphology. The hypomorphic mice, ATG16L1^{HM}, expressed ATG16L1 at 30% of the wildtype level. They exhibited notable abnormalities in the granule exocytosis pathway, with disorganized lysozyme-positive granules, decreased granule number as well as reduced extracellular lysozyme-mucus co-localization. ATG16L1- and ATG5-deficient Paneth cells showed similar aberrations and Paneth cells of patients homozygous for the ATG16L1 risk allele bore resemblance to those abnormalities[58] (see Figure 1-5).

Finally a recent issue points out that ATG16L1 might have an even more extensive function contrary to the expectations. The virus-plus-susceptibility thesis demonstrates a new aspect of the interplay between pathogenesis, gene interaction and a virus factor. Cadwell et al. suggest that interaction between a specific virus infection and a mutation in the Crohn disease susceptibility gene ATG16L1 induces intestinal pathologies in mice. They state that virus-plus-susceptibility gene interaction generates abnormalities in granule packaging and in gene expression patterns of Paneth cells, but yet the molecular mechanism remains unexplained.[59]

1.4 Inflammatory bowel disease

Crohn disease (CD) and ulcerative colitis (UC) are chronic inflammatory disorders of the intestine that are known collectively as inflammatory bowel disease (IBD). IBD is characterized by chronic inflammation of the intestinal tissue and by subsequent progressive destruction of the mucosal integrity[60]. Clinical symptoms include frequent and chronically relapsing diarrhea, abdominal pain, rectal bleeding and malnutrition[61]. UC is restricted to the colon, which is affected by severe mucosal inflammation that is accompanied by extensive superficial mucosal and submucosal ulcerations[62]. CD in contrast is characterized by discontinuous, transmural inflammation that affects all layers of the intestine in the whole gastrointestinal tract with cardinal incidence in the terminal ileum and colon[63] (see Figure 1-4).

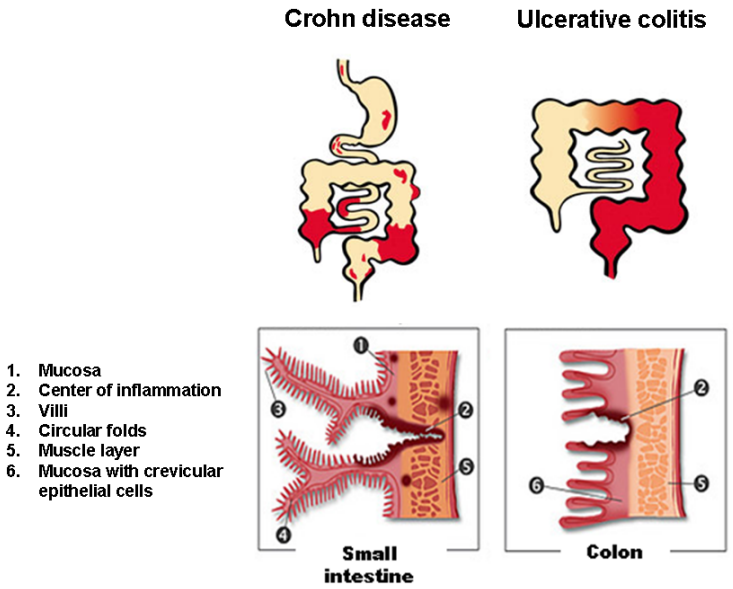

Figure 1-4: Characterization of CD and UC.
Crohn disease is characterized by a completely inflamed intestine whereas Ulcerative colitis affects only the intestinal mucosa. Source: http://www.inflammation-at-interfaces.de; http://www.internisten-im-netz.de/de.

1.4.1 Genetics in inflammatory bowel disease

Genome-wide association studies (GWAS) have identified 71 risk loci in CD and 47 risk loci in UC. An interesting and unexpected finding from the GWA studies is the important role of autophagy in CD pathogenesis, as the two genes *ATG16L1* and *IRGM*, were found to be significantly associated in multiple GWAS[64-68], as well as a third autophagy-associated gene, *LRRK2*[66,69]. Genetic variations in these genes are supposed to have a major impact on the response of the innate immune system to intestinal microbiota and susceptibility to IBD. A link to innate immunity has been made by molecular studies demonstrating a physical interaction between ATG16L1 and NOD2, a pattern recognition receptor that recognizes bacterial products of the enteric flora[70-72]. Interestingly, several risk loci identified through GWAS are common for ulcerative colitis and CD, whereas *ATG16L1*, *IRGM* and *NOD2*, seem to be more specific for CD[73]. Hence, the discovery of the association of NOD2 polymorphism with susceptibility to Crohn disease led to the hypothesis that Crohn disease results from a genetic-based failure in host response to luminal bacteria [61]. In addition, NOD2 is described to be involved in Muramyldipeptide (MDP) induced autophagy[49,74,75], whereas the Crohn disease associated variant NOD2-L1007fsinsC leads to diminished xenophagy (selective autophagy for degradation of intracellular bacteria)[49,74]. Equally, a loss-of-function of the above mentioned ATG16L1-T300A Crohn disease variant was described, as leading to reduced xenophagy, as

well[48,49,74-76]. This led to the received opinion that the increased risk of Crohn disease is caused by impaired bacterial handling and lowered rates of bacterial capture by the autophagy machinery. As NOD2 is described to recruit ATG16L1 to the plasma membrane at the bacterial entry side[49], this might be a hind for a crosstalk of NOD2 and ATG16L1 in xenophagy, further underscoring the observed cooperative effect of the CD-associated variants.

1.4.2 The role of ATG16L1 in Crohn disease

The allelic variant in *ATG16L1* as risk variant for CD was first discovered by our group in 2006. A genome-wide association study using 735 Crohn disease cases and 368 healthy controls was performed resulting in the identification of the coding SNP rs2241880. The variant, typed T300A, results in an amino acid exchange from threonine to alanine at position 300 of the amino acid sequence (see Figure 1-3). A three-dimensional model of the WD-repeat domain structure of human ATG16L1 was designed via in silico protein analysis. The WD-repeat is assumed to consist of 32 β-strands forming an eight-bladed β-propeller with the location of the variant amino acid T300A in strand β3.[64] A following meta-analysis expanded the correlation of the ATG16L1 T300A polymorphism to susceptibility to Crohn disease to a further predisposition to Ulcerative Colitis. Hence, confirming the role for autophagy in the pathogenesis of inflammatory bowel diseases (IBD)[77].

Functional information regarding the role of autophagy in humans in the context of CD is almost lacking. But relevant information regarding ATG16L1 has been obtained in *in vitro* studies and *in vivo* in mice. Kuballa et al. showed a diminished capacity of the CD risk variant ATG16L1^{T300A} in the capture of internalized *Salmonella typhimurium* within autophagosomes by using human epithelial cell lines. They concluded that the association of the ATG16L1 T300A variant with increased risk of Crohn disease is due to impaired bacterial handling and lowered rates of bacterial capture by the autophagy machinery[48]. This observation fits with the current focus on adherent-invasive *E.coli* (AIEC) as one of the microbial malefactors in CD[78] and has been replicated by several groups[49,74-76]. Except in one publication the authors did not see significant effects of the T300A variant in an over-expression experiment[79]. Interestingly, in contrast to bacterial internalizing autophagy (xenophagy), Kuballa et al. asserted that the T300A variant has no impact on basal autophagy in HeLa cells[48]. Additionally, Saitoh et al. described higher IL-1β and IL-18 signaling in ATG16L1-deficient macrophages after stimulation with the TLR-4 ligand LPS. It is

known, that IL-1β increases the intestinal epithelial tight junction permeability[80]. In a mouse model with ATG16L1 lacking in hematopoietic cells, they showed that the animals were highly susceptible to chemically induced colitis[44] (see Figure 1-5).
Recent data of Plantinga et al. shows that the *ATG16L1* polymorphism is associated with an increased production of proinflammatory cytokines upon stimulation with NOD2-ligands, but not with TLR2 or TLR4 agonists. This study is the first to link the ATG16L1 polymorphism with increased production of IL-1β and IL-6 in humans[81].

1.4.3 Immunity in inflammatory bowel disease

In IBD the inflammatory response is characterized by an imbalance between pro- and anti-inflammatory cytokines, which leads to a defective activation of the intestinal immune system. This imbalance is characterized by a domination of pro-inflammatory (TNFα, IL-1β, IL-6, IL-8)[82-84] and a lack of anti-inflammatory cytokines (IL-10, IL-13)[85]. In CD a shift to advanced levels of Th1-type pro-inflammatory cytokines such as *interferon gamma* (IFN-γ), TNFα and IL-6 is described, whereas UC seems to exhibit a Th2-type cytokine profile such as IL-13[62,86-89]. Confirmative, Plantinga et al. recently showed that the ATG16L1 risk variant is associated with increased IL-1β and IL-6 production in humans[81] (see Figure 1-5). Finally, autophagy serves as a guardian of immunological tolerance by appropriate selection of naive T cells before they exit to the periphery. This seems to be important, as genetic disruption of *Atg5* in thymic epithelial cells leads to an altered selection of certain MHC class II restricted T-cell specificities and autoimmunity. The animals develop multiorgan inflammation, including colitis[90].

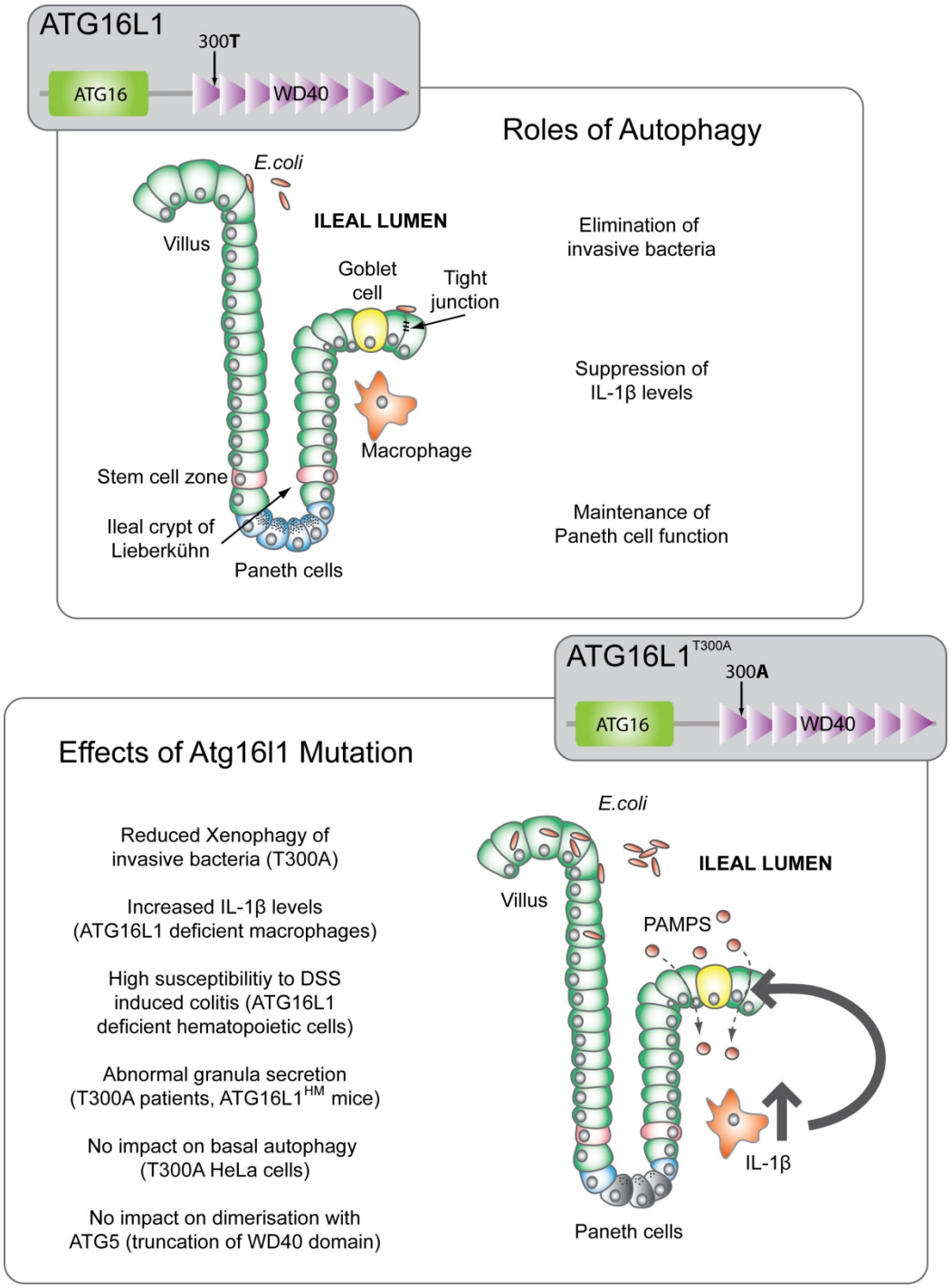

Figure 1-5: ATG16L1 in inflammation
Grey boxes schematically illustrate the autophagy factor ATG16L1 identified as Crohn disease susceptibility locus. *ATG16L1* alleles encode either a protective ATG16L1 300T (top) or a risk form ATG16L1 300A (bottom). Top panel shows intestinal epithelium with different cell types along with the proposed functions of autophagy in the intestinal epithelium. Bottom panel lists six findings regarding the effect of ATG16L1 mutations in different cell lines or patients carrying the risk variant. (modified from Deretic and Levine, Cell Host & Microbe 5, June 2009)

1.4.4 Microbial flora in inflammatory bowel diseases and the link to autophagy

IBD has often been characterized by the failure of tolerance to the normal gut flora and antigens, which finally results in inadequate immunologic responses[91]. Recent

studies in rodents confirm that colonic inflammation is accompanied with changes in bacterial composition[92]. The bacterial concentrations are increased, whereas microbial diversity is diminished, as an increase of *Enterobacteriaceae*, including *E.coli*, is described for IBD along with a decrease in *Firmicutes phyla* members compared to controls[93].

A common hypothesis is that a subset of CD is caused by defective clearance of commensal, opportunistic or pathogenic bacteria with subsequent initiation of compensatory antibacterial effector T cells that cause tissue damage[94,95]. A link to autophagy is given by polymorphisms of genes, regulating clearance of intracellular pathogens and observed defects in innate antimicrobial function. For example, secretion of both α- and β-defensins is defective in CD[96,97], whereat NOD2 deficient mice exhibit decreased expression of α-defensin defcr-4[98]. Deletion of the autophagy gene *ATG16L1* or the endoplasmic reticulum stress protein XBP-1 results in abnormal Paneth cell morphology and reduced expression of antimicrobial peptides[38,58]. Furthermore, the risk variant ATG16L1 T300A causes a decline in bacteria degrading autophagy (xenophagy)[48,49,74-76].

Decreased antimicrobial peptide secretion, as well as reduced xenophagy could lead to overgrowth, increased mucosal adherence and translocation of commensal bacteria, while defective clearance of invasive or phagocytosed bacteria promotes persistence of viable intracellular bacteria[99].

1.4.5 Mouse models for intestinal inflammation

Animal models of intestinal inflammation progressed the understanding of inflammatory bowel disease. The common used chemically induced models of intestinal inflammation are trinitro benzene sulfonic acid (TNBS), oxazolone or dextran sodium sulfate (DSS) colitis[100]. TNBS as well as oxazolone are haptenating substances and are given intrarectal (in ethanol) with the following effect: ethanol has the effect of breaking the mucosal barrier integrity, whereas TNBS and oxazolone induce a T cell mediated response against hapten-modified autologous proteins or luminal antigens. Contrary, DSS affects the integrity of the mucosal barrier by acting directly toxic to gut epithelial cells of the basal crypts[100]. It is applied to mice in their drinking water and induces an acute colitis, which is characterized by bloody diarrhea, ulcerations and infiltrations with granulocytes[101]. Importantly, it is shown, that the adaptive immune system is only secondary involved in this model as T and B cell deficient mice also develop severe intestinal inflammation after DSS

administration[102]. Therefore, the DSS-induced colitis is a useful model to study the involvement of innate immune mechanisms to colitis.

1.5 Aim of the work

In this work, the specific function of ATG16L1 was studied in mice *in vivo* in a DSS induced colitis model and *in vitro* in intestinal epithelial cells and bone marrow derived macrophages. Therefore three mouse models have been compared, the wildtype mice (WT), which express the complete protein; the ΔWD40 mice, which express a truncated form of the ATG16L1 protein lacking the WD40 repeat domain and furthermore, the ΔIEC mice as conditional Villin-Cre knockout mice with ATG16L1 deletion in the intestinal epithelium (see Figure 1-6).

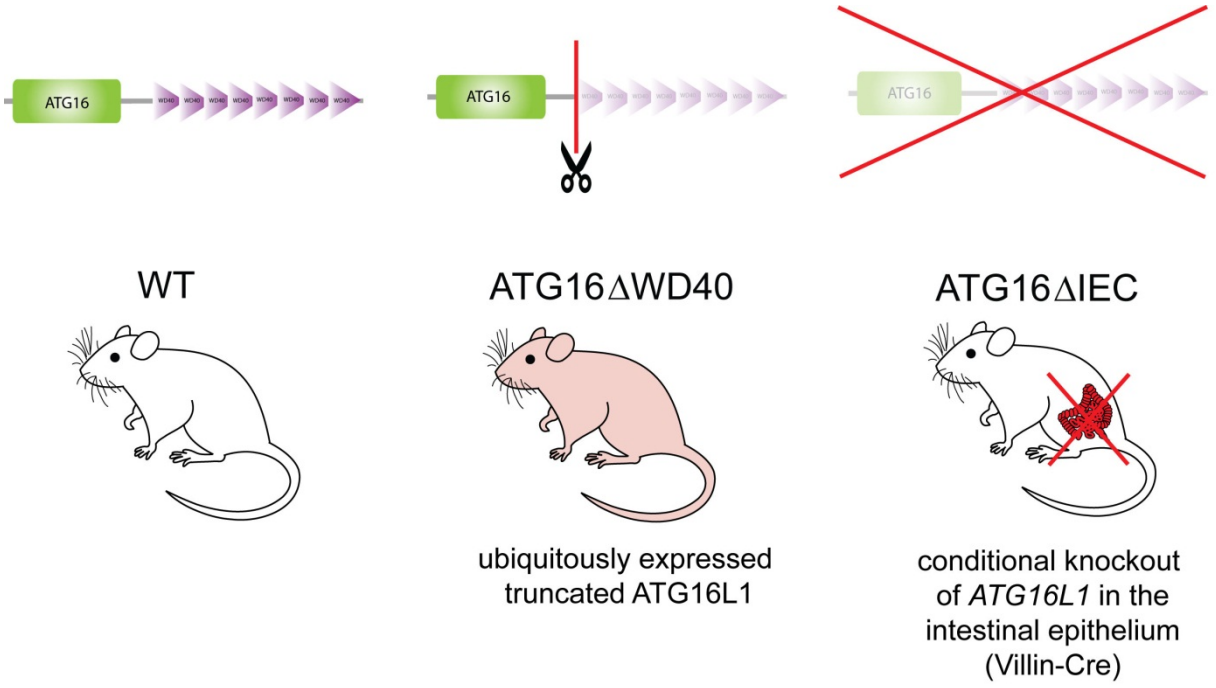

Figure 1-6: Mouse models with genetically altered *Atg16l1*
WT: The wildtype mice which express the complete protein; **ATG16ΔWD40:** the ΔWD40 mice, which express a truncated form of the ATG16L1 protein lacking the WD40 repeat domain; **ATG16ΔIEC:** the ΔIEC mice as conditional Villin Cre knockout mice with ATG16L1 deletion in the intestinal epithelium.

ATG16L1 is assumed to have unique protective functions, including Paneth cell antimicrobial peptide release and the negative regulation of pro-inflammatory cytokine production. A deletion of this protein leads to high susceptibility to Dextran sodium sulfite (DSS) induced colitis. Especially the ATG16L1 WD repeat domain is suggested to fulfill a distinct function in higher eukaryotes, because it is absent in the dimeric coiled coil structure of the yeast APG16 protein in contrast to the structure of the mammalian protein[103]. Until now, no interaction partner for the WD40 domain is

described. It is shown that the truncation of the whole WD40 domain has no impact on dimerization with ATG5. Hence, Fujita et al. concluded that the WD40 domain in ATG16L1 is dispensable for canonical autophagy[79]. But the risk associated variant T300A is located within this domain. The exchange of threonine to alanine at that position has an impact on Paneth cells of patients carrying the risk variant, as they show abnormal packaging and secretion of their antimicrobial granules. The same phenotype is described for hypomorphic mice, expressing only 30% of ATG16L1. Further it is demonstrated that the risk variant T300A leads to diminished xenophagy which in turn might be a link to impaired gut homeostasis.
However, it is unclear how ATG16L1 independently or as part of the classical autophagy pathway interacts with the ER connected vesicle export pathway and how it arranges his influence on the gut homeostasis. Further it is unclear, which specific role does the WD40 repeat domain play within these events.

Therefore, the specific goals of this thesis were:

- to investigate the consequence of an ATG16L1 truncation or deletion in intestinal inflammation in a mouse model

- to monitor the role of ATG16L1 in the autophagic machinery in intestinal epithelial cells and myeloid immune cells (bone marrow derived macrophages)

- to study the contribution of ATG16L1 on vesicle export in Paneth cells

- to investigate a presumed link of ATG16L1 and ER stress in intestinal epithelial cells and myeloid immune cells (bone marrow derived macrophages).

2 MATERIAL AND METHODS

2.1 Material

2.1.1 Organisms

C57BL6/J mice (WT mice)	Jackson Laboratory
ATG16L1 conditional knockout mice (ΔIEC mice)	genOway
ATG16L1 knock-in mice (ΔWD40 mice)	genOway

2.1.2 Chemical

Acryl amide/bisacryl amide (30:0.8)	BioRad
Agarose SeaKem LE	Biozym
Amphotericin	Sigma
Bovine serum albumin (BSA, Fraction V)	ICN Biomedicals Inc.
BrdU	CalBiochem
DEPC	Sigma
DNA Smart Ladder	Eurogentec
dNTPs	Fermentas
DTT	Fermentas
Dimethyl sulfoxide (DMSO)	Roth
Dextran sulfate sodium (DSS, MW 40.000 Da)	TdB Cosultancy
EDTA	Gibco
Ethanol	Merck
Fetal calf serum (FCS)	PAA
Formaldehyde	Roth
FITC-Dextran 4000	Sigma-Aldrich
Glycine	Roth
Glycerol	Roth
HCl	Roth
Hepes	Biochrom KG
Isopropanol	Roth
LD-MDP	Bachem
2-Mercaptoethanol	Merck
Methanol	Roth

Milk powder	Roth
PageRuler™ Plus Prestained Protein Ladder	Fermentas
Penicillin/Streptomycine (P/S)	PAA
Polyacrylamide Rotiphorese Gel 30	Roth
rm M-CSF	Immunotools
Sodium chloride	Roth
Sodium dodecyl sulfate (SDS)	Roth
Sodium hydroxide	Roth
Sulfuric acid	Sigma-Aldrich
SYBR Safe	Invitrogen
N,N,N',N'-tetramethylethan-1,2-diamin	Roth
TEMED	Sigma
TRIS	Merck
Tween 20	Roth
Yeast extract	Roth

2.1.3 Media

DMEM Dulbecco's minimal essential medium	Sigma
MMM Mouse Macrophage medium	Sigma
HBSS calcium-magnesium-free medium	PAA
LB medium	10g NaCl, 10g tryptone, 5g yeast extract, ad 1l Milli-Q H2O, autoclaved
MEM minimal essential medium	PAA, supplemented with 10% (v/v) FCS, 1% (v/v) P/S

2.1.4 Buffers and solutions

2.1.4.1 SDS-polyacrylamide gelelectrophoresis and Western blot

Anode buffer 1	30 mM Tris base, 20% (v/v) methanol
Anode buffer 2	300 mM Tris base, 20%(v/v) methanol
Cathode buffer	25 mM Tris base, 20%(v/v) methanol, 40

	mM 6-amino-caprone acid
5x Protein loading buffer (Fermentas)	0.313 M Tris HCl (pH 6.8 at 25°C),10% (w/v) SDS, 0.05% (w/v) bromophenol blue, 50% (v/v) glycerol, 2M DTT
4x Separation buffer	1.5 M Tric/HCl (pH 8.8), 0.4% (w/v) SDS
4x Stacking buffer	0.5 M Tris/HCl (pH 8.8), 0.4% (w/v) SDS
Stripping buffer	62.5 mM Tris/HCl (pH 6.8), 2% (w/v) SDS, 0.7 % (v/v) b-mercaptoethanol
TTBS	20 mM Tris, 137 mM NaCl, 0.1% (v/v) Tween20
Blocking solution 3% (w/v)	milk powder in TTBS

2.1.4.2 Immunohistochemistry

Shadon Gill III Hematoxylin	Thermo Scientific
Giemsa's azure eosin methylene blue	Merck
AEC substrate	Dako
Blocking reagent	Dako
Antibody Diluent	Dako
DAPI (20mg/ml)	Sigma-Aldrich

2.1.4.3 Cell stimulation

Bafilomycin	Sigma
LD-MDP	Bachem
Rapamycin	Sigma
Tunicamycin (*Streptomyces lysosuperficus*)	Calbiochem

2.1.5 Antibodies

Table 1: List of Antibodies

Antibody	Species, Type	Dilution	Manufacturer	Cat. number
Anti-ATG16L1	Mouse, monoclonal	1:500	MBL	M150-3
Anti-CD3	Rabbit, polyclonal	1:50	Abcam	Ab5690
Anti-ATF4	Rabbit, polyclonal	1:100	Santa Cruz	Sc-200
Anti-goat-FITC		1:300	Jackson ImmunoResearch	
Anti-goat-HRP		1:1000	Amersham Biosciences	1025
Anti-grp78	Rabbit, polyclonal	1:500	ENZO	ADI-SPA-826-D
Anti-LC3	Rabbit, polyclonal	1:300 (IHC) 1:500 (WB)	Novus	ND100-2331
Anti-Lysozym (α)	Goat, polyclonal	1:500	Santa Cruz	Sc-27958
Anti-mouse-Alexa fluor ^{555}		1:300	Invitrogen	A21425
Anti-mouse-HRP		1:1000	GE healthcare	NA931V
Anti-PDI	Rabbit, polyclonal	1:500	Abcam	Ab3672
Anti-rabbit-Alexa fluor ^{555}		1:300	Invitrogen	A21430
Anti-rabbit-HRP		1:1000	GE healthcare	NA934V
Anti-β-actin	Mouse, monoclonal	1:60000	Sigma Aldrich	A-5441

2.1.6 Oligonucleotides

All oligonucleotides used were synthesized from Metabion. Sequences are shown inTable 2.

Table 2: Used Primers and their sequences

Primer	Orientation	Sequence (5'→3')	T_{anneal} (°C)	Amplicon (bp)
ATG16l1_ A(167-423)	sense antisense	GGAAGCGTCACATCGCGGAGG CTCCCCACGCTTCTTGTGCAGT	65	278
ATG16l1_ B(767-1128)	sense antisense	CCAGGAGGCGTCAAGCACGG CAGTGGCCAGCAACCGGGAG	65	381
CD4	sense antisense	CGTGCTGGGTGGCTCCTTCG AGAGCAGAAGGCCGGAGGCA	66	282
CHOP	sense antisense	CTGCCTTTCACCTTGGAGA CGTTTCCTGGGGATGAGATA	60	118
Defa3	sense antisense	TGGCCTTCCAGGTCCAGG GACCCTTTCTGCAGGTCC	62	216

Defa5	sense antisense	AGGCTGATCCTATCCACAAAACAG AGCATCAGTGGCCTCAGACC	62	282
DES	sense antisense	GCGCCAAGCCAAGCAGGAGA GAGGACGGGGCCAGGACACT	66	503
G3PDH	sense antisense	TGAAGGTCGGAGTCAACGGATTTGGT CAGTGGGCCATGAGGTCCACCAC	55	720
Hspa5	sense antisense	CCCCTGTCGCCCTCAGACCA TGCGTCCGATGAGGCGCTTG	65	416
Krt18	sense antisense	GCGCCAGTCTGTGGAGAGCG AGGGTGCGTCTCAGCTCCGT	66	387
Lyz	sense antisense	ACTGCCCAGGCCAAGGTCTACA TCGCCATGCCACCCATGCTC	60	381

2.1.7 Marker

DNA-Ladder

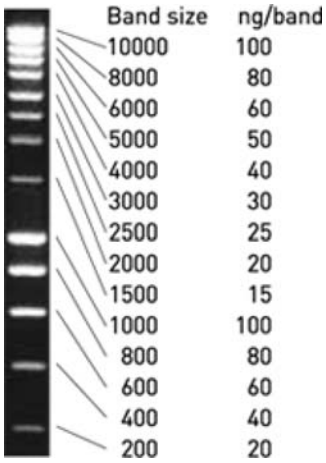

Figure 2-1: 1kb DNA smart Ladder from Fermentas.

Protein-Ladder

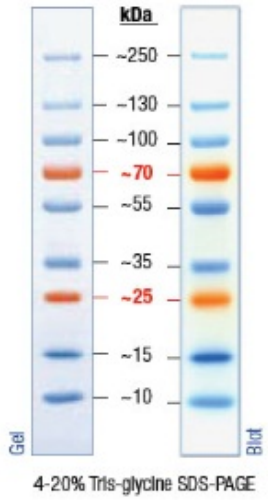

Figure 2-2: Prestained Protein Molecular Marker (10-250 kDa) from Fermentas.

2.1.8 Kits

Advantage RT-for-PCR	BD Bioscience/ Clontech
BrdU In-Situ Detection Kit	BD Pharmingen
ECL-PLUS	Amersham
GoTaq DNA polymerase	Promega
QiaShredder	Qiagen
RNeasy Kit	Qiagen

2.1.9 Electric devices and other materials

2.1.9.1 Centrifuges

Centrifuge 5417R	Eppendorf
Varifuge 3.0R	Haraeus

2.1.9.2 Incubators

HeraCell CO_2-Incubator	Heraeus Instruments
Orbital Incubator SI50	Stuart Scientific

2.1.9.3 Electrophoresis devices and power supplies

Geldok 2000	Biorad
PP 4000 Programmable High Voltage Power Pack	Biometra

2.1.9.4 Microscopes

Fluorescence microscope with integrated Apotome	Carl Zeiss Micro Imaging GmbH

2.1.9.5 Other devices

Gene Amp PCCP System 9700	AppliedBiosystems
NanoDrop ND-1000 spectrophotometer	Thermo Scientific
Sterile working bench	HeraSafe Heraeus
Heating block	Grant Instruments

2.1.9.6 Consumables

0.5ml, 1.5ml and 2ml micro tube	Sarstedt
Pipette tips	Sarstedt
Tube 15ml and 50ml	Sarstedt
Hyperfilm Amersham	Biosciences
PVDF-membrane Highbond P	Amersham Biosciences

Tissue culture dish 6-well	Sarstedt
100 Sterican size 18	Braun
Injekt-F (1ml)	Braun
Surgical Disposable Scalpels	Braun

2.2 Methods

2.2.1 Isolation of RNA

Extraction of RNA from mouse intestinal epithelial cells and bone marrow derived macrophages was performed using the RNeasy Kit from Quiagen according to manufacturer's protocol.

2.2.2 cDNA synthesis

cDNA synthesis was performed using Advantage® RT-for-PCR kit from BD Bioscience/Clontech according to manufacturer's protocol.

2.2.3 Polymerase chain reaction (PCR)

Nucleic acid sequences can be amplified by using polymerase chain reaction. This method can be divided into three different steps: (i) denaturation, (ii) annealing and (iii) elongation. After DNA denaturation specific primers bind during the annealing phase to the template and the defined region of the DNA is replicated during the elongation phase. By repeated denaturation, annealing and elongation for several cycles the specific DNA sequence is amplified exponentially. Standard PCR was performed using the components shown in Table 3. The PCR was carried out with the following PCR program: 95°C 5min, up to 35x (95°C 1min, T_{anneal} 1min, 72°C 1min), 72°C 5min. T_{anneal} equals the primer annealing temperature as estimated by the program UCSC In-Silico PCR. PCR products were analyzed by agarose gel electrophoresis and finally detected under UV light.

Table 3: Components of a standard PCR

Component	Volume [µl]
cDNA Template	2
GoTaq Buffer (5x)	4
dNTP mix (each 10mM)	0,5
Primer mix (each 10µM)	0,5
GoTaq DNA Polymerase	0,25
Milli Q H_2O	12,75

2.2.4 Reverse-transcriptase (RT) PCR

RT-PCR is a PCR amplification of a product from the reverse transcription (RT) reaction, whereby a template mRNA is translated into a single-stranded cDNA. In this study, a RNA-dependent DNA polymerase (=reverse transcriptase) derived from the retrovirus moloney-murine leukemia virus (MMLV) was used in combination with oligo-(dT)18 primer to ensure its binding at the 3' poly(A) tail of the mRNA. All used components originate from the Advantage® RT-for-PCR kit (BD Bioscience/Clontech). The following reaction mixture was used:

RNA	1 µg
Oligo (dT)	1 µl
DEPC treated H2O	add 13.5 µl

The mixture was heated at 70°C for 5 min and then cooled on ice. The following components were subsequently added:

Reaction buffer (5x)	4 µl
dNTPs 10 mM each	1 µl
RNase-Inhibitor	0.5 µl
Reverse Transcriptase (200 U/ml)	1 µl

The reaction mix was incubated for 1 hour at 42°C. Afterwards the Reverse Transcriptase was heat inactivated at 70°C for 10 min. The mixture was filled add 100 µl with DEPC treated H_2O. 2 µl of the resulting cDNA was used directly for the subsequent PCR.

2.2.5 Agarose gel electrophoresis

Nucleic acids were separated in 1% (w/v) agarose gels supplemented with 0.3% (v/v) SYBR safe. The electrophoresis was performed in horizontal gel chambers at 90 to 120 V. Fragment sizes were estimated using DNA ladders.

2.2.6 Protein extraction

Protein extracts were prepared as described by Laemmli et al.[104] by resuspending cell pellets in denaturing lysis buffer containing 2% (w/v) SDS, 0.06M Tris (pH 6.8), 0.05% (w/v) bromophenol blue, 50% (v/v) glycerol and 0.1M Dithiothreitol (DTT), shearing them up to ten times through syringe needle (sterican size 18, braun) and boiling them for five minutes at 100°C in a heating block. Purified supernatant was applied directly to a SDS-polyacrylamide gel or transferred into a fresh microcentrifuge tube and stored at +4°C for one week.

2.2.7 Sodium dodecyl sulfate polyacrylamide gel electrophoresis (SDS-PAGE)

SDS-PAGE is a method to separate proteins according to their electrophoretic mobility and allows the analysis of proteins via staining or Western blotting. Furthermore, molecular weight of analyzed proteins can be determined using molecular weight marker. Proteins were separated by discontinuous gel electrophoresis. Compositions of the different gels are shown in Table 4. Electrophoresis was performed in 1x SDS running buffer. Protein samples were supplemented with 5x protein loading buffer and loaded onto the gel. Electrophoresis was carried out at 120-180V for 90 to 120min.

Table 4: Gel components for SDS-PAGE

Component	Stacking gel [µl]	Separating gel [µl]
A. bidest	1950	2500
4x Stacking buffer	750	-
4x Separation buffer	-	2500
(Bis) Acrylamide	300	5000
10% APS	30	100
TEMED	3	10

2.2.8 Western Blot

After separation of protein samples by SDS-PAGE, proteins were transferred onto a polyvinylidene difluoride (PVDF) membrane (Millipore, Schwalbach) at 0.8mA/cm2 and 1 to 1.5 hours. After blocking for one hour with 5% (w/v) low-fat milk powder in TTBS, membranes were probed with specific primary antibodies overnight at 4°C, washed and incubated with horseradish peroxidase (HRP)-conjugated IgG as secondary antibody for one hour at room temperature. After another washing step proteins were visualized by chemiluminescence (ECL, Amersham Biosciences). To determine even transfer and equal loading, membranes were stripped and reprobed with antibody specific for β-actin. The bands were quantified by densitometry.

2.2.9 Animal treatment

All experiments were performed according to German guidelines for animal care and protection (V742-72 241.121-3 (20-2/04) and (76-7/00) as well as V312-72241.121-3). Mice were maintained in a 12h light-dark cycle under standard conditions and were provided with food and water ad libitum. All animals were pathogen free as assessed by regular microbiological screening and kept under barrier conditions at 21°C ± 2°C and 60% ± 5% humidity in individually ventilated cages.

2.2.10 Induction of DSS-colitis and determination of clinical scores

Chronic colitis was induced by administration of 2 % dextran sulfate sodium (DSS) in the drinking water for 5 d followed by 5 d of regular drinking water over a period of 30d. Acute colitis was induced by 4 %DSS in the drinking water for 5 d. Groups of four to 11 mice were used to monitor the disease activity index (DAI) or after sacrifice via Immunhistochemistry of sections of the Colon the histological scoring (see Table 5). Clinical parameters were recorded daily. DAI displaying the combined score of weight loss, stool consistency, and rectal bleeding, was performed as previously described by Siegmund et al[105]. A high resolution mouse video endoscopic system was used (HOPKINS® Optik 64019BA; KARL STOLZ AIDATM VET, Berlin, Germany). Histological scoring was obtained by combination of the score of inflammatory cell proliferation and tissue damaging as described by Siegmund et al.[106] and Atreya et al.[107].

Table 5: Components of DAI and histological scoring

DAI	Histological scoring
Weight loss	Inflammatory cell infiltration
Stool consistency	Tissue damaging
Rectal bleeding	

2.2.11 FITC dextran and BrdU administration

Intestinal permeability was assessed by administration of the non-metabolizable macromolecule FITC-dextran 4000 (Sigma-Aldrich, Deisenhofen, Germany). FITC-dextran was administered by gavage (0.6 g/kg body weight) 4 h before sacrifice. Whole blood and serum were obtained by cardiac puncture and centrifugation at 5,000 rpm for 15 min respectively. Dilutions of FITC-dextran 4000 in PBS were used as a standard curve and absorption of 100 µl serum or standard was measured in a fluorometer at 488 nm.

BrdU (5-bromo-2-deoxyuridine) is a synthetic nucleoside that is an analogue of thymidine and provides a simple technique for labeling and identifying proliferating cells. BrdU can be incorporated into the newly synthesized DNA of replicating cells (during the S-phase of the cell cycle), substituting for thymidine during DNA replication. To study proliferation of epithelial cells 50mg BrdU/kg body weight (CalBiochem, Schwalbach, Germany) was injected intraperitoneally 2h before sacrifice.

2.2.12 Statistical analysis

All parametric data are presented as the means ± standard deviation. Data from two groups were analyzed for significance using a student's unpaired t-test (http://www.physics.csbsju.edu/stats/t-test.html). A p value of $p<0.05$ was considered as statistically significant (*) and $p<0.01$ was considered strong significant (**) and $p<0.001$ was considered as highly significant (***). Experiments and measurements were replicated at least three times.

2.2.13 Densitometrical analysis with ImageJ

The densitometrical analysis of pictures or X-ray films received from agarose gel electrophoresis combined with UV light visualization and detection of proteins by chemiluminescence was performed with the non-commercial software ImageJ (http://rsb.info.nih.gov/ij/).

2.2.14 Immunohistochemistry

2.2.14.1 Processing of tissues

Jejunum tissue and colon tissue, especially the distal part, was removed and fixed in 4 % paraformaldehyde in 1xPBS for 24 h. Tissues were dehydrated in an ascending ethanol and xylol series. Samples were embedded in paraffin and dissected with 5 µm using a microtome (Leica RM2165).

2.2.14.2 Hematoxylin-Eosin (HE) staining

Processed tissue sections were incubated in Shadon Gill III Hematoxylin, differentiated in 0.5% acetic acid, washed and stained with Giemsa's azur eosin methylen blue solution. The stained sections were analyzed by microscopy.

2.2.14.3 BrdU staining

To visualize BrdU incorporation sections were stained with 1:500 dilution of mouse anti-BrdU mAb in Antibody diluent overnight. Sections were then incubated for 1h with biotinylated anti-mouse secondary antibody (1:50 in Antibody Diluent) and developed with AEC substrate. Counterstaining was performed with Shadon Gill III Hemytoxylin. Stained sections were analyzed by microscopy.

2.2.14.4 Immunofluorescence staining

Sections were boiled in citrate buffer for 3 or 20 min (depending on the primary antibody) followed by sequential incubation with blocking reagent. Slides were then

incubated for 1 h at room temperature with primary antibody. After washing with PBS, slides were incubated for 45 min at room temperature with Alexa fluor^{555}- or FITC-labeled secondary antibodies (see Table 1). Nuclei were counterstained with DAPI (4',6-diamidino-2-phenylindole; 20 mg/ml).

2.2.14.5 Electronmicroscopy and Toluidine blue staining

Electronmicroscopy and Toluidine blue staining of semi thin sections was performed at Institute of Anatomy (AG Lucius) according to standard protocols[108,109].

2.2.15 Isolation of primary cells

2.2.15.1 Intestinal epithelial cells (IECs)

Briefly, mouse Jejunum was everted and incubated in calcium-magnesium-free HBSS with 1 mM EDTA for 30 min at 37°C with gentle shaking to liberate intestinal epithelial cells (IECs). The isolated cells were seeded in 6-well plates (Nunc) at 1x10^6 cells/well in minimal essential medium (MEM), supplemented with 20 % fetal calf serum (FCS) and 1 % Penicillin/Streptomycin (P/S) and were left resting for 3 h before stimulation.

2.2.15.2 Bone marrow derived macrophages (BMDMs)

Primary bone marrow-derived macrophages (BMDM) were obtained from femoral bone marrow. In brief, cells from the femur were isolated and cultured at 10^6 cells/ml for 7 days in 1:1 Dulbecco's minimal essential medium (DMEM, Sigma) and Mouse Macrophage Medium (MMM, Sigma), supplemented with 10 % fetal calf serum (FCS), Penicillin/Streptomycin (1x), Amphotericin (2.5 µg/µl) and rm M-CSF (20 ng/ml). At 3 days after washing and reculturing in fresh medium, the cell preparation contained a homogenous population of >95 % macrophages. The BMDMs were plated in 6-well culture plates (8x10^5 cells/well).

2.2.16 Stimulation of BMDMs or IECs

For stimulation experiments, seeded cells were stimulated with the following stimuli or were left untreated:

Table 6: Reagents used in cell culture experiments.

Reagent	Concentration (Time)
Rapamycin	50µg/ml (20min)
Bafilomycin	100nM (20min)
LD-MDP	100µg/ml (2h)
Salmonella typhimurium	MOI 100 (1h)
Tunicamycin	5µg/ml (4h)

2.2.17 Transgenic animals

2.2.17.1 Generation of *Atg16l1* conditional knockout mice (∆IEC)

The *Atg16l1* knockout mice were generated in collaboration with GenOway. The *Atg16l1* targeting strategy was designed to introduce a single distal loxP site upstream *Atg16l1* gene exon 1, within the promoter region, and a loxP site together with an FRT flanked neomycin selection cassette within the intron 1, and leading to conditional disruption of the translation of all *Atg16l1* isoforms by partial gene deletion. The resulted mouse line was bred with deleter-mice constitutively expressing the Flp-recombinase to remove the neomycin selectin cassette and thus creating a line of floxed mice in which *Atg16l1* gene exon 1 is flanked by loxP sites. This floxed mouse line then was mated with Cre-recombinase expressing mice (under the direction of the mouse villin 1 promoter) to obtain a tissue specific *Atg16l1* knock-out model (recombination occurs in villi and crypt cells of the small and large intestines).

2.2.17.2 Generation of *Atg16l1* knock-in mice (∆WD40)

The *Atg16l1* knock-in mice were generated in collaboration with GenOway. The targeting strategy was designed for insertion of a Stop-polyadenylation signal cassette in 3' of *Atg16l1* exon 10, and leading to the constitutive expression of truncated *Atg16l1* isoforms missing the C terminal region encoding for the WD40 domains. The resulting lines of mice were bred with deleter-mice constitutively expressing the Flp-recombinase, in order to remove the neomycin selection cassette and thus create the *Atg16l1* Knock-in mouse line devoid of selection cassette.

3 RESULTS

3.1 The role of ATG16L1 in DSS induced colitis.

Autophagy-related protein 16-1 (ATG16L1) is a component of a large protein complex essential for autophagy. As autophagy is described to be genetically linked to Crohn's disease with a polymorphism in ATG16L1 as revealed by our group in a genome wide association study in 2007[110], it was interesting to understand the specific role of the ATG16L1 WD40 repeat domain, which comprises the Crohn associated coding variant T300A (threonine-to-alanine substitution), in inflammatory bowel disease. Three mouse models have been compared: the wildtype mice (WT), which express the complete protein; the ΔWD40 mice, which expressed a truncated form of the ATG16L1 protein lacking the WD40 repeat domain and furthermore, the ΔIEC mice as conditional Villin-Cre knockout mice (see Figure 3-1 A). Before testing the gene expression of *Atg16l1* in intestinal epithelial cells (IECs) a purity control was performed to estimate the extent of contamination by further cell lineages in the isolated IECs. Therefore, the expression of the transcripts *Cd4*, *Des* and *Krt18* was investigated via RT-PCR. *Cd4* encodes for the protein CD4, expressed on the surface of $CD4^+$T cells, additionally *Des* encodes for the Protein desmin, a subunit of intermediate filaments in skeletal muscle tissue. *Krt18* encodes for the protein keratin 18, a type I cytokeratin which is expressed in single layer epithelial tissues. As depicted in Figure 3-1 B, the RT-PCR of the intestinal epithelial cells shows that in fact IECs were isolated (387bp), only low expression of *Cd4* (282bp) and no expression of *Des* was detected which indicates that due to the method of primary IEC isolation, there is a negligible low grade of contamination with immune cells and no contamination with muscle cells.

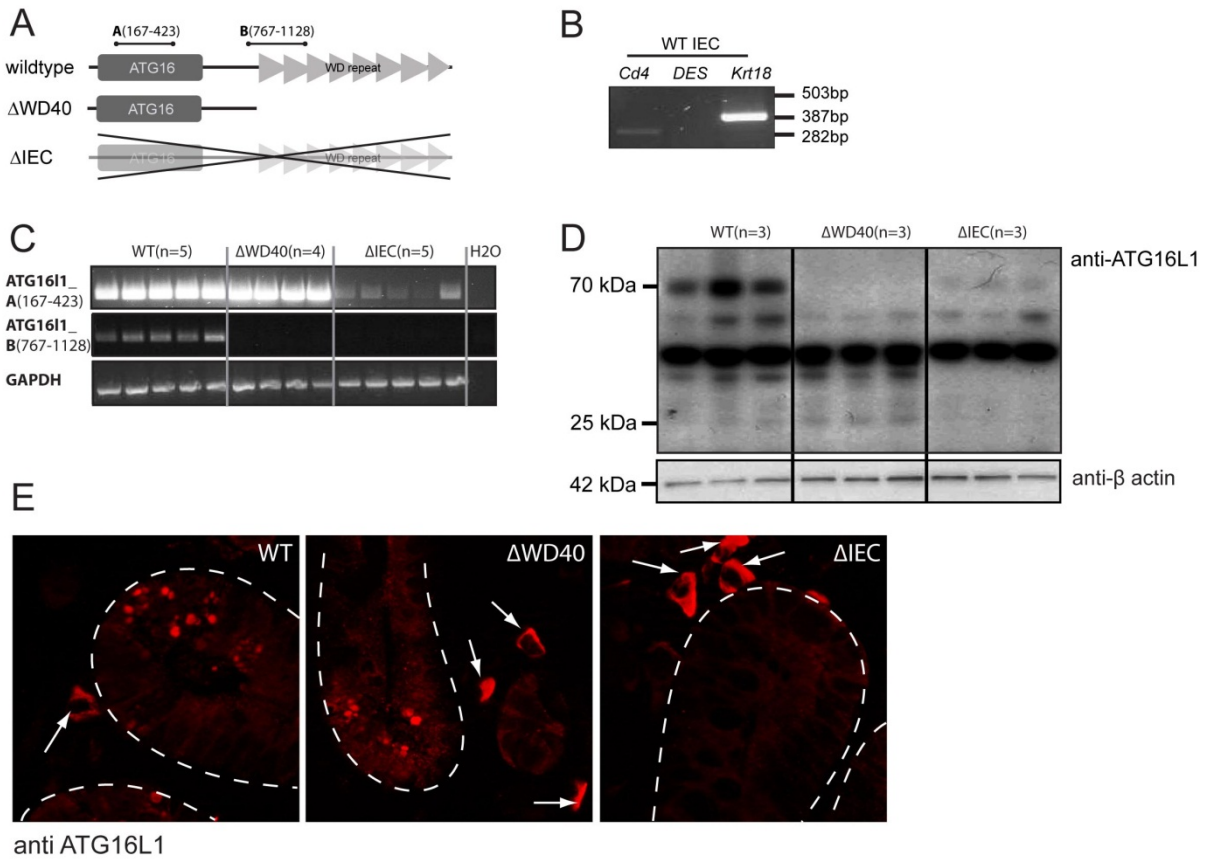

Figure 3-1: Domain structure and expression profile of murine ATG16L1 displaying the three variants of genotypes.
A) The N-terminal domain (ATG16) of the ATG16L1 protein is involved in complexation of essential autophagy proteins ATG5 and ATG12 and self-dimerisation. The C-terminal eight WD repeats are of unknown function and comprise the Crohn disease associated coding SNP T300A. The wildtype mice express the whole protein, the ΔWD40 ubiquitously express the truncated form, missing the WD40 repeat domain, and the ΔIEC mice do not express ATG16L1 in the IECs. Marked with bars are the DNA binding sites for the primer pairs A(167-423) and B(7667-1128). **B)** Intestinal epithelial cells were isolated from WT mice and RT-PCR experiments were performed with cDNA and sequence-specific primers for *CD4*, *DES* and *Krt18*. **C)** RT-PCR experiments were performed with cDNA and sequence-specific primers for *Atg16l1* in the area of the ATG16 domain coding sequence (A167-423) and of the beginning of the WD40 repeat domain coding sequence B(7667-1128) and *G3PDH*. **D)** Protein extracts of intestinal epithelial cells of WT, ΔWD40 and ΔIEC mice (each n=3) were separated by SDS-PAGE and immunoblotted against ATG16L1 and β-actin; representative image. **E)** Jejunum tissue section of WT, ΔWD40 and ΔIEC mice stained with anti-ATG16L1 (red). Arrows show ATG16L1 positive, non-epithelial cells; dotted line denotes crypt unit; representative images.

Furthermore, for genotype validation the expression of the *Atg16l1* gene was tested in intestinal epithelial cells (IECs) by RT-PCR via two different pairs of oligonucleotides. One pair (**A**(167-423)) amplified a DNA fragment from nucleotide 167 to 423 in the DNA sequence coding for the coiled coil domain, the other one (**B**(767-1128)) a fragment from nucleotide 767 to 1128 within the DNA sequence coding for the WD40 domain (see Figure 3-1 A,C). In wildtype mice with both primer pairs the desired DNA sequences were amplified, whereas in ΔWD40 mice only primer pair A bound to the DNA sequence coding for the coiled coil domain. In ΔIEC

mice no bands were detected apart from very weak amplifications, which can be explained by contamination of the intestinal epithelial cells by $CD4^+$ T cells. *G3PDH* was used as a loading control (see Figure 3-1 C). Additional genotype validation was performed by investigating the protein expression of ATG16L1. After preparation of whole protein extracts from intestinal epithelial cells, SDS PAGE and immunoblotting were performed with a specific antibody raised against the N-terminal region of ATG16L1 and β-actin as equal loading control of proteins. Figure 3-1 D shows that ATG16L1 could be detected in WT mice with a protein size of ~70 kDa. Again, a very weak signal was observed in ΔIEC mice, which can be explained by contamination with non-intestinal epithelial cells. For the truncated version of ATG16L1 in ΔWD40 mice no specific signal was detected via immunoblotting, which is assumed to be a complicacy with the antibody especially in this analysis method.

At last, ATG16L1 protein expression was validated via immunohistochemistry in Jejunum sections of all three genotypes using the same ATG16L1 antibody as before. As depicted in Figure 3-1E ATG16L1 positive signals were detected in intestinal epithelial cells of WT and ΔWD40 mice. ΔIEC Jejunum sections exhibit no ATG16L1 positive epithelial cells. All three genotypes show ATG16L1-stained non-epithelial cells (see Figure 3-1, E).

These results indicate on the one hand that the isolation method for the intestinal epithelial cells is sufficient for further experiments and on the other hand that the mouse models generated in collaboration with genOway are validated.

ATG16L1 is described to be linked with Crohn disease[64], but two different opinions exist about its role during DSS induced colitis. Cadwell et al. detected no differences in responses to DSS-induced intestinal injury in mice expressing ATG16L1 at 30 % of the wildtype level[59]. Contrariwise Saitoh et al. reported higher responsibility to DSS treatment for chimeric mice deficient for *Atg16l1*[44]. Hence, it was interesting to compare Cadwells and Saitohs findings with our mouse models.

Wildtype mice as well as ΔWD40 and ΔIEC mice were either treated with 2 % DSS in the drinking water for five days followed by five days of water over a period of 30 days (chronic colitis) or with 4 % DSS in the drinking water for 5 days (acute colitis). During this DSS induced colitis almost all mice developed loose stools or diarrhea. DSS is toxic to gut epithelial cells of the basal crypts and affects the integrity of the mucosal barrier[111] via extensive crypt and epithelial cell damage. Significant

infiltration of granulocytes and mononuclear immune cells and decreased epithelial cell proliferation are observed consequenses[112]. The wall appears thickened, and stricture appears early in the disease. Coloscopical examination indicated that in both experiments all strains developed colitis as exemplarily depicted in Figure 3-2 for acute colitis.

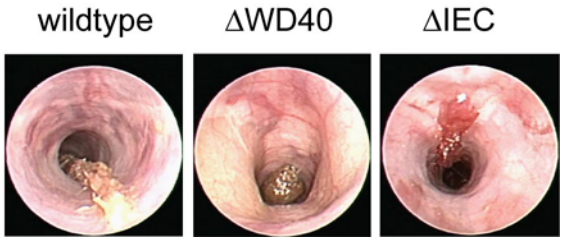

Figure 3-2: Colonoscopy of DSS treated WT, ΔWD40 and ΔIEC mice.
Acute Colitis was induced by giving animals 4% DSS in the drinking water for 5 days. On the last day of the experiment colonoscopy was performed.

Disease severity was investigated daily by weight progression, hemoccult test and stool consistency, thus termed the disease activity index (DAI) (see Figure 3-3 A). The combined score ranged from 0 (no changes) to 12 (strong disease severity with weight loss >20 %, liquid stools and gross rectal bleeding). A group of six to ten wildtype, eight to eleven ΔWD40 and five to seven ΔIEC animals were used. The DAI validation sustained the above described coloscopical findings in mice of all three strains. Interestingly, compared to WT as well as to ΔWD40 mice the ΔIEC mice exhibited a significantly higher responsibility to DSS in both colitis experiments, as already shown likewise by Saitoh et al.[44]. No clear differences appeared by comparison of ΔWD40 mice with WT mice. All WT and ΔWD40 mice survived, but one ΔIEC mouse died.

As displayed in Figure 3-3 B and C, during chronic and acute DSS colitis the ΔIEC mice exhibited significantly increased intestinal injury response, whereas no clear difference could be observed between ΔWD40 and WT mice.

A

Index \ Score	0	1	2	3	4
Weight loss	0	1-5%	6-10%	11-20%	>20%
Stool consistency	well-formed pellets	-	pasty and semiformed pellets that did not adhere the anus	-	liqid stools that did not adhere to the anus
Rectal bleeding	no blood by using hemoccult	-	positive hemoccult	-	gross bleeding

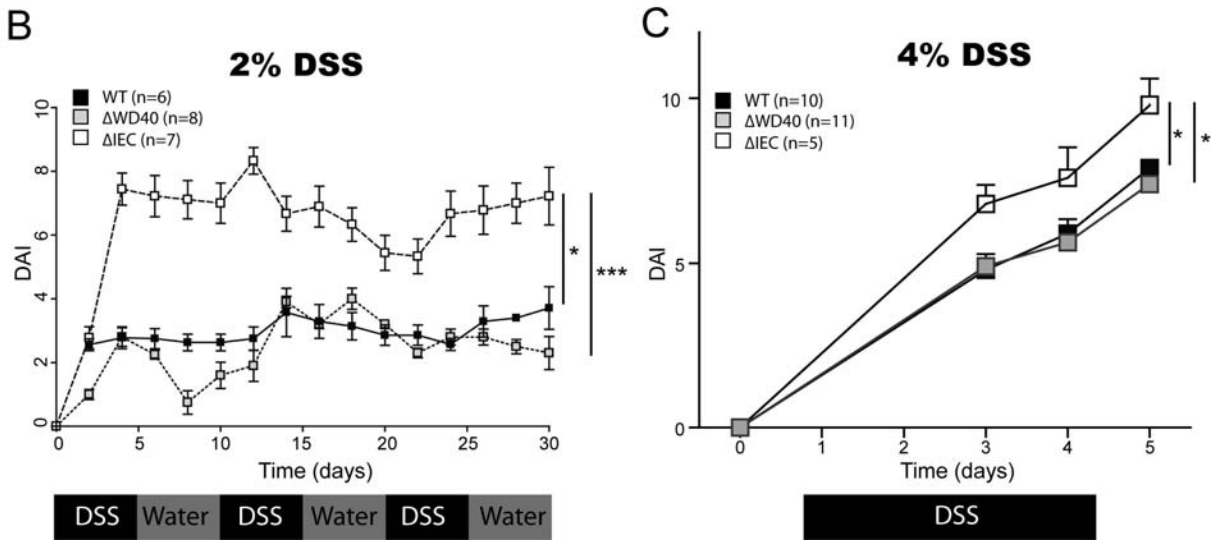

Figure 3-3: DAI score during DSS-treatment.
A) Components of the disease activity index (DAI). **B)** DSS was applied in drinking water for 5d followed by 5d of drinking water over a period of 30d. The disease activity index (DAI) displays the results of daily assessment of change in body weight, diarrhea score, and bleeding score during chronic colitis or **C)** acute colitis (index with values are shown as means ± SEM;*, p≤0,05).

HE staining of the colon of mice treated with DSS affirmed fewer signs of inflammation in WT and ΔWD40 mice but strong signs in ΔIEC mice. In all three genotypes the epithelium was afflicted by DSS toxicity to gut epithelial cells. A clear difference was detected in the architecture of the crypts. In mildly inflamed mice like WT and ΔWD40 animals the crypts are almost intact. In higher inflamed ΔIEC mice the crypt structure was occasionally lost after day five (see Figure 3-4 A).

Histological scoring is the combined score of inflammatory cell infiltration (score 0-3) and tissue damage (score 0-3)[106,107] (Figure 3-4 B). The combined score ranged from 0 (no changes) to 6 (extensive cell infiltration and tissue damage). As shown on Figure 3-4 C, the histological score is significantly increased in all three genotypes from untreated mice to DSS challenged mice (p≤0.001), and it is significantly elevated in DSS treated ΔIEC mice compared to WT mice (p≤0.05).

A

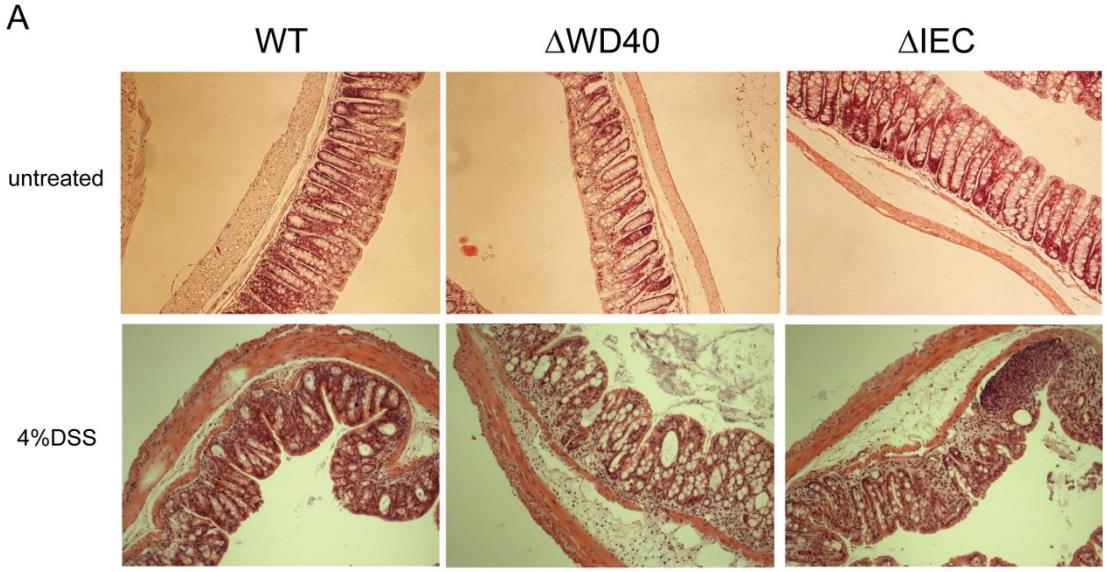

B

Score / Index	0	1	2	3
Inflammatory cell infiltration	Occasional inflammatory cells in the lamina propria	Increased numbers of inflammatory cells in the lamina propria	Confluence of inflammatory cells extending into the submucosa	Transmural extension of the Infiltrate
Tissue damage	No mucosal damage	Lymphoepithelial lesions	Surface mucosal erosion or focal ulceration	Extensive mucosal damage and extension into deeper structures of the bowel wall

C

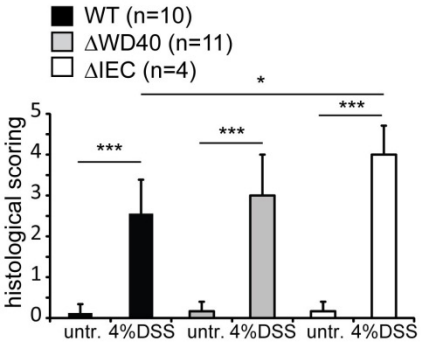

Figure 3-4: Histological scoring for unchallenged and DSS treated WT, ΔWD40 and ΔIEC mice. A) HE staining of colons from WT, ΔWD40 and ΔIEC mice challenged for 5d with 4%DSS or left untreated; at a magnification of 100. B) Components of histological scoring. C) The histological displays the inflammatory cell migration, as well as tissue the tissue damage of WT (n=10), ΔWD40 (n=11) and ΔIEC (n=4) mice. Values are shown as means ± S.D; * p≤0.05; *** p≤0.001.

To confirm the above findings, infiltration of immune cells was visualized by immune fluorescent staining with anti-CD3 as marker for infiltrating T-Lymphocytes. An optical evaluation was performed with Colon sections of three DSS treated animals per genotype, depicted representatively on Figure 3-5. It shows a high increase of CD3 positive cells in the Lamina propria of ΔIEC mice, whereas the rate of infiltration was less severe in WT and ΔWD40 mice.

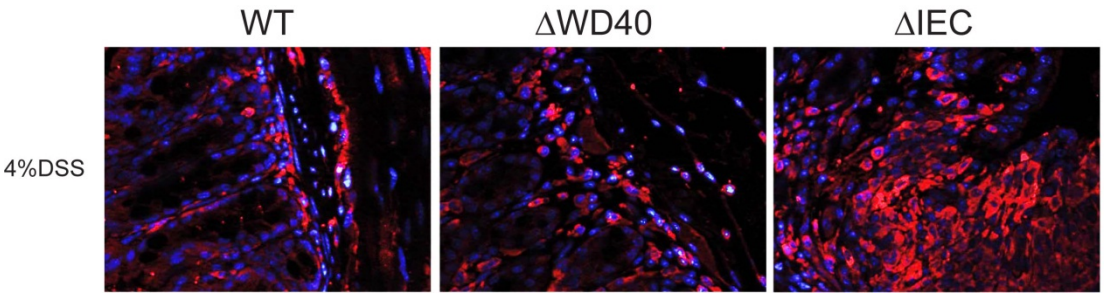

Figure 3-5: CD3 positive T cells in intestinal tissue sections of DSS-treated, ΔWD40 and ΔIEC mice.
Colonic tissue sections of WT, ΔWD40 and ΔIEC mice stained with anti-CD3 antibody to visualize CD3 positive T cells

A possibility to explain higher susceptibility to DSS induced colitis in ΔIEC mice might be the impairment of regenerative proliferation of epithelial cells. To analyze the regenerative response of the gut epithelium during DSS-induced colitis, cell proliferation was measured via Bromdesoxyuridine (BrdU) staining. Cells were labeled by intraperitoneal injection of BrdU two hours before sacrifice. As shown on Figure 3-6 A, the cell proliferation during DSS-induced colitis decreases from WT mice to ΔWD40 and from ΔWD40 mice to ΔIEC mice. This observation was confirmed by counting ~3 BrdU positive cells per crypt in 154 crypts of 5 WT animals, ~2 positive cells in 327 crypts of 5 ΔWD40 and ~1 positive cell in 312 crypts of 5 ΔIEC mice. The decrease of proliferation from WT mice to ΔWD40 and to ΔIEC mice is highly significant ($p \leq 0.001$), as well as the decrease of proliferating cells from ΔWD40 to ΔIEC mice ($p \leq 0.01$).

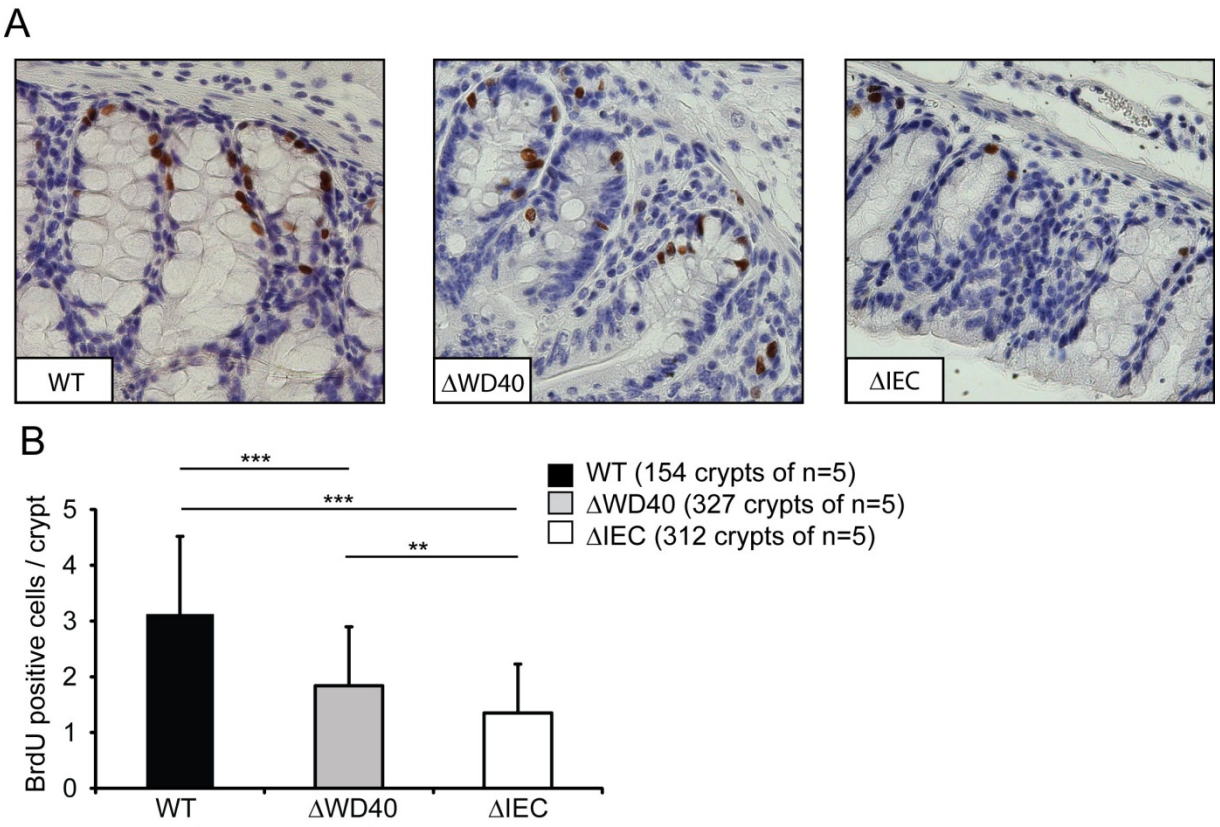

Figure 3-6: BrdU Immunohistochemistry in the colon of DSS treated WT, ΔWD40 and ΔIEC mice.
A) BrdU staining of colons from WT, ΔWD40 and ΔIEC mice challenged for 5d with 4%DSS. Magnification of 100. **B)** BrdU positive cells per crypt (154 crypts of 5 WT, 327 crypts of 5 ΔWD40 and 312 crypts of 5 ΔIEC mice). Values are shown as mean ± S.D; ** p≤0.01, *** p≤0.001.

For maintaining the intestinal barrier function an efficient regenerative response is required. A fast and severe progression of the disease is the result of impaired barrier integrity. Therefore, general membrane condition in the gut was measured by permeability for FITC-Dextran[114] in unchallenged mice. Four hours before sacrifice FITC-Dextran was administered by gastric gavage. Afterwards, blood samples were collected and serum was analyzed for presence of FITC-Dextran. As a positive control, Agr2 KO mice were used, which are characterized by impaired intestinal homeostasis with developing spontaneous colitis[115]. In unchallenged WT, ΔWD40 and ΔIEC mice, no difference in permeability could be detected (Figure 3-7). These results indicate that no general barrier impairment exists in the more disease susceptible ΔIEC mice.

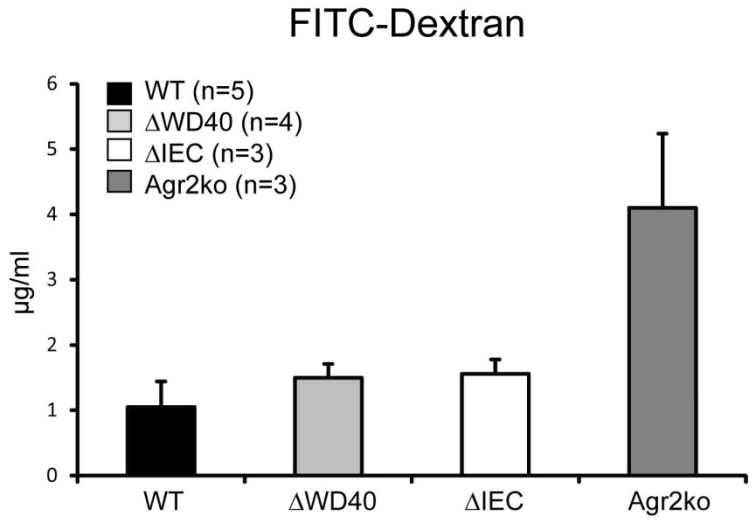

Figure 3-7: Intestinal permeability of WT, ΔWD40 and ΔIEC mice.
Plasma FITC-dextran concentrations in WT (n=5), ΔWD40 (n=4), ΔIEC (n=4) and agr2ko (n=3) mice 4h after FITC-dextran administration; values are shown as means ± S.D.

3.2 Influence of ATG16L1 truncation or deletion on autophagy

Afterwards, it was investigated whether primary bone marrow-derived macrophages (BMDMs) or intestinal epithelial cells (IECs) of the three genotypes show different autophagic activity. As a reliable marker of autophagosomes, LC3, a mammalian homolog of yeast Atg8, was used to determine the autophagic activity. The PE-conjugated form localizes both on the isolation membrane and the autophagosome membrane[116,117]. The unconjugated (LC3-I) and conjugated forms (LC3-II) of LC3 can be separated by SDS-PAGE. Because the amount of LC3-II correlates with the number of autophagosomes, the conversion of LC3 can be used to monitor autophagic activity[116]. Untreated cells were applied to display the basal level of autophagy, whereas the induced turnover could be analyzed by treating cells with either Rapamycin (50 µg/ml; 20 min.) or Rapamycin in combination with Bafilomycin (100 nM; 20 min.). Rapamycin, the inhibitor of mTOR, induces autophagy[118]. In this experimental setup it was used to increase the amount of LC3-II to measure the induced autophagic activity. But as half-life of LC3-II is short because autophagosomes are transient structures, LC3-II represents the autophagic activity at the moment in time[119]. Hence, Bafilomycin, a specific inhibitor of the vacuolar type H(+)-ATPase (V-ATPase) in cells[120] and therefore an inhibitor of the lysosomal degradation, was used. It blocks the autophagosome degradation and allows an assessment of the induced turnover. Bone marrow derived macrophages of ΔIEC mice were used as control, as they are not affected by the conditional knockout.

In 2009 Fujita et al. described that the deletion of the ATG16L1 WD repeat domain deletion has little impact on canonical autophagy[79]. In contrast, this work indicates that the truncation of the ATG16L1 WD repeat domain leads to lower LC3 expression levels and reduced LC3-II conversion in basal autophagy (exemplarily shown on Figure 3-8 A and B). As expected, BMDMs of ΔIEC mice did not show any difference compared to the WT. The fold induction of the amount of LC3-II to LC3-I depicts more detailed the autophagic activity (see Figure 3-8 C and D). The results show no significance, but clear tendency. Thus it becomes apparent that in comparison of the WT (11.68 fold induction) to the ΔWD40 mice (7.44 fold induction) the basal autophagic activity was reduced about 46 %. Stimulation with Rapamycin led to an induced autophagic activity of about 32.29 fold induction in WT and 11.38 in ΔWD40 mice. This is a reduction of about 65 % in ΔWD40 mice. As lower LC3-II level might follow from high lysosomal activity, the stimulation of Bafilomycin in combination with Rapamycin gives information about this possibility. Monitoring the induced turnover via inhibiting the lysosomal degradation caused autophagic activity of 41.38 fold induction in WT and 19.41 in ΔWD40 mice with a reduction of about 53 %. Again, no difference was observed by comparing autophagic activity of WT and ΔIEC mice.
These results indicate that the ΔWD40 mice have a lower autophagic activity compared to the WT mice.

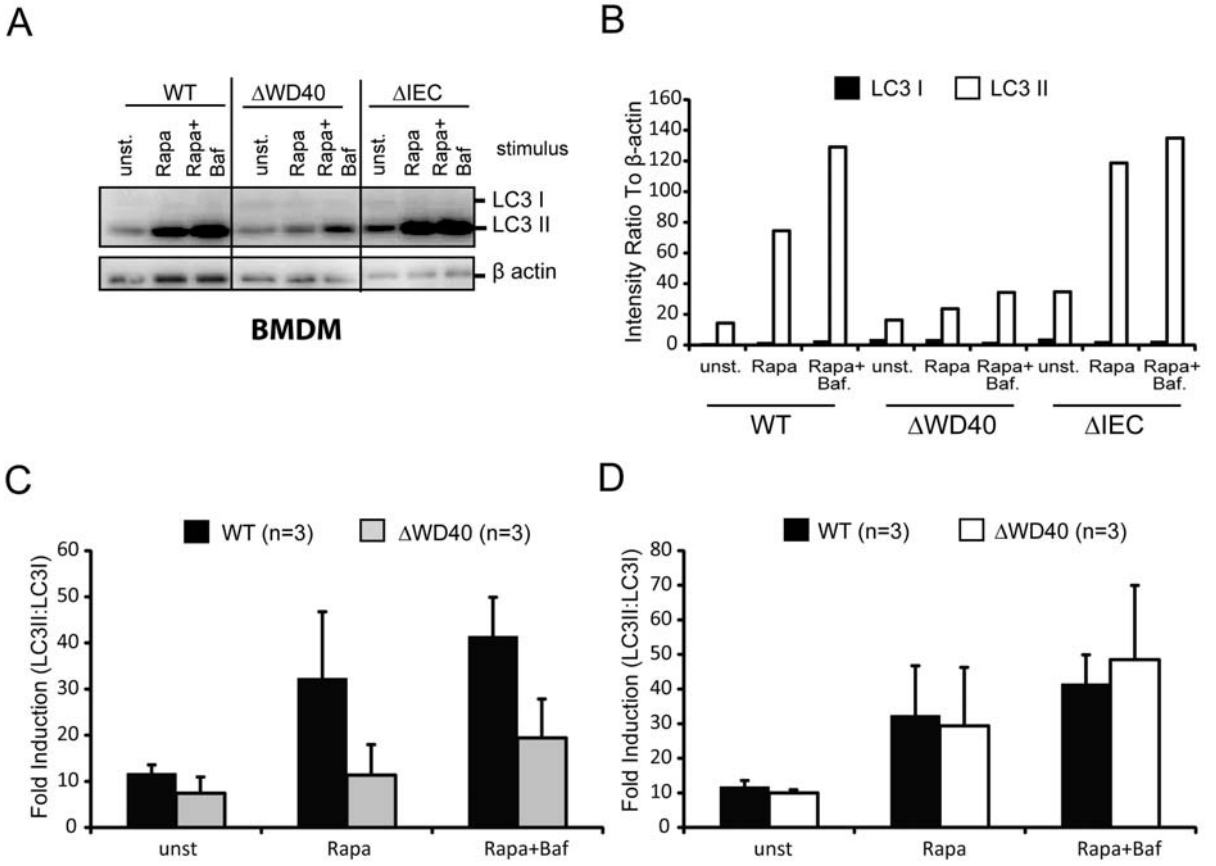

Figure 3-8: LC3 expression in bone marrow derived macrophages.
A) Bonemarrow derived macrophages (BMDMs) were stimulated with Rapamycin (50µg/ml for 20minutes) or with Rapamycin and Bafilomycin (100nM for 20minutes) or were left untreated. Protein extracts were separated by SDS-PAGE and immunoblotted against LC3 and β-actin; representative image. **B)** Detected bands for LC3-I and LC3-II were densitometrically analyzed by ImageJ and related to β-actin; representative result of 3 independet experiments. **C)** Fold induction was assessed by determing the ratio between LC3-II and LC3-I; WT and ΔWD40 or **D)** ΔIEC mice (values are shown as means ± S.D; n=3).

To further monitor the autophagic activity of cells with either truncated or deleted ATG16L1, the above described experiments were repeated in intestinal epithelial cells (IEC). The results reflect the above findings for ΔWD40 cells regarding reduced autophagic activity. As depicted exemplarily in Figure 3-9 A and B there is a distinct reduction of LC3-II amount and autophagic activity in ΔWD40 intestinal epithelial cells. The assessment of the fold induction of LC3-II to LC3-I could strengthen this result by displaying strong significant decrease of LC3 conversion in all three parameters: the basal autophagy was reduced about of 44 % from WT to ΔWD40 mice (unst. $p \leq 0.001$), the Rapamycin induced autophagic activity was reduced about 52 % (Rapa $p \leq 0.01$) and the accumulation of LC3-II by stimulation with both Rapamycin and Bafilomycin was reduced about 48 % (Rapa+Baf $p \leq 0.01$). As illustrated in Figure 3-9 A and B the basal autophagy was completely inhibited in

ATG16L1 deficient IECs, as no LC3-II conversion was observed. Even stimulation with the mTor inhibitor Rapamycin did not return this dysfunction.

Again, the absence of the WD repeat domain led to reduced autophagic activity in IECs as already shown for BMDMs.

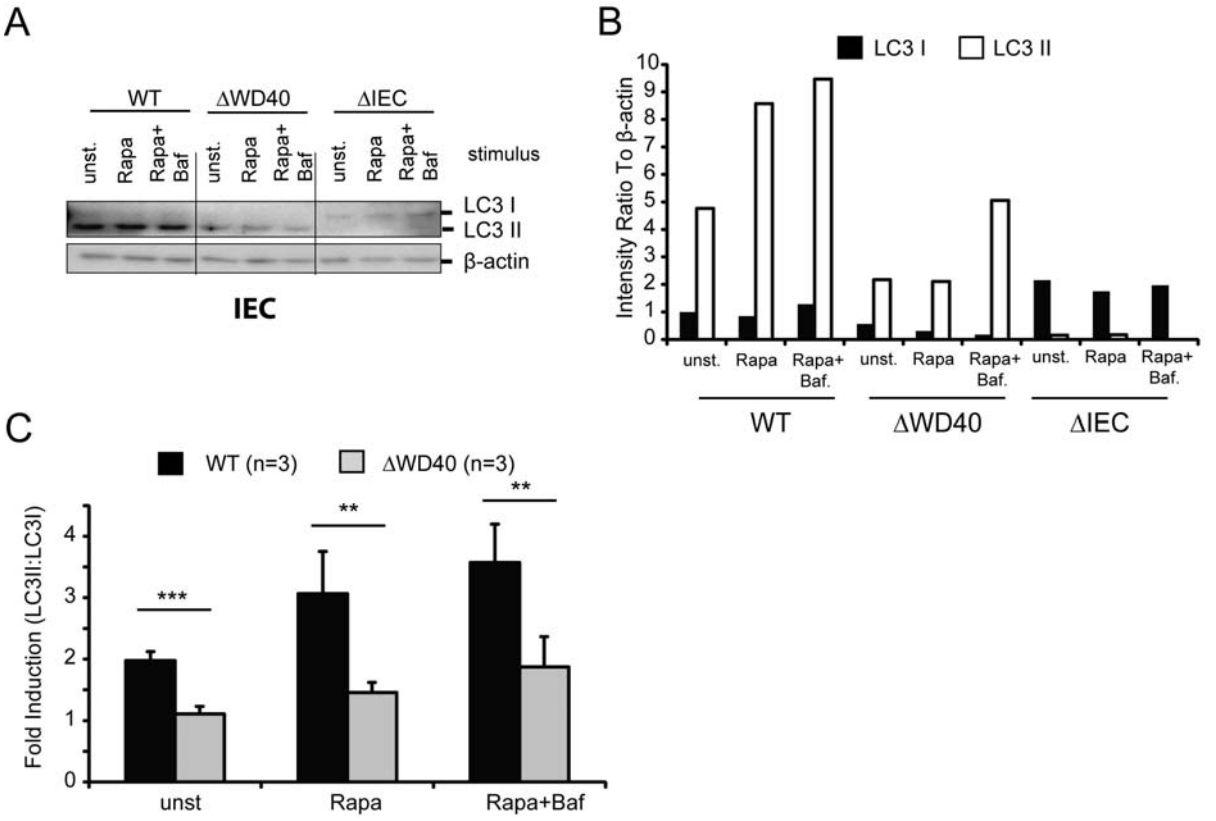

Figure 3-9: LC3 expression in intestinal epithelial cells.
A) Intestinal epithelial cells (IECs) were stimulated with Rapamycin (50 µg/ml for 20 minutes) or with Rapamycin and Bafilomycin (100 nM for 20 minutes) or were left untreated. Protein extracts were separated by SDS-PAGE and immunoblotted against LC3 and β-actin; representative image. **B)** Detected bands for LC3-I and LC3-II were densitometrically analyzed by ImageJ and related to β-actin; representative experiment. **C)** Fold induction was assessed by determing the ratio between LC3-II and LC3-I; WT and ΔWD40 (values are shown as means ± S.D; n=3; **p≤0,01; ***p≤0,001).

3.3 Evident morphological alterations in Paneth cells in ΔWD40 and ΔIEC mice

In intestinal epithelial cells the truncation of the WD40 repeat domain and the knockout of *Atg16l1* led to either less LC3 expression or even suppression of LC3 conversion. Furthermore the colitis experiments developed that ΔIEC mice are high susceptible to DSS-induced colitis. As Cadwell et al. hypothesized that Paneth cells might have unique sensitivity to autophagy gene disruption[58], this led us focus on the Paneth cells. They are described as critically important intestinal innate immune cells.

More precisely Paneth cells are secretory epithelial cells of the small intestine. They are thought to play a role in the control of intestinal microbiota via secretion of granule contents including antimicrobial peptides and lysozyme[121]. Cadwell et al.[58] discovered that mice, expressing ATG16L1 at 30 % of the wildtype level (hypomorphic mice), exhibited striking abnormalities in the granule exocytosis pathway of Paneth cells. The following investigations are based on their experimental setup but in contrast, for the present study mice were used with a total deletion of *Atg16l1* in the intestinal epithelial cells (ΔIEC) and mice with a general deletion of the ATG16L1 WD40 domain (ΔWD40). For quantifying abnormalities in secretory granules lysozyme staining was performed in sections of the Jejunum. Lysozyme is normally packed in the secretory granules of Paneth cells [121]. Afterwards, based on Cadwells work Paneth cells were divided into four patterns of lysozyme positive granules (see Figure 3-10 A): normal (D_0), disordered (D_1), depleted (D_2) and diffuse (D_3)[58]. As illustrated in Figure 3-10 B and C the WT Paneth cells show normal patterns of lysozyme expression (70 % of total Paneth cells), whereas the ΔIEC Paneth cells show a significant large population ($p \leq 0.01$ compared to WT; $p \leq 0.05$ compared to ΔWD40) of cells with diffuse lysozyme staining (64 % of total Paneth cells). Interestingly, the ΔWD40 Paneth cells displayed different pattern. They exhibited a striking population of cells with significantly disordered lysozyme positive granules (52 % of total Paneth cells; $p \leq 0.01$ compared to WT; $p \leq 0.05$ compared to ΔIEC).

These results imply that due to the deletion of the WD40 domain a regular formation of granules might not be possible in Paneth cells leading to a disordered granula allocation. Furthermore, the total lack of ATG16L1 leads to a totally disabled lysozyme packaging to the granules. A diffuse lysozyme allocation is the result.

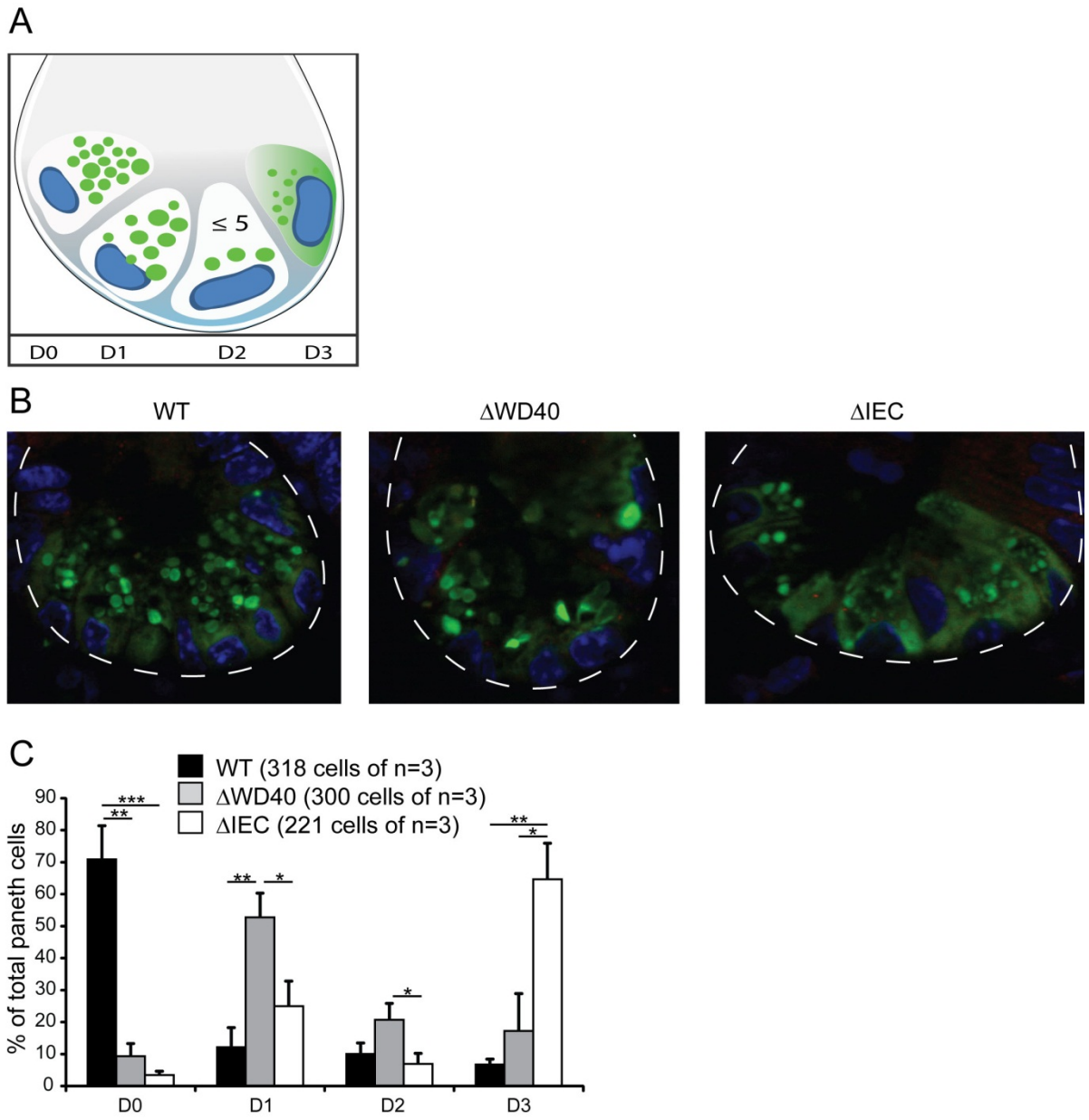

Figure 3-10: Lysozyme allocation in Paneth cells.
A) Lysozyme expression and allocation patterns are sorted to the following four classes (lysozyme represented in green, white represents areas that exclude lysozyme): normal (D0), disordered (D1), depleted (D2), and diffuse (D3) as described by Cadwell et al.[58] **B)** Representative images of indirect immunofluorescence of jejunum sections stained for lysozyme (green) in WT, ΔWD40 and ΔIEC mouse crypts (dotted line denotes crypt unit), magnification of 600. **C)** Number of Paneth cells of WT, ΔWD40 and ΔIEC mice displaying each pattern of lysozyme expression (n=318 cells from 3 WT mice, 300 cells from 3 ΔWD40 mice and 221 cells from 3 ΔIEC mice; values are shown as means ± S.D; * p≤0,05; ** p≤0,01; *** p≤0,001.

Afterwards the characteristics of lysozyme (*Lyz1*) mRNA expression in IECs and BMDMs were investigated by RT-PCR analysis as shown exemplarily on Figure 3-11 A. *GAP3H* was used as a loading control. Figure 3-11 B illustrates quite clearly the significant down regulation of *Lyz1* in ΔWD40 and ΔIEC cells on basal level in unstimulated IECs (p≤0.05 in ΔWD40 and p≤0.001 in ΔIEC compared to WT). By

contrast, the basal *Lyz1* mRNA expression level in the BMDMs of ΔWD40 mice was significantly higher than in BMDMs of WT or (as control) ΔIEC mice (p≤0.01 or p≤0.05) (Figure 3-11 C).

To investigate the influence of different stimuli on the expression of *Lyz1*, the IECs were treated with Rapamycin (50 µg/ml; 20 min.), MDP-LD (100 µg/ml; 2 h), *Salmonella typh.* (MOI 100; 1 h) and Tunicamycin (5 µg/ml; 4 h). Afterwards the mRNA expression was evaluated semi quantitatively via RT-PCR and following densitometry of the gel-bands. It appeared that in contrast to the WT IECs the *Lyz1* expression was not affected in ΔWD40 and ΔIEC cells by one of the stimuli.

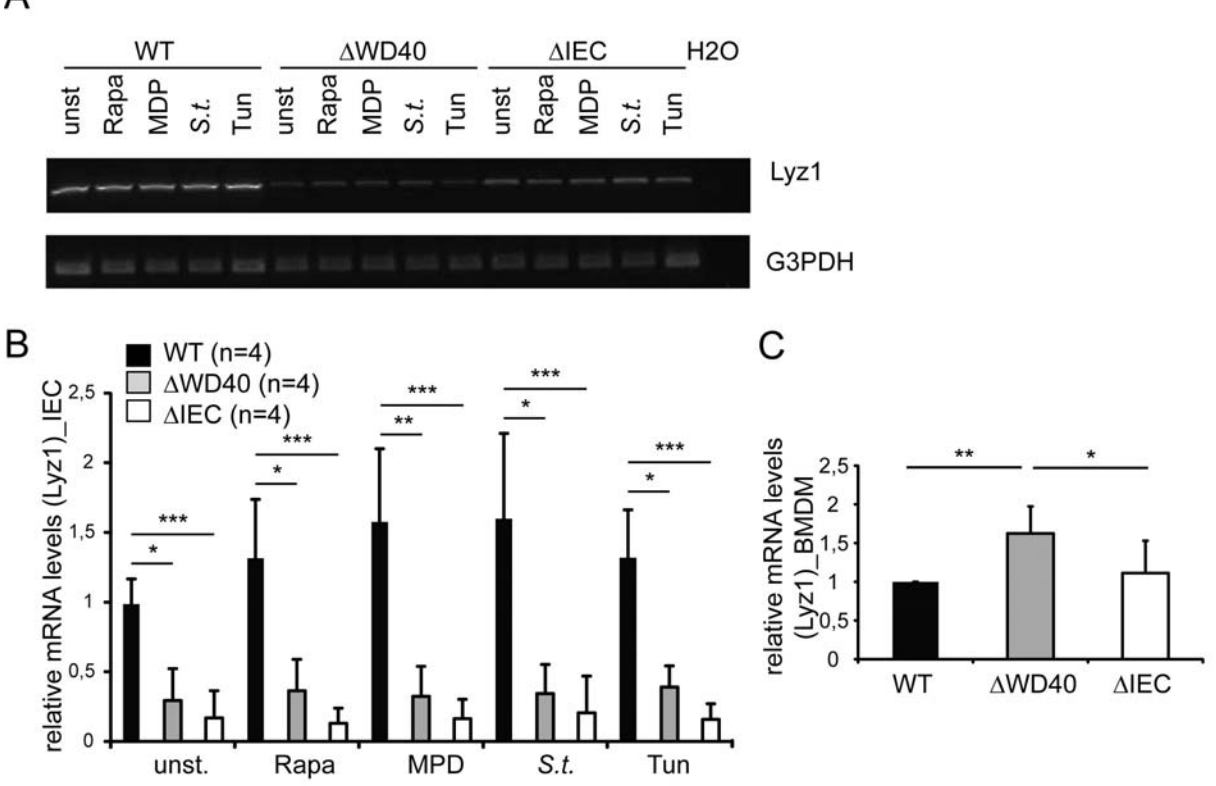

Figure 3-11: *Lyz1* mRNA expression in IECs and BMDMs.
A) IECs of WT, ΔWD40 and ΔIEC mice were stimulated with Rapamycin (50µg/ml, 20min.), MDP-LD (100µg/ml, 2h), *Salmonella typh.* (MOI100, 1h), Tunicamycin (5µg/ml, 4h) or left untreated. mRNA expression of *Lyz1* and *G3PDH* was performed by RT-PCR and analyzed by agarose gel electrophoresis (representative image). **B)** Detected bands for *Lyz1* were densitometrically analyzed by ImageJ and first related to *G3PDH* and afterwards to WT unstimulated. **C)** Relative basal mRNA expression levels for *Lyz1* were quantified by RT-PCR and following densitometrically analysis in BMDMs of WT, ΔWD40 and ΔIEC mice; values as means of n=4 independent experiments ± S.D; n=4; * p≤0.05; ** p≤0.01; *** p≤0.001.

To further monitor the connection between ATG16L1 truncation or deletion and vesicle export, the number of vesicles was counted in Paneth cells of Jejunum sections stained with toluidine blue (see Figure 3-12 A for exemplary images). As diagrammed in Figure 3-12 B, two classifications of vesicle numbers have been

compared (less than 10 and more than 10 vesicle per Paneth cell). There is a significant higher amount of 'less than 10' vesicles per Paneth cell in ΔWD40 (p≤0.001) or ΔIEC mice (p≤0.01) compared to the WT. Furthermore a significant difference between ΔWD40 and ΔIEC mice was detected as well, as the ΔWD40 genotype represents more cells in the ≤10 class (p≤0.05). The distribution of vesicle numbers in the classification of 'more than 10' showed that WT mice were most frequently represented here, whereas the Paneth cells of the ΔWD40 (p≤0.001) and the ΔIEC mice (p≤0.05) displayed significant lower ratio in this class. Again, a significant difference between ΔWD40 and ΔIEC mice was monitored with higher amount of ΔIEC cells in this category (p≤0.05).

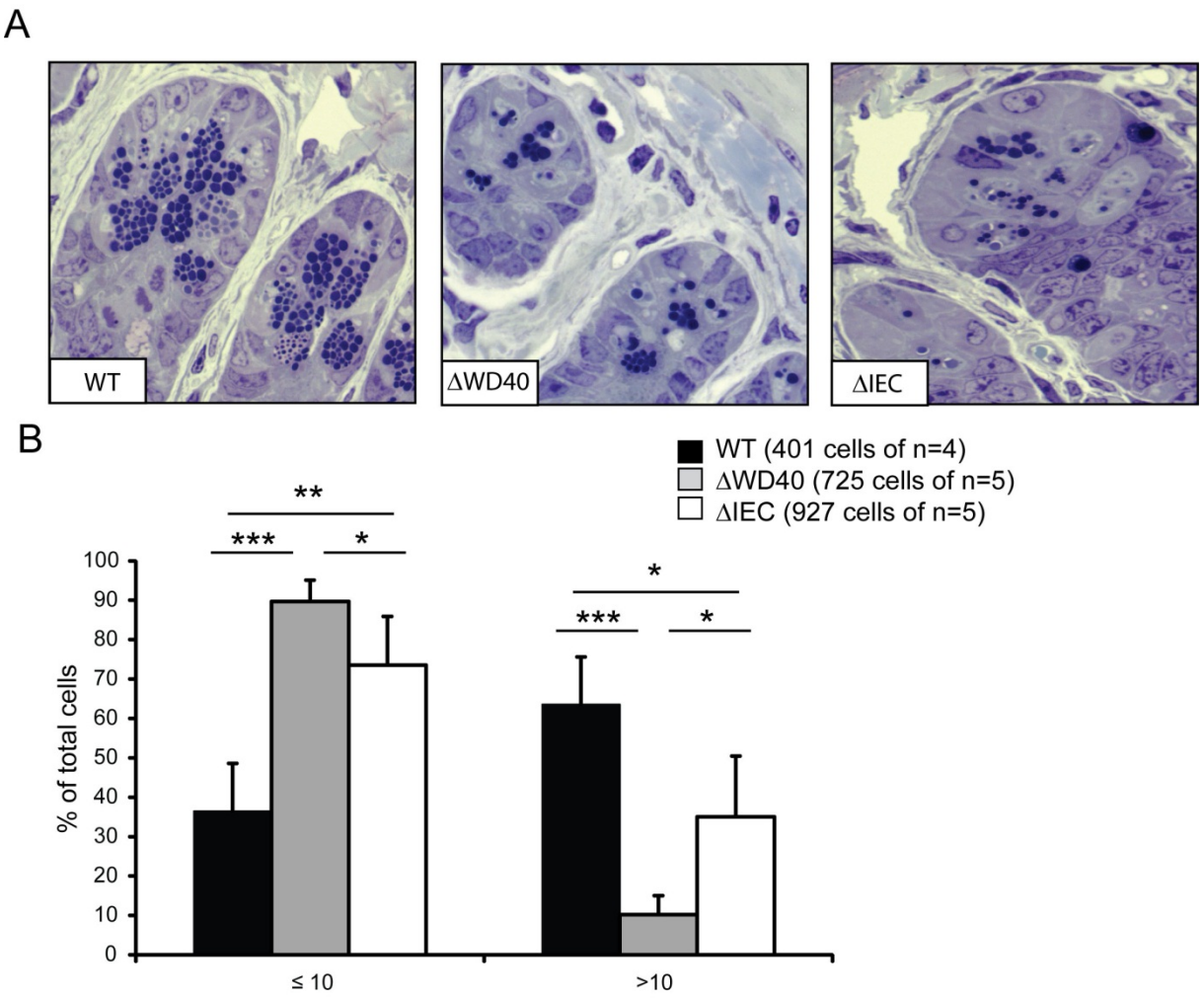

Figure 3-12: Number of vesicles in Paneth cells.
A) Representative images of jejunum sections stained with Toluidine blue in WT, ΔWD40 and ΔIEC mouse crypts, magnification of 600**. B)** Vesicles were counted and divided into two groups: ≤10 or >10 vesicles per Paneth cell. (n=401 cells from 4 WT mice, 725 cells from 5 ΔWD40 mice and 927 cells from 5 ΔIEC mice); values are shown as means ± S.D; * p≤0.05; ** p≤0.01; *** p≤0.001.

To determine if the above investigated abnormalities were limited to Paneth cells as already described by Cadwell et al.[58], the numbers of goblet cells per crypt on the one hand and on the other hand the numbers of Paneth cells per crypt were counted. The number of Goblet cells was determined via Periodic acid-Schiff (PAS) staining. As depicted in Figure 3-13 A and B, the number of goblet cells differed in neither of the three mouse genotypes. In contrast the difference in numbers of Paneth cells, which was determined via Lysozyme staining, was significantly distinct in all three mouse strains (see Figure 3-13 C). The WT mice exhibited the highest number of Paneth cells with about 6 per crypt. Whereas the ΔWD40 mice showed 38% less Paneth cells with about 4 per crypt (p≤0.001) and the ΔIEC mice 71% less with about 2 per crypt (p≤0.001) in comparison to WT mice. The decrease in number of cells from ΔWD40 to ΔIEC is highly significant as well (p≤0.001).

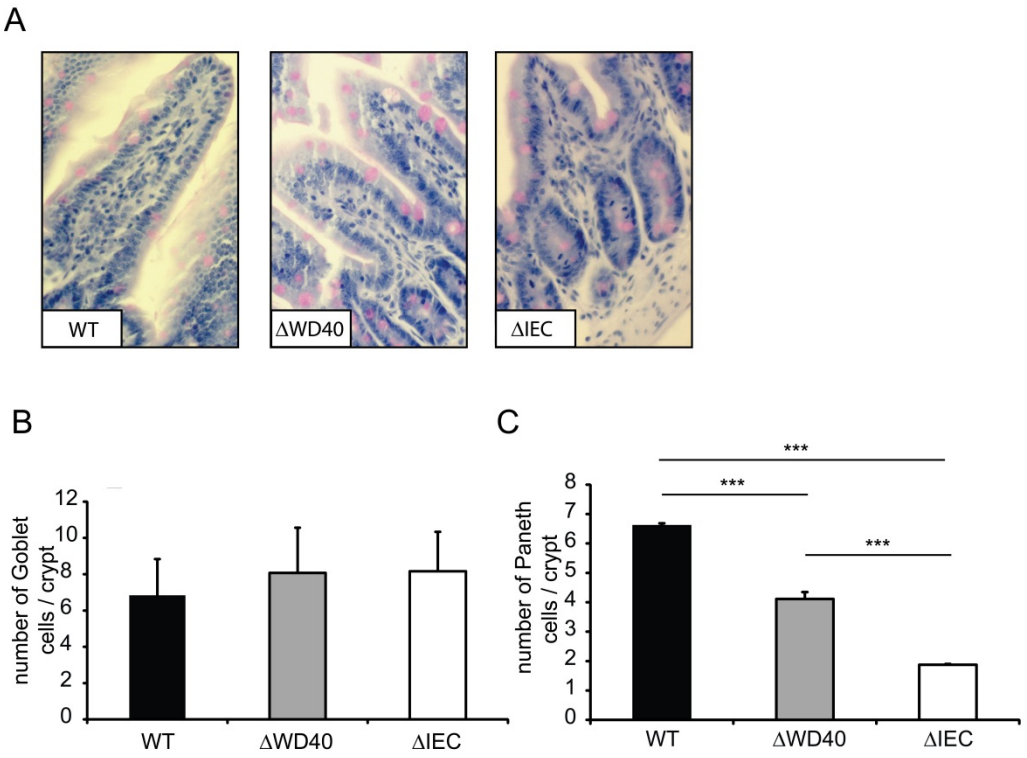

Figure 3-13: Number of Goblet cells and Paneth cells per crypt.
A) Representative PAS-staining images for Goblet cells of jejunum sections in WT, ΔWD40 and ΔIEC mouse crypts, magnification of 200**. B)** Goblet cells were counted and normalized to crypt length (n=40 crypts from 3 WT mice, 46 crypts from 3 ΔWD40 mice and 44 crypts from 5 ΔIEC mice) **C)** Lysozyme stained Paneth cells (see Figure 3-10) were counted (n=181 cells from 3 WT mice, 157 cells from 3 ΔWD40 mice, and 225 cells from ΔIEC mice); values are shown as means ± S.D; ***p≤0,001.

Electron microscopy of Jejunum sections of three animals per genotype was performed to clarify more detailed the phenotypically differences within the Paneth cells of the genetically altered mouse strains. As illustrated exemplarily in Figure 3-14 ΔIEC mice exhibited a comparable phenotype to the hypomorphic mice shown by

Cadwell et al[58]. Highlighted in red, large areas of structurally altered cellular components were detected in ΔWD40 mice and more evident in ΔIEC mice, compared to the WT. Cadwell et al. discussed these areas as accumulated cytoplasmic vesicle[58], but another explanation might be a dilated endoplasmatic reticulum.

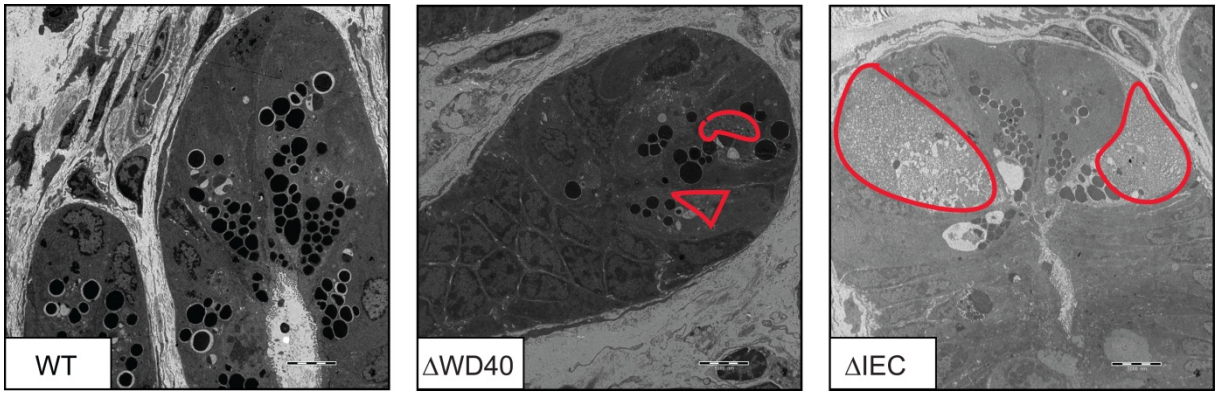

Figure 3-14: Electron microscopy of Jejunum sections.
EM of Jejunum sections of WT, ΔWD40 and ΔIEC crypts (red lines accent the assumed area of dilated endoplasmatic reticulum).

Paneth cell secretory granules are loaded with diverse host defense proteins and peptides, including the above described lysozyme, but also α-defensins[121,122]. Since defensins were first identified as antimicrobial peptides, it is suggested that defensins interact with host immune cells, thereby playing important roles in both innate and adaptive immune responses against bacterial infection[123,124]. Thus it was interesting to investigate the expression of α-defensins/cryptdins in intestinal epithelial cells. mRNA expression of *Defa3* and *Defa5* was analyzed by RT-PCR and densitometrically evaluated. Figure 3-15 A and B illustrate quite clearly the significant down regulation of basal *Defa3* and *Defa5* expression in ΔWD40 and ΔIEC mice ($p \leq 0.01$ or $p \leq 0.05$) compared to WT mice. *GAP3H* was used as loading control.
Consequently a deficiency of ATG16L1 not only influences the Lysozyme expression in intestinal epithelial cells, it also influences the expression of α-defensins on mRNA level.

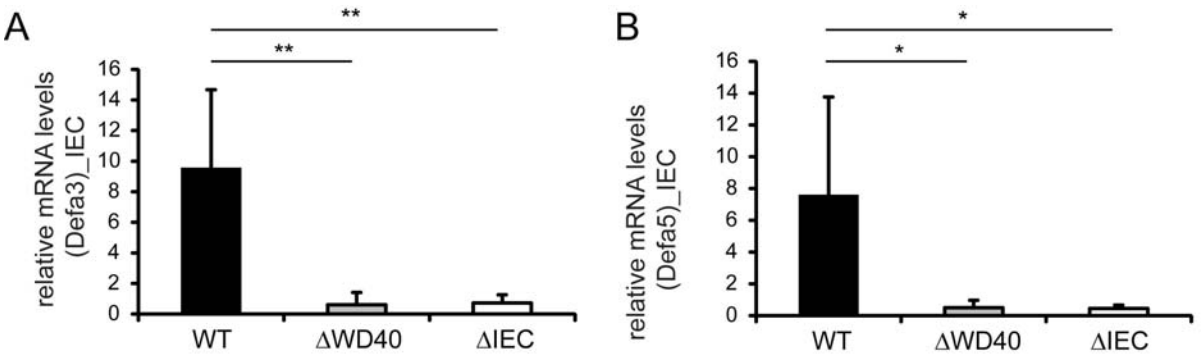

Figure 3-15: Defa3 and Defa5 mRNA expression in IECs.
A) After RT-PCR and agarose gel electrophoresis the detected bands for *Defa3* or **B)** *Defa5* were densitometrically analyzed by ImageJ and related to *G3PDH*; values are shown as means ± S.D; (Defa3 n=5; Defa5 n=4); * p≤0.05; ** p≤0.01.

Further, the relation between lysozyme expression and LC3 expression in Jejunum sections of all three genotypes was investigated via LC3 and lysozyme co-staining of 3 animals per genotype. As illustrated exemplarily in Figure 3-16, the LC3 expression decreased from WT to ΔIEC mice. The WT sections showed clear LC3 dots, whereas in the ΔIEC sections diffuse LC3 staining could be detected. Interestingly, the ΔWD40 sections showed both, clear LC3 dots and diffuse LC3 expression, as well (i-iii).

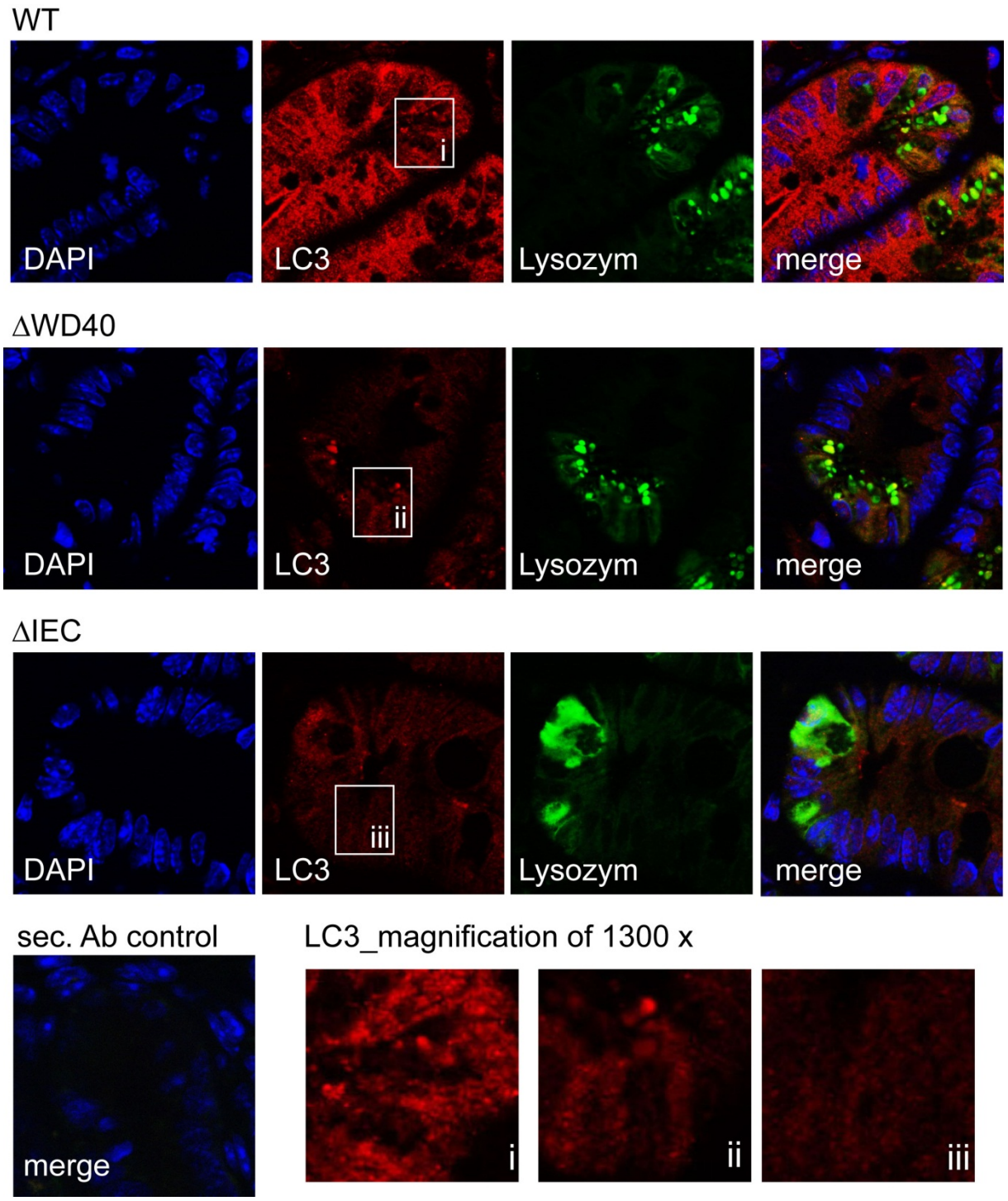

Figure 3-16: LC3 and lysozyme staining in Jejunum tissue sections of WT, ΔWD40 and ΔIEC mice.
Jejunum tissue sections of WT, ΔWD40 and ΔIEC mice stained with anti-LC3 (red) and anti-lysozyme (green) antibodies; magnification of 600 x; representative images of n=3 animals per genotype. i, ii and iii show sections of the LC3 staining in magnification of 1300 x to visualize LC3-dots. Counterstaining of nuclei with DAPI appears in blue. Colocalization appears in yellow. Representative images of n=3 per genotype. Optical investigation was performed in n=150 cells from 3 WT mice, n=170 cells from 3 ΔWD40 mice and n=88 cells from 3 ΔIEC mice.

Interestingly, the LC3 signals in Paneth cells of WT and ΔWD40 mice overlaid with some of the lysozyme filled vesicles (see Figure 3-17). High magnification (of 3000 x) showed that the colocalization appeared congruent within the lysozyme filled vesicles for both genotypes. In contrast, no comparable co-staining of LC3 and lysozyme could be observed in the ΔIEC cells.

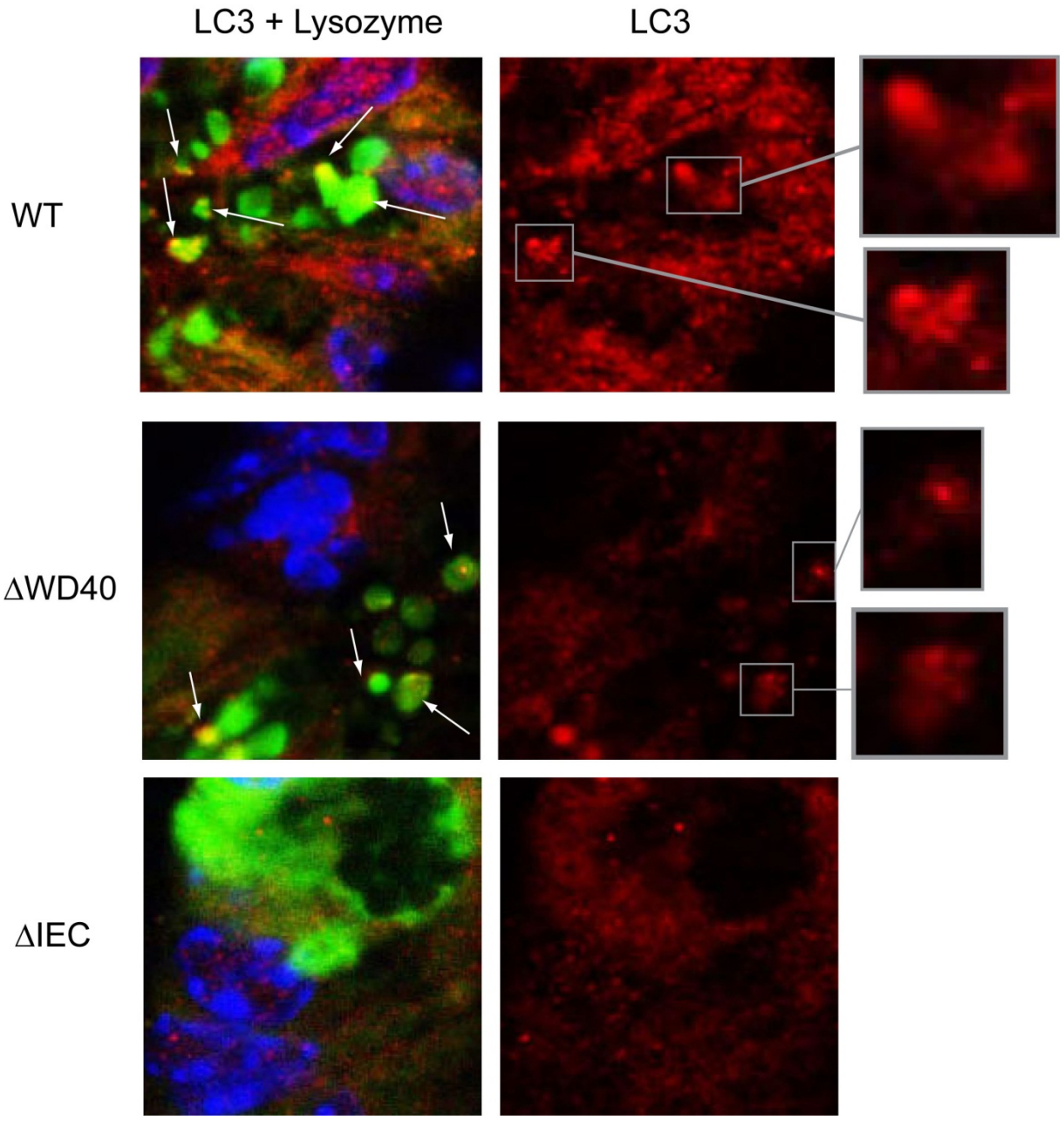

Figure 3-17: Colocalization of LC3 and lysozyme expression in Jejunum tissue sections of WT, ΔWD40 and ΔIEC mice.
Partial excerpt of Figure 3-16: magnification of 1300 x LC3 + lysozyme merged and LC3 single stained images of WT, ΔWD40 and ΔIEC mice. Arrows indicate colocalization of LC3 and lysozyme expression within a cell (yellow).Small boxes indicate details of LC3 images in magnification of 3000 x. Representative images of n=3 per genotype. Optical investigation was performed in n=150 cells from 3 WT mice, n=170 cells from 3 ΔWD40 mice and n=88 cells from 3 ΔIEC mice.

Afterwards, the correlation between lysozyme expression and ATG16L1 expression was analyzed, as well, in Jejunum sections of 3 animals per genotype via ATG16L1 and lysozyme co-staining. As depicted in Figure 3-18 the ATG16L1 staining showed remarkable colocalization with lysozyme positive granules of WT and ΔWD40 mice. Expectedly, no ATG16L1 protein expression was observed in ΔIEC mice apart from unspecific signals.

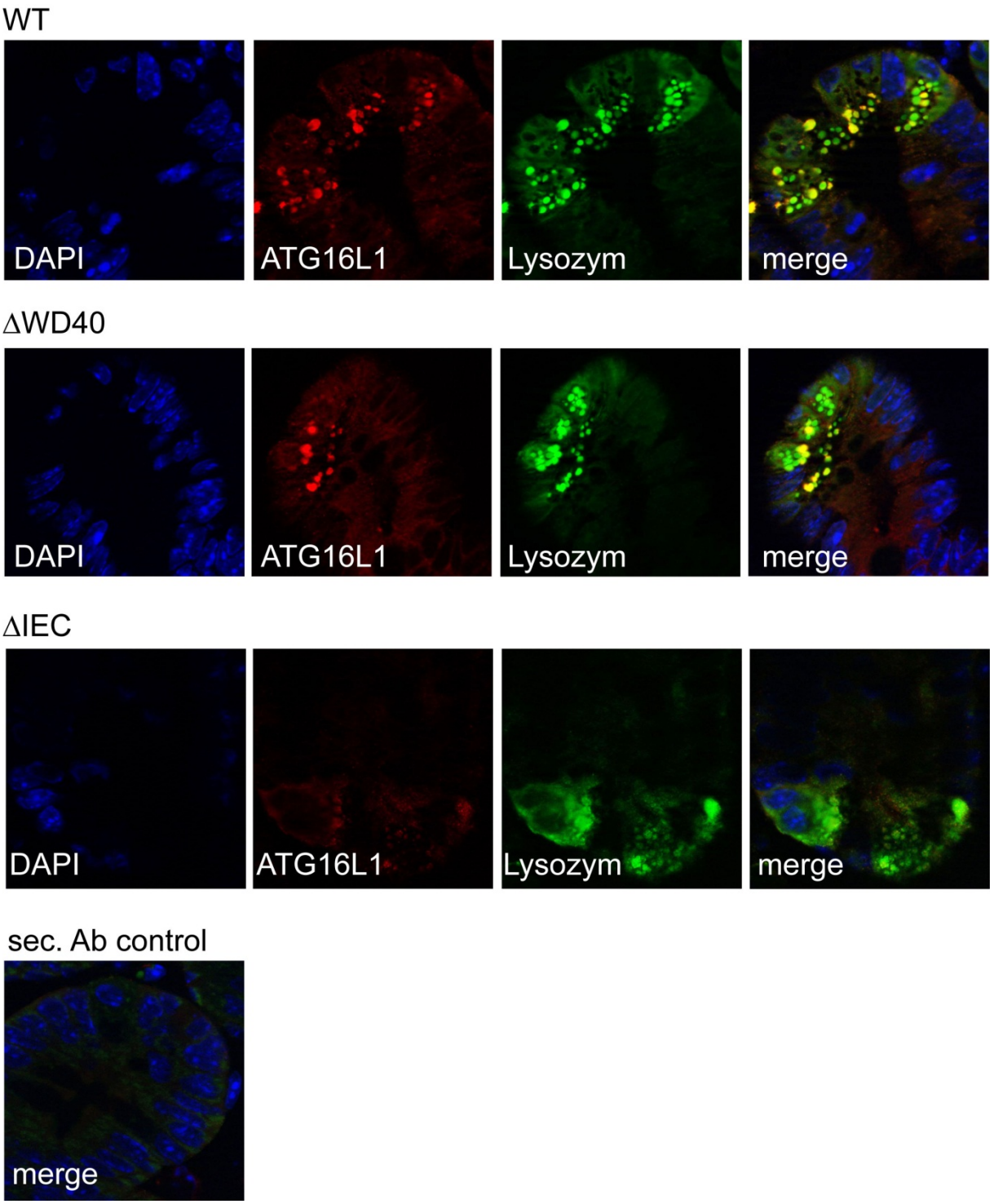

Figure 3-18: ATG16L1 and lysozyme staining in Jejunum tissue sections of WT, ΔWD40 and ΔIEC mice.
Jejunum tissue sections of WT, ΔWD40 and ΔIEC mice stained with anti-ATG16L1 (red) and anti-lysozyme (green) antibodies to visualize potential colocalization. Counterstaining of nuclei with DAPI appears in blue. Colocalization appears in yellow; magnification of 600 x. Representative images of n=3 per genotype. Optical investigation was performed in n=117 cells from 3 WT mice, n=79 cells from 3 ΔWD40 mice and n=41 cells from 3 ΔIEC mice.

More detailed, the colocalization could be illustrated in higher magnification of 1300 x (investigated in 3 animals per genotype). In WT mice nearly all lysozyme positive

vesicles exhibited ATG16L1 co-staining, whereas this seems to decrease in ΔWD40 mice (see Figure 3-19). High magnification of 3000 x showed that the ATG16L1 staining is congruent with the lysozyme filled vesicles. Again, ΔIEC cells showed no ATG16L1 staining apart from unspecific signals.

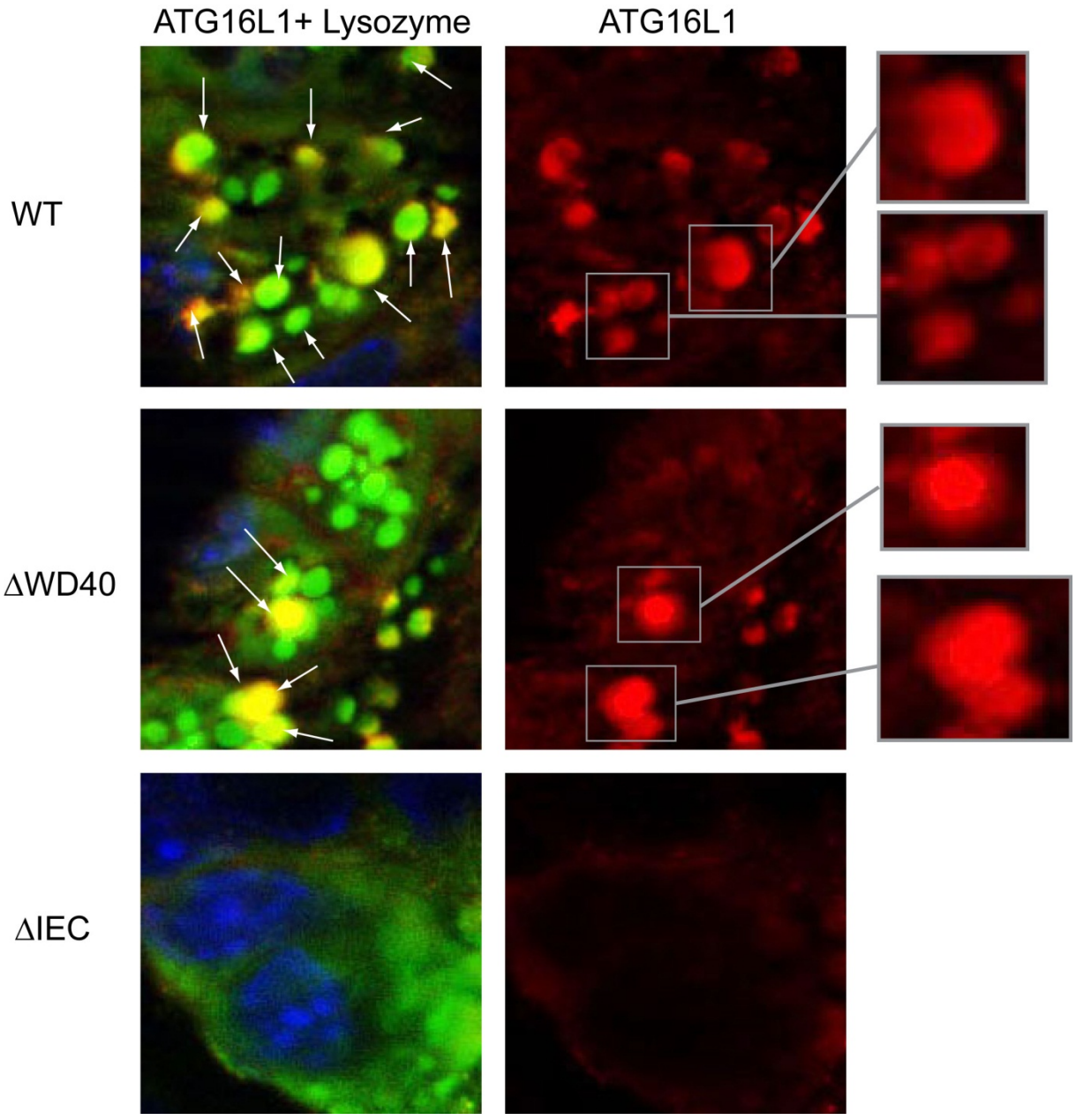

Figure 3-19: Colocalization of ATG16L1 and lysozyme expression in Jejunum tissue sections of WT, ΔWD40 and ΔIEC mice
Partial excerpt of Figure 3-18: magnification of 1300 x of ATG16L1 + lysozyme merged and ATG16L1 single stained images of WT, ΔWD40 and ΔIEC mice. Arrows that indicate colocalization (yellow) of ATG16L1 and lysozyme within a cell. Small boxes indicate details of ATG16L1 images in magnification of 2800 x. Representative images of n=3 per genotype. Optical investigation was performed in n=117 cells from 3 WT mice, n=79 cells from 3 ΔWD40 mice and n=41 cells from 3 ΔIEC mice.

In this study it could be shown by abnormal lysozyme expression patterns that the vesicle export might be constrained in case of ΔWD40 and especially ΔIEC mice. Hence, it was interesting to visualize a putative connection between the endoplasmic reticulum (ER) and the lysozyme allocation via anti-PDI antibody (Protein Disulphide Isomerase). The investigation was performed optical, using three animals per genotype. As the ER is involved in vesicle packaging and export, Paneth cells exhibit a unique morphology that is characterized by an extensive endoplasmic reticulum and Golgi network[125] as seen in Figure 3-20. It becomes apparent that in WT and ΔWD40 mice the lysozyme filled granules were separated from the ER. Whereas in Paneth cells of ΔIEC mice the total sources of lysozyme was inside the ER. Additionally, these pictures demonstrate clearly the decline of number of Paneth cells from WT, to ΔWD40 and to ΔIEC mice, that was already described in Figure 3-13, C.

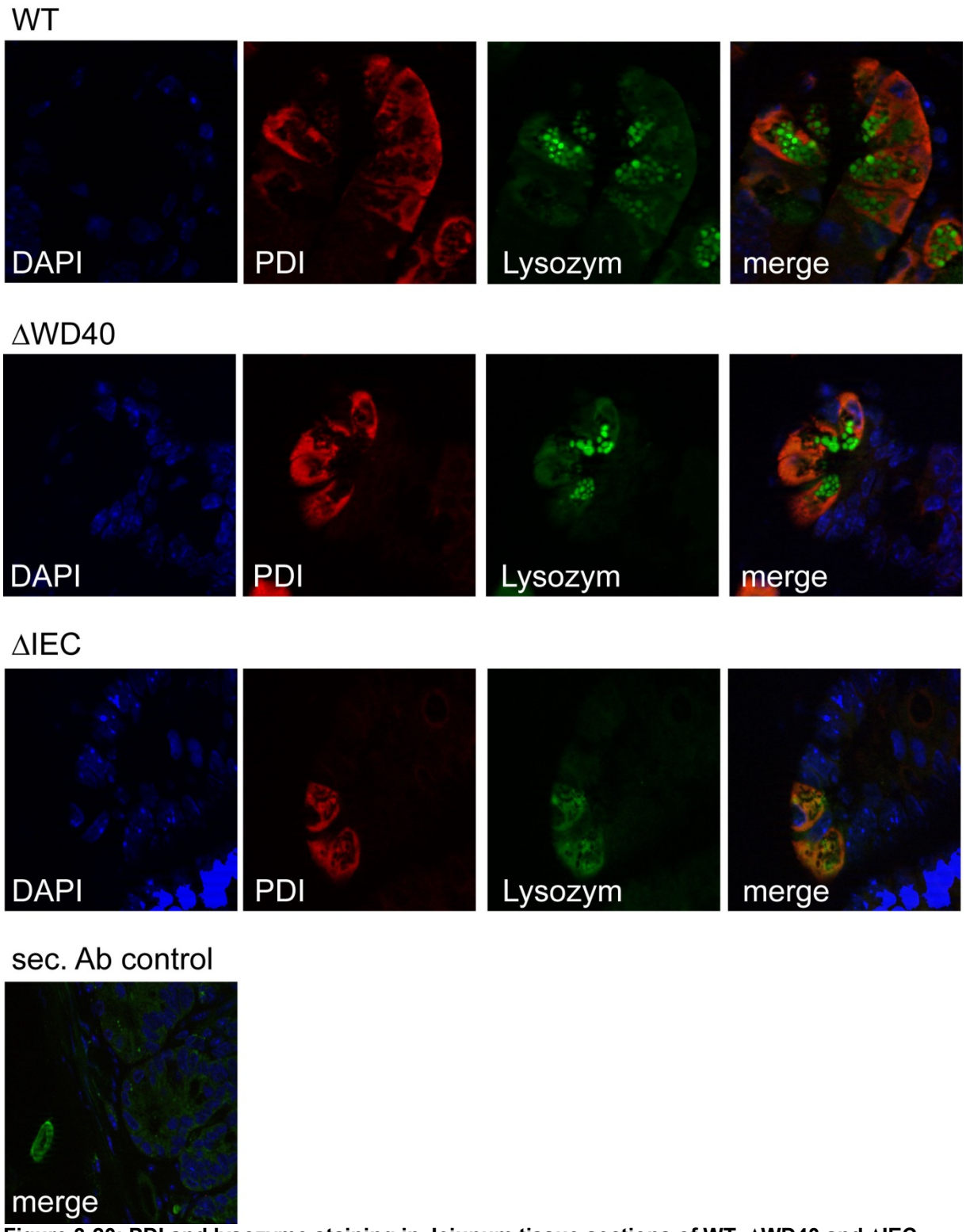

Figure 3-20: PDI and lysozyme staining in Jejunum tissue sections of WT, ΔWD40 and ΔIEC mice.

Jejunum tissue sections of WT, ΔWD40 and ΔIEC mice stained with anti-PDI (red) and anti-lysozyme (green) antibodies to visualize potential colocalization. Counterstaining of nuclei with DAPI appears in blue. Colocalization appears in yellow; magnification of 600x. Representative images of n=3 per genotype. Optical investigation was performed in n=166 cells from 3 WT mice, n=119 cells from 3 ΔWD40 mice and n=65 cells from 3 ΔIEC mice.

3.4 ER-stress in intestinal epithelial cells of ΔIEC and ΔWD40 mice

The results suggested that the observed abnormalities in Paneth cell morphology might be linked with the endoplasmic reticulum. It is known that the unfolded protein response (UPR) is connected closely to autophagy[30,126]. Thus I analyzed if the modification of ATG16L1 leads to higher susceptibility to ER stress in the ΔWD40 or ΔIEC mice.

ΔIEC as well as ΔWD40 and WT mice were treated with Tunicamycin (5 µg/ml for 4h), a commonly used ER stress inducer, by inhibiting the GlcNAc phosphotransferase (GPT), which catalyzes the transfer of N-actelyglucosamine-1-phosphate from UDP-N-acetylglucosamine to dolichol phosphate in the first step of glycoprotein synthesis[127,128], or were left untreated. Afterwards the transcripts of two specific ER-stress markers were examined by expression analysis: Heat Shock 70 kDa Protein 5 (*Hspa5*), also referred to as 78 kDa glucose-regulated protein (GRP78) and CCAAT/enhancer binding protein (C/EBP) homologous protein (*CHOP).* Figure 3-21 A illustrates exemplarily the significant increase of mRNA expression of *Hspa5* and *CHOP* in intestinal epithelial cells of both ΔWD40 and ΔIEC mice. Densitometric analysis showed that on basal level the expression of *Hspa5* and *CHOP* was significantly increased in ΔWD40 (*Hspa5*: $p \leq 0.05$; *CHOP*: $p \leq 0.01$) and ΔIEC mice (*Hspa5*: $p \leq 0.01$; *CHOP*: $p \leq 0.01$) compared to the WT mice. Stimulation with Tunicamycin induced a significant upregulation of *Hspa5* in WT mice ($p \leq 0.05$), but not in ΔWD40 or ΔIEC mice, whereas *CHOP* was significantly upregulated in both, WT ($p \leq 0.05$) and ΔWD40 mice ($p \leq 0.01$), but again not in ΔIEC mice after stimulation. In contrast, in BMDMs no difference between ΔWD40 and WT mice occurred. ΔIEC mice were used as a control and showed no difference to the WT mice. All genotypes show an upregulation of *Hspa5* and more evident of *CHOP* on basal level or after stimulation with Tunicamycin. The stimulation with other stimuli like MDP, *Salmonella typh.* or Rapamycin did not affect the expression of *Hspa5* or *CHOP* in both IECs or BMDMs (data of relative mRNA expression not shown).

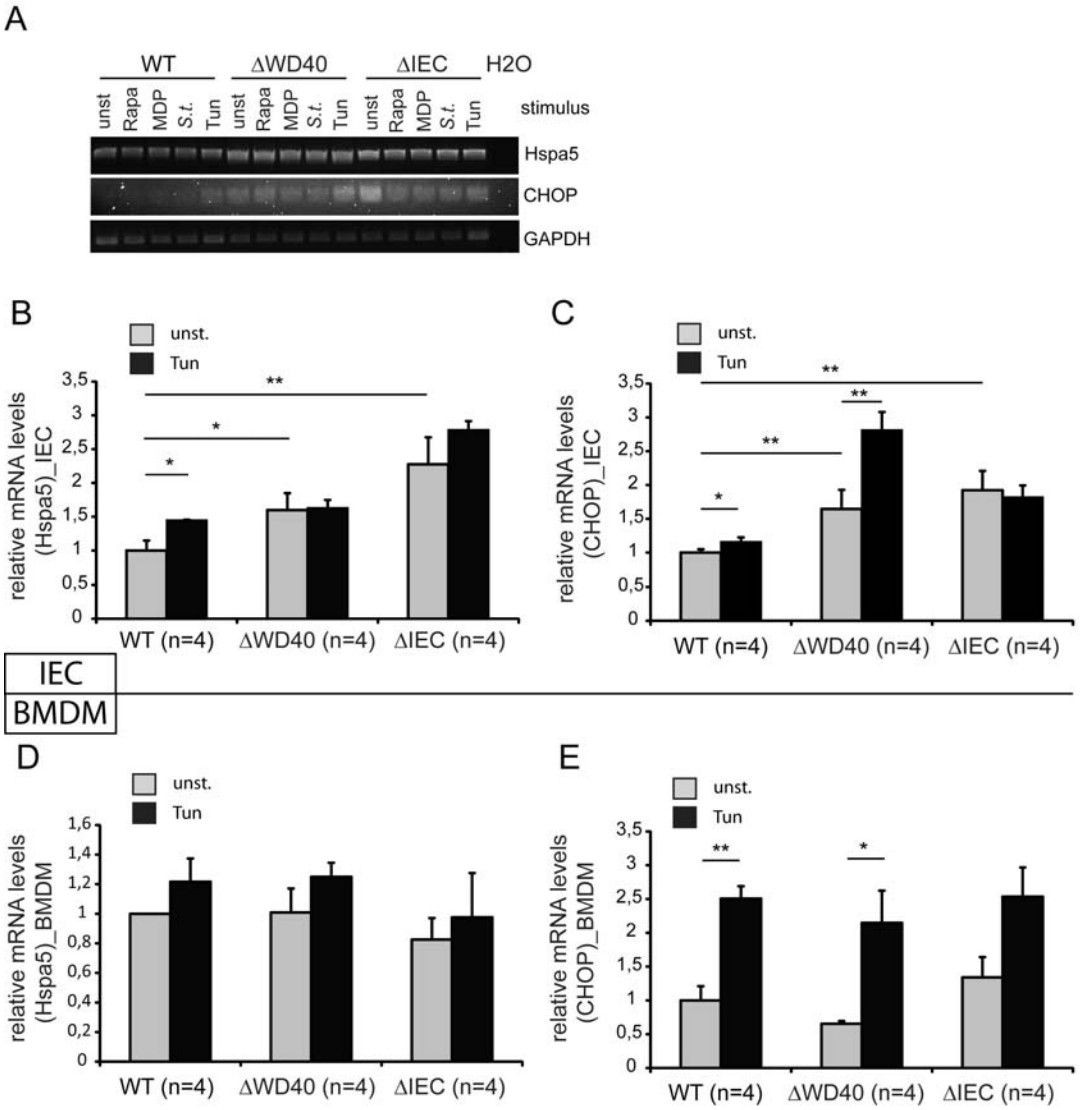

Figure 3-21: Hspa5 and CHOP mRNA expression in IECs and BMDMs.
A) IECs of WT, ΔWD40 and ΔIEC mice were stimulated with Rapamycin (50µg/ml, 20Min), MDP-LD (100µg/ml, 2h), *Salmonella typh.* (MOI100, 1h), Tunicamycin (5µg/ml 4h) or left untreated. mRNA expression of Hspa5, CHOP and GAPDH was performed by RT-PCR and analyzed by agarose gel electrophoresis (representative image). **B)** Detected bands for Hspa5 and **(C)** CHOP of unstimulated und Tunicamycin stimulated IECs were densitometrically analyzed by ImageJ, first related to *G3PDH* and afterwards to WT unstimulated. **D)** Detected bands for Hspa5 and **(E)** CHOP of unstimulated und Tunicamycin stimulated BMDMs were densitometrically analyzed by ImageJ, first related to *G3PDH* and afterwards to WT unstimulated; values are shown as means ± S.D; n=4; * p≤0.05; ** p≤0.01.

The above findings were demonstrated exemplarily by antibody staining against activation transcription factor 4 (ATF4) of Jejunum sections of all three genotypes (see Figure 3-22). ATF4 is a transcription factor downstream of CHOP and a marker for ER stress. Comparable to the results shown in Figure 3-21: Hspa5 and CHOP mRNA expression in IECs and BMDMs.Figure 3-21 C, an increase of ATF4 expression is illustrated in untreated ΔWD40 and ΔIEC mice, versus untreated WT mice.

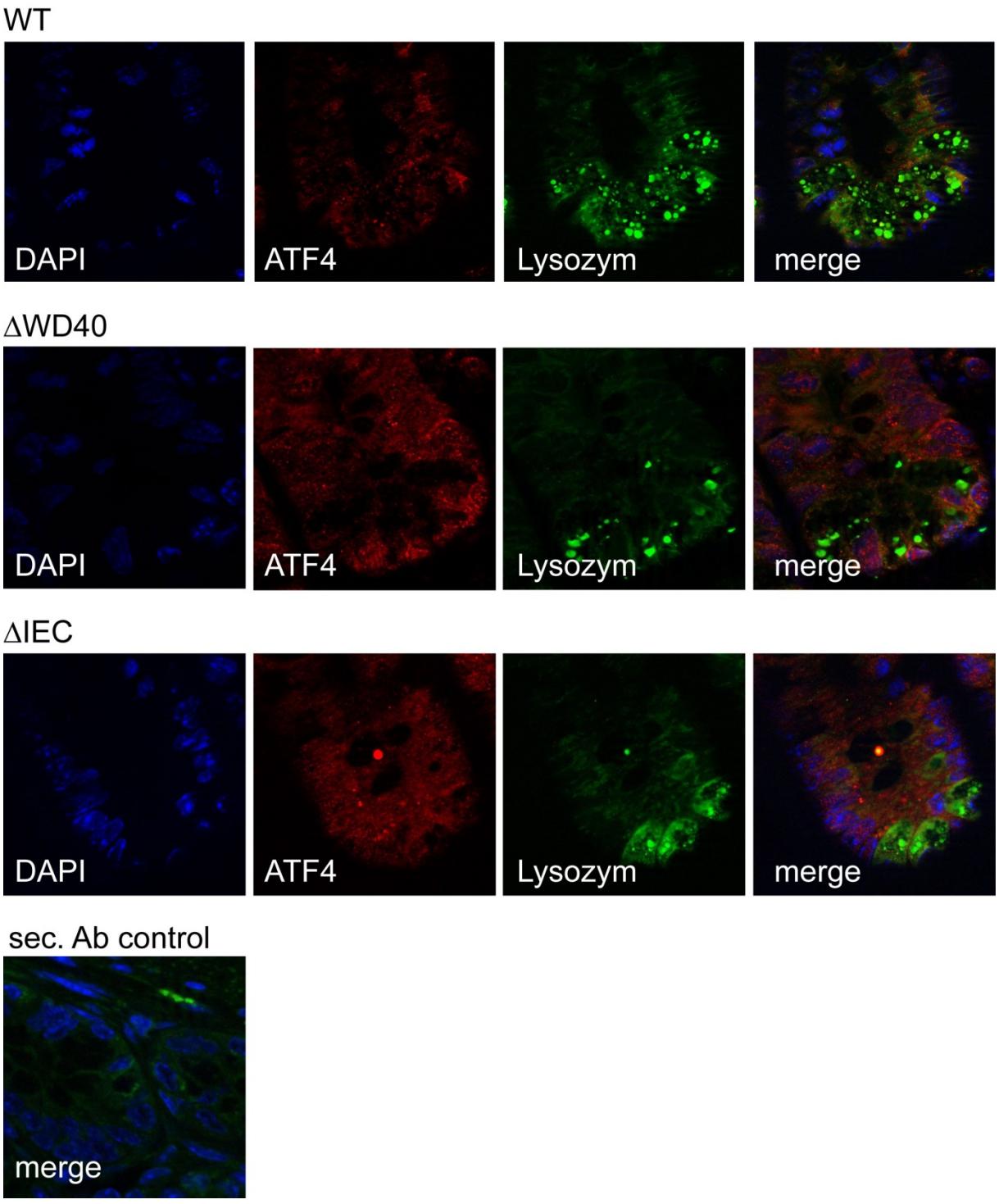

Figure 3-22: ATF4 and lysozyme staining in Jejunum tissue sections of WT, ΔWD40 and ΔIEC mice.
Jejunum tissue sections of WT, ΔWD40 and ΔIEC mice stained with anti-ATF4 (red) and anti-lysozyme (green) antibodies to visualize ER stress; magnification of 600 x. Counterstaining of nuclei with DAPI appears in blue.

4 DISCUSSION

The autophagy protein ATG16L1, as crucial part of the phagophore assembly mechanism, is considered to play a role in gut homeostasis by holding protective functions. *Atg16l1* deficient mice are not viable. As shown by other groups, mutations of this protein lead to reduced xenophagy, increased IL-1β levels, high susceptibility to Crohn disease and abnormal granula secretion in Paneth cells. The special function of ATG16L1 in these events is still unknown, especially the role of the WD40 repeat domain. The aim of the present study was to clarify the specific role of ATG16L1 in DSS-induced colitis, Paneth cell vesicle export with antimicrobial peptide expression, in the autophagic machinery and ER stress. I hypothesized, that by using the two genetically modified mouse lines (ΔIEC and ΔWD40) I could explain the functions of ATG16L1 and the special purpose of the WD40 repeat domain in the intestinal epithelium.

4.1 Influence of ATG16L1 deletion on DSS-induced colitis

A deregulation of the immune response to commensal microorganisms in the gut may evoke dysfunctional immune activation resulting in inflammation of the intestine[129,130]. Neutrophilic infiltration and the development of ulcerations and bloody diarrhea are the characteristics of acute DSS colitis[112]. Colitis can be induced in mice with severe combined immunodeficiency lacking T and B cells. Therefore the DSS induced model appears to be independent of a T cell response[131] and is an appropriate tool to study the innate mechanisms of colitis[111]. Within this model the mechanism of inflammation is believed to involve the direct toxic effect of DSS on colonic epithelium leading to the direct activation of immunological cells[132].

In the present study the results of the DSS induced colitis were assessed by disease activity index (DAI) and evaluating colon tissue by histological examinations (histological score and infiltration of $CD4^+$ cells). Possible causes for the different phenotypes as diminished regenerative proliferation of inflamed intestinal epithelial cells or general impaired intestinal barrier function were determined on the one hand via *in vivo* administration of BrdU and on the other hand by the administration of FITC-Dextran.

In my experiments I could recapitulate results of other studies (Saitoh and Cadwell) suggesting that ATG16L1 deficiency leads to an increased susceptibility to intestinal

inflammation[44]. In contrast to Cadwell et al., who used *Atg16l1* hypomorphic mice, the present study employed a complete deletion of ATG16L1 in the intestinal epithelium. 30 % of the normal amount of ATG16L1 in the case of Cadwells study seemed to be enough to conserve the ability of the cells, affected of DSS treatment, to resist against inflammation[58]. Here we could show that during DSS induced colits only the ΔIEC mice differ from the wildtype mice, whereas the ΔWD40 mice do not clearly differ from the wildtype mice phenotype, which could be revealed by DAI, colon length and infiltration of $CD4^+$ cells. But histological investigations showed contradictory results. In case of the histological score and the regenerative response of the intestinal epithelial cells, the ΔWD40 mice exhibit a phenotype, which is located between the WT and the ΔIEC mice. This leads either to the assumption that the WD40 repeat domain is not involved in the development of inflammation, as for example being involved in pathways for activating further immune cells like dendritic cells or macrophages, and that the remaining part of the protein can accommodate with the situation. But another possible reason should be kept clearly in mind, as most of the following examinations of this study show clear differences between the WT and the ΔWD40 mice. The analogy of the achieved results during DSS induced colitis of the WT and the ΔWD40 mice might be due to the large margin that was detected between single individuals especially of the ΔWD40 strain during assessing the DAI. All following experiments that will be discussed later, led to the assumption that a higher number of animals might reveal differences between the wildtype and ΔWD40 strains, as well.

An explanation for the higher susceptibility to DSS induced colitis of the ΔIEC mice might be a dysfunctional intestinal barrier of the ΔIEC mice, as it was shown in a mouse model with *Atg16l1* deficient hematopoietic cells and cells of patients carrying the T300A risk variant[44,81]. The IL-1β levels of these mice were increased, whereas IL-1β itself increases the intestinal epithelial tight junction permeability, as shown by Al-Sadi and Ma[80]. A functional intestinal barrier is important for the gut homeostasis. Thereby the para cellular pathway functions as gate keeper with apically located tight junctions and lateral adherent junctions and desmosomes[133]. The present study could show that neither truncation of the ATG16L1 WD40 domain nor deletion of the whole ATG16L1 protein in the intestinal epithelium had impact on the intestinal barrier function in unchallenged mice, shown by FITC administration. Hence, no general barrier dysfunction exists in ΔIEC mice. The cause for the high susceptibility

to DSS treatment in these mice might have another explanation, as impairment of regenerative proliferation during inflammation could be one possibility. The regenerative proliferation was tested by BrdU staining and was approved to be impaired in the ΔIEC mice. Interestingly, the regenerative response is impaired in the ΔWD40 mice as well, leading to the above mentioned assumption that the ΔWD40 genotype might also cause to increased susceptibility to DSS-induced colitis. As DSS is toxic for the IECs[132], an impaired regenerative response during inflammation could lead to a directly impaired immunological function of the intestinal epithelium. Since the ΔIEC mice have genetically normal immune cells, this impaired IEC response may be caused by inadequate chemokine and cytokine signals and a secondary overreaction of innate immune cells like dendritic cells or macrophages. Hence, the direct activation of immunological cells might proceed inadequate, leading to higher inflammatory responses and higher severity of the colitis.

4.2 Discussion of the methodology of in vitro studies for autophagy

The autophagic process consists of continuous dynamic membrane formation and fusion. Hence, it is important to estimate autophagic activity accurately and quantitatively when studying autophagy in vitro.

4.2.1 Estimation of autophagy

Many methods for monitoring autophagy have been established, including GFP-LC3[134], tandem fluorescent LC3[135], and LC3-II turnover assay[136]. In this study the estimation of autophagy was performed by a LC3-II conversion assay, a measurement of autophagic turnover in which LC3-II is assayed by immunoblotting with anti-LC3 antibody in the presence and absence of a lysosomal inhibitor[136]. Bafilomycin A1 (an inhibitor of V-ATPase[120]) was chosen as lysosomal inhibitor for monitoring the LC3-II turnover. The accumulation of LC3-II reflects the activity of the process delivering LC3-II into lysosomes, that is, autophagic turnover. V-ATPases are multisubunit complexes organized in two domains. These evolutionary highly conserved enzymes acidify a wide array of intracellular organelles and pump protons across the plasma membranes of numerous cell types. At low concentrations bafilomycin A1 (BafA1) inhibits the V-ATPase by binding to the proteolipid subunit[137,138]; subunit a might also participate in binding[139]. At these low concentrations, BafA1 is highly specific for V-ATPases[140,141]. Therefore, these

inhibitors have been widely used in studies of V-ATPase mediated acidification[142,143]. The vacuolar H+-ATPases (V-ATPases) are responsible for establishing and maintaining intracellular pH gradients across specialized organellar membranes, including the trans-Golgi network (TGN), secretory granules, endosomes and lysosomes. Hence it has to be noted, that Bafilomycin as V-ATPase contributes to the acidification of other organelles, including Golgi and endosomes and therefore may show off-target effects[144,145].

4.2.2 Primary cell culture of intestinal epithelial cells

Intestinal epithelial cells play a key role in the homeostasis of the organ. The main functions are to absorb and assimilate selected nutrients and to produce secretions with protective (mucous barrier) or signaling (growth factors or cytokines) properties[146,147]. They also have the ability to protect the organism from various pathogens and toxins, which are found even under normal conditions in the intestine. Hence, they provide an effective barrier to the complex antigenic load of intestinal contents[148]. The epithelium of the small intestine is one of the most rapidly proliferating tissues in the body. A process, involving cell generation and migration from stem cells located at the bottom of the crypt to the extrusion of the terminally differentiated cells at the tip of the villus, ensures that the epithelium is continuously renewed[149]. The proliferation, migration and differentiation events are tightly regulated by a variety of growth factors and macromolecules of the extracellular matrix[150]. So far the study of human intestinal cell regulation has been limited to cell cultures generated from experimental animals[151] and human cancer tissues[152] as primary cells can only be obtained in short-term cultures at low amounts. The normal physiology of the intestinal epithelium has been studied on the whole organ and mucosal preparations, which are limited both by rapid necrosis and degeneration of the epithelium. Finally, it is impossible to differentiate between the functions of the different mucosal cytotypes[149].

Significant advances have been made in single-cell preparation and maintenance in short-term cultures [153]. It is assumed that proliferation of normal gut epithelium *ex vivo* is dependent on the maintenance of the structural integrity of this tissue. Thus, for the present study a preparation of IECs was tried to be performed after Evans et al.[154]. They established an isolation method of the epithelia by preservation the three-dimensional integrity with the result of epithelial cells detaching as intact units, called organoids. But this preparation method failed for the present study, wherefore

single cell preparation and short term culture were chosen. But recently, Sato et al. established other long-term culture conditions for generating crypt-villus organoids[155]. These organoids are built by single crypts undergoing multiple crypt fission events. Thereby the fissioned crypts simultaneously generate villus-like epithelial domains in which all differentiated cell types are present. They showed that single sorted Lgr5+ stem cells can also initiate these crypt–villus organoids. Thus, a future prospect will be to generate such crypt-villus organoids for further experiments with intestinal epithelial cells.

However, it is also evident that an important limitation of these systems is that observations made with experimental animal models cannot always be transferred to humans. A fact possibly due to the difference of brush border enzyme expression and its regulation by hormones and growth factors. Further, the fundamental differences between animal and human tissues in the composition of the epithelial basement membrane along the crypt-villus axis are important[156].

According to anatomical data obtained with mouse small intestine[157,158] it is important to take care that contamination by stromal cells (fibroblasts) or immune cells (macrophages, lymphocytes) is difficult to control. In this study a purity control was performed to estimate the extent of contamination of the isolated epithelial cells by further cell lineages. But only low expression of $CD4^{+}$T cells was obtained.

4.2.3 Primary cell culture of bone marrow derived macrophages

Macrophages are central players in both the innate and the adaptive immune system. They have a crucial phagocytic function and are involved in important cytotoxic activity and in the destruction of microorganisms. Macrophages present antigens to primed T-Lymphocytes and secrete a number of important cytokines and chemokines, which regulate a wide range of immune responses[147]. Both mature Macrophages and macrophage precursors have their source in the bone marrow. By harvesting immature cells from the femurs of mice and culturing them with specific growth factors, large numbers of macrophages can be derived from bone marrow precursors. This results in a quite homogenous population of cells[159].

The cells undergo differentiation and polarization into macrophages with variable functional properties, in response to the *in vivo* microenvironment. Cytokines and microbial products function alone or in combination to induce differences in functional phenotypes, affecting capacity for phagocytosis and inflammatory responses[160]. This should be kept in mind for *ex vivo* cellular interaction studies. They rely on

macrophage differentiation of harvested cellular populations and are performed under largely artificial condition. Further, differences in media components could have an influence on macrophage phenotypes. Currently, *ex vivo* studies variably rely on culture in recombinant MCSF, or culture in conditioned medium from one of several cell lines that are known to produce MCSF[161].

In this study BMDMs were used as a contrast to epithelial cells. Differences in the results would be a hint for cell specific characteristics. Further this cell line provided in contrast to IECs a negative control for the ΔIEC mice with the *Atg16l1* knockout only in the intestinal tissue.

4.3 Influence of ATG16L1 truncation or deletion on autophagy

For the CD associated risk variant ATG16L1 T300A it was shown by several groups that bacterial handling is impaired[48,49,74-76] which might be a reason for reduced autophagic activity. In this study, the autophagic activity was examined by LC3-II turnover. In contrast to the work of Fujita et al., who described that an ATG16L1 WD repeat domain deletion has little impact on canonical autophagy[44], it could be shown in the present study that the truncation of the WD40 repeat domain leads to lower LC3 expression levels and reduced LC3-II conversion in basal autophagy in both intestinal epithelial cells and in bone marrow derived macrophages. Even stimulation with the mTor inhibitor Rapamycin or lysosomal inhibition by Bafilomycin did not lead to an enhancement. The truncation of the WD40 repeat domain leads to a decreased autophagic activity of about 50 %, indicating a specific role for the WD40 repeat domain during basal autophagy, especially during LC3-II turnover. The fact, that in ΔWD40 mice the conversion of LC3 is still functional, but in a minor extent, indicates that on the one hand, due to the binding of ATG5 on the N-terminal site of ATG16L1, the complex accumulation of ATG5, ATG12 and ATG16L1 is still running, but on the other hand especially the WD40 repeat domain might be involved in ensuring an accurate and compact complex formation and therefore by missing this domain the complex formation is reduced or loosely. The findings of this study suggest that the function of the ATG16L1 WD40 repeat domain might be the intensifying of the protein interactions during complex formation. The WD40 domain therefore might not be essential for the complex formation and following LC3 conversion, but it strengthens it. But how does this phenotype fit to the results of the DSS induced colitis? There, no striking difference to the WT mice could be shown via DAI. But the distinct reduction

of the autophagic activity enforces the assumption that with more animals a difference in the DAI of the colitis experiment could appear as well.

The ΔIEC mice showed high sensitivity to DSS treatment which might be due to an impaired intracellular bacterial killing by autophagic mechanisms. Komatsu et al.[43] and Saitoh et al.[44] described that *Atg16l1*-deficiency hinders the recruitment of the ATG12-ATG5 conjugate to the isolation membrane, resulting in the loss of LC3 conjugation to phosphatidyl ethanolamine (PE) and the complete inhibition of the basal autophagy machinery. This study confirms these findings. ATG16L1 deletion in the intestinal epithelium leads to the loss of LC3-II turnover and to higher susceptibility to DSS induced colitis. Interestingly, the untreated animals of this genotype do not differ from the wildtype mice in their outward appearance or in histology of the gut. This leads to the assumption, that missing autophagic activity in the intestinal epithelial cells must be absorbed by other mechanisms, whereas during DSS treatment, this failure cannot be compensated anymore and leads to the distinct phenotype.

4.4 Influence of ATG16L1 truncation or deletion on the secretory pathway

Paneth cells are part of the intestinal barrier with the main function of secreting antimicrobial peptides including α-defensins and lysozyme[50,52]. These cells increasingly got into focus in the context of their abnormal behavior in inflammatory bowel disease associated with autophagy. For example, mice with reduced expression of the ATG16L1 protein (Atg16l1^{HM}) show that Paneth cell packaging of antimicrobial proteins into granules and thus their proper export into the lumen of the gut is defective[58]. Further *Atg5* Villin-Cre and *Atg7* Villin-Cre mice display morphological abnormalities in their Paneth cells that are indistinguishable from the Atg16l1^{HM} mice. Moreover these mice do not display obvious morphological abnormalities outside the Paneth cells within the ileal epithelium[58,162].

In this study histological analyses were performed to investigate the effect of the *Atg16l1* Villin-Cre deletion or the truncation of the WD40 repeat domain on the morphology of Paneth cells. First, the lysozyme allocation was compared. As this antimicrobial peptide is normally packaged in the secretory granules of Paneth cells[121], this study confirms the findings of Cadwell et al. Comparable to the morphology of their ATG16L1^{HM} mice[58], in this study the Paneth cells of the ΔIEC

mice display diffuse lysozyme staining (64 % of total Paneth cells), which implies that the total lack of the autophagy protein ATG16L1 causes a totally disabled lysozyme packaging, resulting in diffuse allocation of this antimicrobial peptide within the Paneth cell.

Interestingly, yet the truncation of the WD40 repeat domain leads to an altered morphology. The ΔWD40 mice exhibit a striking population of Paneth cells with disordered allocation of lysozyme positive granules (52 % of total Paneth cells). This indicates that already the deletion of the WD40 repeat domain causes abnormal granula formation, leading to the assumption that the WD40 repeat domain is involved in the procedure of the secretory pathway.

Already the mRNA expression of lysozyme (*Lyz1*) is modified due to the deletion or truncation of ATG16L1. Both genotypes ΔWD40 and ΔIEC show significantly decreased *Lyz1* mRNA levels in intestinal epithelial cells. But in contrast, BMDMs of ΔWD40 mice exhibit significantly increased mRNA levels of lysozyme. This might be one explanation why the truncation of the WD40 repeat domain does not lead to higher susceptibility to DSS induced colitis. These animals exhibit macrophages with higher mRNA expression of lysozyme. In case of higher expression on protein levels, the cells might be highly effective against intracellular bacteria because of the enzymatic activity of lysozyme. It hydrolyses glycosidic bonds and is thus able to hydrolyse the cell wall peptidoglycans of some micro-organisms and thereby kill the harmful organism[163]. The high antimicrobial potency of the macrophages might compensate the reduced lysozyme level of the intestinal epithelial cells in ΔWD40 mice, whereas the ΔIEC lack such compensation due to normal lysozyme expression in their non-epithelial cells, which in turn leads to higher susceptibility to DSS induced colitis. But the question why the genetically altered *Atg16l1* leads to such different expression levels of lysozyme in different cell lines still remains unsolved.

Further, the association between the autophagy proteins ATG16L1 and LC3 and lysozyme positive granules was monitored via fluorescence staining. LC3 dots, representing autophagosomes, decreased from WT mice to ΔWD40 mice and were not detectable in ΔIEC mice. This is concordant with the results of the reduced or inhibited LC3-II conversion, obtained from the LC3 turn-over experiments. Interestingly, both proteins ATG16L1 and LC3 show colocalization with lysozyme in the WT mice. This is still existent in the ΔWD40 mice, but seems to be decreased due to the truncation of the WD40 repeat domain. This leads to the assumption that

there is an interaction between Paneth cell lysozyme filled secretory vesicles, and LC3, as well as ATG16L1. This interaction might be implemented by ATG16L1, and strengthened by the WD40 repeat domain. But if this interaction is a function of the autophagy protein, autonomous from the autophagy machinery, still remains to be answered. Further, a direct connection between autophagy, Paneth cell vesicle export and the ER could be demonstrated by co-fluorescent staining of PDI (Protein Disulphide Isomerase) as ER marker and lysozyme. This study could demonstrate that in WT mice and ΔWD40 mice the lysozyme filled granules are separated from the ER, whereas the total sources of lysozyme in ΔIEC mice are within the ER. Another evidence for the association of ATG16L1 truncation or deletion on Paneth cell vesicle export is given by subsequent morphological changes, shown by examination of granule numbers in Paneth cells as well as detected by electron microscopy of Jejunum sections of the different mouse genotypes. Cadwell et al. described reduced vesicle numbers in the ATG16L1^{HM} mice[58] which could be confirmed by this study. The numbers of granules differ between WT, ΔWD40 and ΔIEC mice. Both, the truncation of the WD40 repeat domain and the deletion of the ATG16L1 protein in the intestinal epithelial cells lead to decreased granule number within the Paneth cell. Via electron microscopy Cadwell et al. detected areas within the Paneth cells of hypomorphic mice, which they construed as areas of increased cytoplasmic vesicles[58]. In this study, comparable morphological changes were shown for ΔWD40 mice and more evident for ΔIEC mice. One reason might be a hindered retrieval vesicle pathway from the endosome to the ER. But in relation to the findings of the PDI staining, where it could be shown, that the lysosome of ΔIEC mice is located within the ER, this supposes that the large area of stained ER might coincide with the altered cellular structures detected by electron microscopy. This might be a hint for dilated ER structures within the genetically altered mouse strains. Hence, this work delineates an association between the autophagy protein ATG16L1 (with special function for the WD40 repeat domain), Paneth cell granula, the endoplasmic reticulum and supposable cytoplasmic vesicular trafficking.

A study of Zhao et al. affirms the association between autophagy proteins and cytoplasmic vesicular traffic. They described that Atg5 expression in phagocytic cells is essential for cellular immunity to intracellular pathogens *in vivo*. They showed that Atg5 was required for the recruitment of the IFNγ-inducible p47 GTPase IIGP1 (Irga6) to the vacuole membrane, while, via electron microscopy, they did not detect

double membrane shaped autophagosomes enveloping *T. gondii*. Therefore they concluded that an autophagy protein can participate in immunity and intracellular killing of pathogens via autophagosome-independent processes such as GTPase trafficking[164]. The present study shows for the first time that both autophagy proteins LC3 and ATG16L1 are located at Paneth cell lysozyme filled granules. Referred to Zhao et al., our findings may indicate an autophagy-independent role for LC3 and ATG16L1 in vesicular trafficking.

Still the question remains why the above named morphological changes are located on Paneth cells within the intestinal epithelium after ATG16L1 deletion or truncation. This study demonstrates that histologically all three genotypes do not seem to differ in the investigated tissue and organ system apart from the one cell lineage in focus, the Paneth cells. Even the number of Paneth cells is significantly decreased by truncation of the WD40 repeat domain and more by ATG16L1 deletion. By contrast, goblet cells as one of the other cell lineages found in the intestinal epithelium are not affected in their number.

4.4.1 Decreased defensin expression by ATG16L1 truncation or deletion

Defensins are antimicrobial peptides produced at a diversity of epithelial surfaces. They assist in maintaining the balance between protection from pathogens and tolerance to normal flora in the intestinal tract and therefore contribute to host immunity. Based on structural differences relating to the bonds between cysteine pairs, defensins are differentiated into two groups, the α- and β-defensins[165]. Although certain Paneth cell α-defensins (cryptdins) also have been detected in different tissues, α-defensins are specific to Paneth cells in the small intestine [166,167]. They are processed from inactive proforms by specific proteolytic cleavage steps, as mediated by matrix metalloproteinase-7 (MMP-7; matrilysin) in Paneth cells. It was shown that, MMP-7-null mice, lacking functional cryptdin peptides, have a defect in clearance of intestinal infections[168]. Thus, altered expression of defensins compromises host immunity and is suggested to be an essential factor in the development of inflammatory bowel disease (IBD) [169]. The group of Shi found out that α-defensins, including mouse Paneth cell defensins cryptdin-3 and cryptdin-4, human neutrophil defensin HNP-1, and human Paneth cell defensin HD-5, blocked the release of IL-1β from LPS-activated monocytes. They concluded that α-defensins may play an important role in intestinal homeostasis by controlling the production of IL-1β[170].

In the present study, quantitative analysis of α-defensin mRNA expression was performed. It could be shown that the truncation or deficiency of ATG16L1 influences the expression of α-defensins in intestinal epithelial cells. A significant downregulation of *Defa3* and *Defa5* mRNA was discovered in both genotypes, which indicates a special function for the WD40 repeat domain in this context. The extreme down regulation of defensin mRNA is likely not explainable by the decreased number of Paneth cells, alone. In that case, a decreasing trend in mRNA levels would have been expected, comparable to the decline of the Paneth cell number from WT to ΔWD40 to ΔIEC mice. An explanation might be the involvement of ATG16L1 in expression pathways that regulate the amount of defensins. It is described that reduced Paneth cell defensin expression has been linked with susceptibility to Crohn disease[96,97]. Hence, the downregulation of *Defa3* and *Defa5* mRNA might be a reason for the high susceptibility to DSS induced colitis in ΔIEC mice.

ΔWD40 mice have the same mRNA level of α-defensins as the ΔIEC mice, whereas during DSS-induced colitis, they instead differ from ΔIEC mice by resembling the WT mice. This leads to the conclusion that always a combination of different factors leads to the development of a disease. But as noted above, a higher number of ΔWD40 animals in the DSS-induced colitis may further strengthen the notion that their phenotype might be located between the WT and the ΔIEC mice.

As NOD2 and ATG16L1 are described to interact during autophagy[49,74,75], the received opinion, that a variety of different factors play a role in the development of Crohn disease, might be supported by the findings of Wehkamp and collegues[171]. They suggest an association between the intracellular receptor NOD2 (which mediates the intracellular recognition of the bacterial cell wall component muramyl dipeptide (MDP) and is also described to recruit ATG16L1 to the plasma membrane at the bacterial entry site), and the mechanisms for regulating the expression of α-defensin[172]. The NOD2 receptor is most highly expressed in circulating blood monocytes and in intestinal epithelial cells, with particularly high expression in Paneth cells[173,174]. In their study, Wehkamp and collegues observed that patients with a NOD2 mutation exhibited a significantly reduced production of Paneth cell *HD5* mRNA compared to CD patients with wild type NOD2[171]. If NOD2 and ATG16L1, which interact during xenophagy, are also connected during the control of defensin production, still remains unsolved.

4.5 ER stress induced by truncation or deletion of ATG16L1

How does a defect of an autophagy protein cause such specific effects on Paneth cells, while other intestinal epithelial cell lineages do not exhibit obvious morphological abnormalities? In contrast to other intestinal epithelial cells, Paneth cells contain an outsized endoplasmic reticulum (ER). The loss or the mutation of key autophagy proteins may disrupt autophagy-mediated organelle turnover, hence disturbing the ER homeostasis. Kaser et al. demonstrated that Paneth cells are particularly sensitive to ER stress by examining the intestinal role of Xbp1, a transcription factor important in ER homeostasis[38]. Further, Cadwell et al. have shown that ATG16L1^{HM} Paneth cells exhibit degeneration of mitochondria and replacement of ER with abundant vesicular structures[58]. As it is known that the unfolded protein response (UPR) is linked to autophagy by affecting the expression of ATG5, ATG12 and LC3 as well as the LC3 conversion[30-33], this study shows that also ATG16L1 is linked to unfolded protein response in intestinal epithelial cells. This study demonstrates that the truncation of ATG16L1 in ΔWD40 mice and even more the deletion in ΔIEC mice exhibit significant higher mRNA levels of *Hspa5* and *CHOP* in comparison to WT mice, approved by histological staining of ATF4 in intestinal epithelial cells. In contrast, in bone marrow derived macrophages, no ER stress, measured by *Hspa5* or *CHOP* expression levels could be observed.

This indicates a specific link between autophagy proteins, intestinal epithelial cells and ER stress.

4.6 Involvement of the autophagy protein ATG16L1 in intestinal inflammation

Despite intensive study of IBD pathogenesis, the mechanisms which contribute to disease initiation and progression still largely remain unknown. The results obtained in this work indicate that many factors are involved in the pathogenesis of DSS-induced colitis. First the function of the autophagy protein ATG16L1 and its WD40 repeat domain during DSS-induced colitis were analyzed. Interestingly, by investigating the DAI, the WT and the ΔWD40 mice did not differ in their phenotype, whereas the ΔIEC mice were significantly higher susceptible to DSS treatment. But as the ΔIEC mice exhibit unaltered and functional immune cells, this works indicates that an inadequate communication between intestinal and immunological cells must be one basis for the high susceptibility of ΔIEC mice. Recent reports suggest that

autophagy takes part in innate and adaptive immunity processes. It was demonstrated that IFN-gamma induces autophagy in macrophages, whereby this immunological induction was achieved through a process that included the GTPase IRGM1[175]. Further, the role of autophagy in MHC II presentation of endogenously synthesized viral proteins or non-viral peptides from cytoplasmic sources was displayed[176,177]. On the one hand ATG16L1 might be directly involved in immunological pathways and its deficiency in intestinal epithelial cells leads to dysfunctions in immunological answers. On the other hand the deficiency of ATG16L1 leads to a blockade of LC3 conversion and therefore to a loss of autophagic activity with reduced intracellular bacterial killing as a result. But also the truncation of the WD40 domain leads to reduced autophagic activity, which would imply that the ΔWD40 mice should differ in their disease severety from WT mice. The ΔWD40 mice ubiquitously exhibit the truncation of the ATG16L1 protein, hence exhibiting the mutation in their immune cells, as well. As demonstrated in this study, the bone marrow derived macrophages of the ΔWD40 mice express a higher level of *Lyz1* mRNA in comparison to the WT mice. Therefore their macrophages might be highly effective against intracellular pathogens, which might be one explanation for no higher susceptibility of the ΔWD40 mice.

Paneth cells play an important role in the maintenance of the intestinal barrier by producing, packaging and exporting antimicrobial proteins[51,81]. Especially the autophagic protein ATG16L1 was described to be involved in morphological and vesicular changes in Paneth cells of *Atg16l1* hypomorphic mice[58] comparable to the cellular morphological changes of patients carrying the Crohn associated risk variant T300A[57]. This study could affirm these findings by demonstrating that the truncation of the WD40 repeat domain leads to diminished lysozyme granula packaging, whereas the deletion of ATG16L1 in intestinal epithelial cells leads to complete inhibition of forming lysozyme filled granula. This was confirmed by the findings of this study that the lysozyme is completely located to the endoplasmic reticulum (ER) in ATG16L1 deficient Paneth cells, while the lysozyme filled granules of WT and ΔWD40 mice are separated from the ER. Interestingly, electron microscopic analysis gives a hint that the ER might be dilated due to genetically alteration or deletion of *Atg16l1*.

Further, this work demonstrates that the autophagy proteins ATG16L1 and LC3 are located to lysozyme filled granules in WT and ΔWD40 mice, indicating that the

granules might interact with these proteins. These findings, and the observation of reduced granula numbers with accompanied supposable increased cytoplasmic vesicles (a possible result of hindered retrieval pathway from the endosome to the ER) due to ATG16L1 truncation or deletion, denote that the autophagy protein ATG16L1 might play an autophagy-independent role in vesicle export. This was already shown for example for ATG5 as participating in immunity and intracellular killing of pathogens via autophagosome-independent-processes such as GTPase trafficking[164]. Further, Huang et al. gave a link from the ER to autophagosomes. They suggested that antibacterial autophagy occurs at omegasomes (cup-shaped projections from the ER that serve as a platform for autophagosome biogenesis in mammalian cells) and revealed that the Rab1 GTPase plays a crucial role in mammalian autophagy[178].

The failure of ΔIEC mice in packaging lysozyme into Paneth cell granules might be another reason for the high susceptibility to DSS-induced colitis, beside the inhibited autophagic machinery in the intestinal epithelial cells. Hence, the intestinal homeostasis is impaired by the lack of exported lysozyme in the mucus[58].

This work furthermore demonstrates that the impaired vesicular trafficking of Paneth cells with ATG16L1 truncation or deletion is accompanied by a strong reduction of α-defensin expression on mRNA level. This implies that ATG16L1 is apparently autophagy-independently involved in the regulation of *Defa3* and *Defa5* production. If directly or indirectly via NOD2 for example (NOD2 is described to be involved in human α-defensin 5 production[171]) is not clear. While it is supposed that α-defensins may play an important role in intestinal homeostasis by controlling the production of IL-1β[170], this leads to the assumption that ATG16L1 might be involved in this regulation. Further it is described that ATG16L1-deficiency causes increased production of IL-1β by Toll/IL-1 receptor domain-containing adaptor inducing IFN-β (TRIF)-dependent activation of caspase-1[44]. This demonstrates that ATG16L1 is an essential component for the control of the inflammatory immune response.

This work describes that intestinal epithelial cells of ΔWD40 and ΔIEC mice show ER stress in an increasing trend from truncation to deletion, whereas the bone marrow derived macrophages are not affected. This implicates that the cause for this phenotype might be found within the physiology of intestinal epithelial cells. Especially the Paneth cells with ATG16L1 truncation or deletion show abnormalities in their morphology, granula export and probably in their cytoplasmic vesicle export.

On the one hand an explanation might be that the hindered vesicle export, shown for Paneth cells, with accompanied accumulation of lysozyme in the ER and further failing autophagosome turnover leads to ER stress. But on the other hand it was recently shown by other groups that ER stress may alter the ER export and the dynamic of post-ER compartments[179], indicating that ER stress might be the reason for the phenotypes of the ΔWD40 and ΔIEC mice. This works strengthens this assumption by showing that an increased expression of ATF4 is detected in all intestinal epithelial cells, with no special role for Paneth cells. This might indicate that ATG16L1 truncation or deficiency directly leads to ER stress in all IECs. As Paneth cells have an exceptional position within the intestinal epithelial cells with an outsized ER and specialized secretory vesicle export, especially these cells show the observed morphological abnormalities after ATG16L1 truncation or deletion. The direct connection between ATG16L1 and the ER is not known but might be the omegasome formation. The omegasome is described to be one possible origin of the autophagosome membrane. It is a specialized subdomain of the ER, and autophagosome formation takes place inside the omegasome[180]. It is not described that ATG16L1 directly interacts with the ER during autophagosome formation, but it might be involved indirectly by interacting with unknown interaction partners. For example, Matsunaga et al. revealed the role of ATG14L in autophagosome formation as it mediates the localization of the autophagy-specific PI3-kinase complex to the ER[181].

But nevertheless the data of this work demonstrate that inflammatory bowel disease is controlled by a complex molecular framework. Many factors lead to morphological and functional changes of Paneth cells, which in turn influence the gut homeostasis and might also trigger immunological answers, finally leading to chronically inflammatory responses. A further interesting aspect regarding the connection between ER stress and intestinal inflammation is illustrated by the group of Kaser et al. They showed that induction of ER stress in intestinal epithelium through XBP1 deletion results in spontaneous intestinal inflammation. The XBP1-deficient IECs show diminished antimicrobial activity and response to inflammatory signals in the local milieu[38].

At last, an important aspect of this work is the fact that the truncation of the WD40 repeat domain does not lead to a loss-of-function phenotype. As the risk variant T300A is located within this domain which is completely missing in the yeast ATG16

protein, it was argued that the WD40 repeat domain might play an important role in eukaryotes[2]. The ΔWD40 mice exhibit a mostly different phenotype to the WT mice but they also differ from the ΔIEC mice. Their phenotype is a phenotype “in between”. This indicates that on the one hand the WD40 repeat domain is dispensable as no loss-of-function is observed. But on the other hand, it has an important function in possibly strengthening the binding of ATG16L1 with interaction partners which might be necessary for ensuring correct autophagic and non-autophagic activity.

4.7 Conclusion

The autophagy protein ATG16L1 seems to play an important role in the maintenance of intestinal homeostasis. A deletion of this protein leads to higher susceptibility to DSS induced colitis with highly inflamed intestinal tissue. This work gives a hint that especially the morphology of Paneth cells is affected by genetically altered *Atg16l1*, and changes within these cells may be involved in the development of inflammation. The deletion or truncation of the ATG16L1 protein might be the trigger for ER stress which in turn is assumed to be the reason for diminished or defective granular packaging within the ER/trans Golgi network, leading to a reduced number of secretory vesicles. Further the retrieval pathway from endosomes to the ER could be affected, as well. Moreover, this work shows that ATG16L1 is involved in regulating the expression of α-defensins on mRNA level. Further, as a reason of reduced or impaired autophagic activity due to the truncation or deletion of ATG16L1, rising numbers of intracellular pathogens might damage the intestinal cells. Taken together all these effects might be involved in intestinal inflammation (see Figure 4-1).

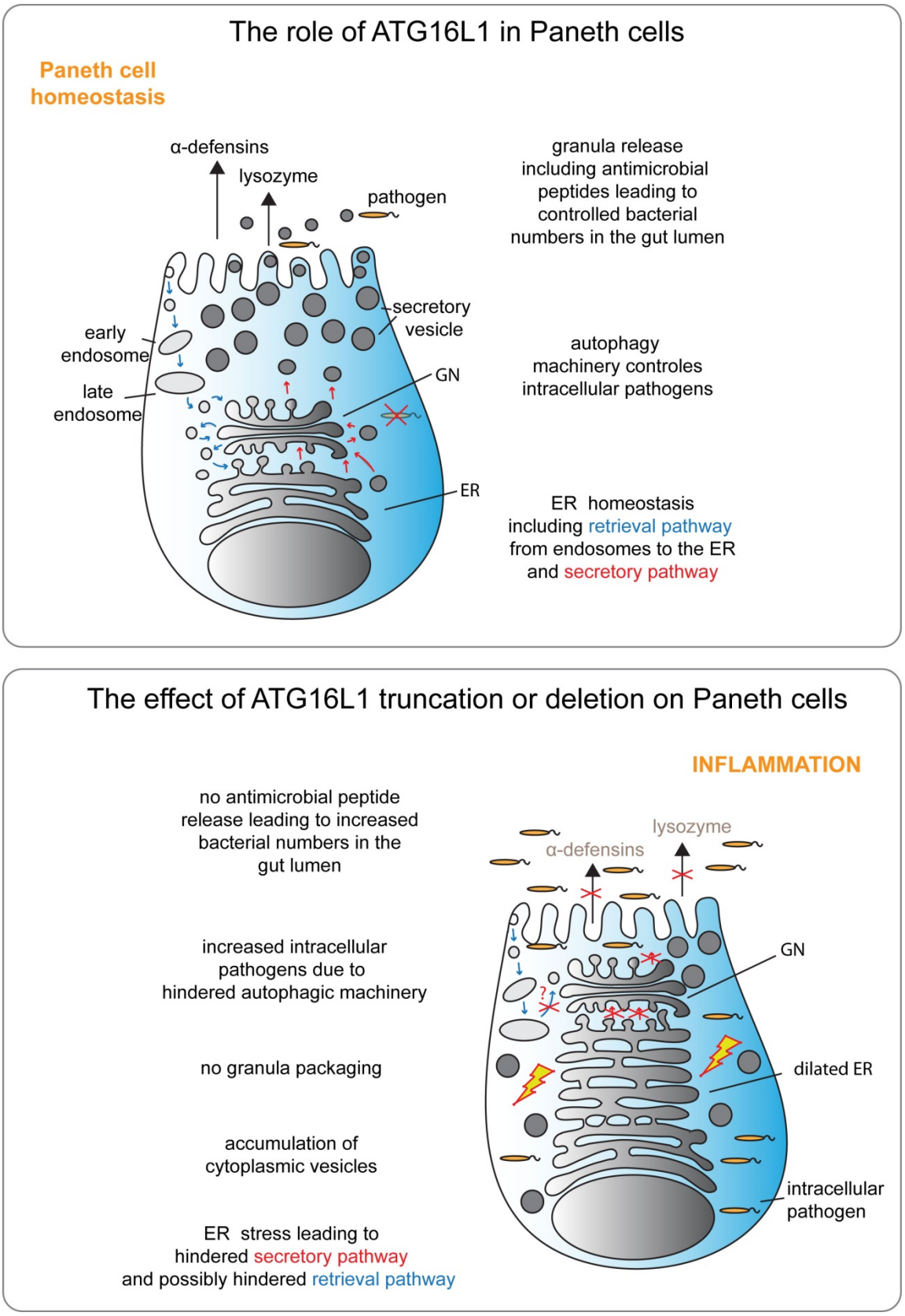

Figure 4-1: Supposed effects of ATG16L1 truncation or deletion on intestinal inflammation
Top panel shows the proposed functions of ATG16L1 in the Paneth cell. Bottom panel shows the assumed effect of ATG16L1 truncation or deletion on the Paneth cell leading to intestinal inflammation. Red arrows indicate the secretory pathway, blue arrows the retrieval pathway to the endoplasmic reticulum. (GN: Golgi Network; ER: Endoplasmic Reticulum)

4.8 Future prospect

ATG16L1 deletion in the intestinal epithelial cells leads to higher susceptibility to DSS induced colitis. Furthermore, ATG16L1 truncation and deletion lead to reduced or impaired autophagic activity in BMDMs and IECs and to morphological changes of Paneth cells with concurrent impaired granula packaging and vesicle export. This might be a result of ER stress. Further the α-defensin production is inhibited.

Based on these findings and interpretations, some future prospects have been derived for additional experiments.

I. The ΔWD40 mice and the ΔIEC mice show decreased or impaired lysozyme packaging into granula and additionally dilated ER. This indicates that the secretory vesicle pathway and possibly the retrieval pathway are impaired. Further, this work leads to the assumption, that the truncation or deletion of ATG16L1 might be the trigger for ER stress. And in turn, that the ER stress might be the reason for the impaired vesicle pathways. Future experiments will have to show how ATG16L1 is involved in ER stress. Is there a direct connection partner during omegasome formation? Or is the correlation between ER stress and ATG16L1 given by different interaction like for example Clathrin, COPI or COPII?

II. The truncation or deletion of ATG16L1 leads to a complete downregulation of *Defa3* and *Defa5* on mRNA level. This indicates that the control of the α-defensin production might be an important function of ATG16L1 for regulating the gut homeostasis. Is ATG16L1 involved in the control of other cytokines or chemokines as well, leading to abnormal immunological responses during DSS induced colitis?

5 SUMMARY

The chronic inflammatory disorders of the gut Crohn disease and Ulcerative colitis are counted among inflammatory bowel disease (IBD) and are characterized by bloody diarrhea, ulcerations and infiltrations of inflammatory cells. The molecular mechanisms of the disease still remain unknown. But it has recently been shown, that genome wide association (GWA) studies are the most productive approach for discovering the genetic variations responsible for IBD susceptibility. As the autophagic proteins ATG16LI and IRGM were implicated in CD by GWA, Genetic and functional studies indicate that autophagy is a key pathway in the pathogenesis of CD.

For ATG16L1, a non-synonymous SNP was identified, which causes an amino acid change at position 300 in the amino acid sequence (alanine to threonine). Following experiments in human cell lines demonstrated that ATG16L1 *300A cells show impaired bacterial handling. Additional experiments indicate that chimeric mice with *Atg16l1*-deficient hematopoietic cells have increased levels of the inflammatory cytokines IL-1β and IL-18 and are high susceptible to dextran sodium sulfate (DSS) induced colitis. *Atg16l1*-deficient mice die shortly after birth and cells derived from such animals show autophagy defects *in vitro*, indicating that the protein ATG16L1 is essential for surviving the period of neonatal starvation. While the functions of the N-terminal domain as well as the central coiled coil domain are known, the function of the C-terminal WD40 domain of the ATG16L1 protein still remains entirely unknown.

The aim of this work was to investigate the function of ATG16L1 as well as of the WD40 domain in the pathogenesis of IBD. Since *Atg16l1* deficient mice are not viable, conditional Villin Cre knock out mice with a deletion of the ATG16L1 protein in the intestinal tissue (ΔIEC) were used for this study, as well as mice with a truncation of the WD40 repeat domain (ΔWD40). To elucidate the role of ATG16L1 in IBD, mice were treated with DSS. Interestingly, ΔIEC mice were highly susceptible to DSS-induced colitis. Furthermore, ATG16L1 truncation or deletion leads to reduced or impaired autophagic activity in BMDMs and IECs and to morphological changes in Paneth cells including impaired granula packaging and vesicle export. This work gives a hint, that these morphological changes might be a result of ER stress, which

in turn was shown to be triggered by ATG16L1 deletion or truncation. Further, it could be shown that the α-defensin production is inhibited on RNA level in both genotypes, demonstrating that ATG16L1 plays an essential role in the control of the inflammatory immune response.

Further, this work indicates that the WD40 domain of the ATG16L1 protein is dispensable, as in ΔWD40 mice the autophagic machinery is reduced but not inhibited and as morphological changes of the Paneth cells are not as drastic as in ΔIEC mice. Further, these animals do not show disease severity as strong as the ΔIEC animals. As ΔWD40 mice can be located phenotypically mostly “in between” the WT and the ΔIEC phenotypes, this indicates that the main function of the WD40 domain might be the strengthening of protein bonds for adequate protein interactions. The loss of the domain does not induce a loss of function but a decrease of function.

Taken together, all results demonstrate that ATG16L1 plays an important role in the homeostasis of Paneth cells, indicating that genetically alteration of *Atg16l1* may play a crucial role in the pathogenesis of intestinal inflammation.

6 ZUSAMMENFASSUNG

Morbus Crohn und Colitis Ulcerosa gehören zu den chronisch entzündlichen Darmerkrankungen und sind durch blutigen Durchfall, Ulzerationen und Einwanderungen von Immunzellen gekennzeichnet. Die zugrundeliegenden molekularen Mechanismen sind bislang ungeklärt. Es wurde jedoch kürzlich gezeigt, dass genomweite Assoziationsstudien (GWA) den bislang produktivsten Beitrag zur Entdeckung von genetischen Variationen, die eine Anfälligkeit für entzündliche Darmerkrankungen herbeiführen, geleistet haben. Die Autophagieproteine ATG16L1 und IRGM wurden mittels solcher Studien in den Fokus von Morbus Crohn gerückt. Nachfolgende genetische und funktionelle Studien zeigten, dass Autophagie einen Schlüsselweg bei der Pathogenese von Morbus Crohn darstellt.

Im Falle von ATG16L1 wurde ein nicht-synonymer SNP (Variation einzelner Basenpaare im DNS-Strang) identifiziert, welcher einen Aminosäureaustausch an Position 300 der Aminosäuresequenz (Alanin zu Threonin) bewirkt. In humanen Zelllinien konnte gezeigt werden, dass die ATG16L1 Variante *300A einen eingeschränkten Wirkungsmechanismus gegen Bakterien hervorruft. Nachfolgende Versuche bei chimären Mäusen mit ATG16L1 defizienten hämatopoetischen Stammzellen bewiesen, dass die Tiere erhöhte Level der inflammatorischen Zytokine IL-1β und IL-18 aufweisen, ebenso wie eine hohe Anfälligkeit für eine durch DSS hervorgerufene Kolitis. Mäuse mit einem komplett ausgeschalteten Gen, welches für ATG16L1 kodiert, sterben kurz nach der Geburt. Mittels *in vitro* Studien konnte gezeigt werden, dass primäre Zellen dieser Tiere Autophagiedefekte aufweisen, was zu der Annahme führte, dass ATG16L1 eine essentielle Rolle während der Phase des neonatalen Nährstoffmangels spielt. Während die Funktion der N-terminalen Domäne und der zentralen coiled coil Domäne des ATG16L1 Proteins bekannt sind, ist die Funktion der C-terminalen WD40 Domäne gänzlich ungeklärt.

Ziel dieser Arbeit war es, die spezielle Funktion von ATG16L1 und der WD40 Domäne während einer chronisch entzündlichen Darmerkrankung zu klären. Basierend auf dem Wissen, dass *Atg16l1* defiziente Tiere nicht lebensfähig sind, wurden für diese Arbeit Tiere mit einem konditionalen Knockout, katalysiert von der Cre Rekombinase unter der Direktion vom Villin Promotor, verwendet (ΔIEC). Folglich ist in diesen Tieren die ATG16L1 Deletion nur auf das intestinale Epithelium

beschränkt. Des Weiteren wurden Tiere untersucht, die eine um die WD40 Domäne verkürzte Variante des ATG16L1 Proteins ubiquitär exprimieren. Um die Rolle von ATG16L1 in chronisch entzündlichen Darmerkrankungen zu untersuchen, wurden die Versuchstiere mit DSS behandelt. Es stellte sich heraus, dass die ΔIEC Mäuse stark anfällig für eine durch DSS hervorgerufene Kolitis sind. Zusätzlich konnte gezeigt werden, dass eine Verkürzung oder Deletion von ATG16L1 zu einer reduzierten oder verhinderten Autophagieaktivität führen. Außerdem wurden morphologische Veränderungen in den Paneth Zellen hervorgerufen, die mit einem eingeschränkten Exportweg für sekretorische Vesikel einhergehen. Die Ergebnisse dieser Arbeit deuten drauf hin, dass die morphologischen Veränderungen in den Paneth Zellen aus im intestinalen Epithel lokalisiertem ER Stress resultieren könnten. Der ER Stress wiederum scheint ein direktes Resultat der ATG16L1 Verkürzung oder Deletion zu sein. Zusätzlich konnte gezeigt werden, dass die α-Defensin Expression auf mRNA Ebene gänzlich inhibiert wurde, was darauf hindeutet, dass ATG16L1 eine wichtige Rolle bei der Regulierung der entzündlichen Immunantwort spielt.
Außerdem konnte gezeigt werden, dass die WD40 Domäne für die Funktion des ATG16L1 Proteins entbehrlich ist. Einen Hinweis darauf geben die mit dieser Arbeit erzielten Ergebnisse, die verdeutlichen, dass zum einen Autophagiemechanismen reduziert aber nicht inhibiert wurden, und dass zum anderen die morphologischen Veränderungen in den Paneth Zellen nicht so drastisch ausfallen wie bei den ΔIEC Tieren. Des Weiteren weisen ΔWD40 Mäuse während der durch DSS hervorgerufenen Kolitis keine vergleichbar starken Symptome auf wie die ΔIEC Tiere. Da der ΔWD40 Phänotyp hauptsächlich zwischen WT und dem ΔIEC Phänotyp anzuordnen ist, führt dies zu dem Schluss, dass die Hauptfunktion der WD40 Domäne beinhaltet, Bindungen zu verstärken, die für eine adäquate Proteininteraktion nötig sind. Ein Verlust dieser Domäne ruft somit keinen Funktionsverlust des Proteins hervor, sondern bewirkt eine Funktionsminderung.

Schließlich deuten alle Ergebnisse dieser Arbeit darauf hin, dass das Protein ATG16L1 eine wichtige Rolle in der Paneth Zell Homöostase spielt. Folglich können Mutationen oder Deletionen dieses Proteins an der Pathogenese von chronisch entzündlichen Darmerkrankungen beteiligt sein.

7 FIGURE LIST

8 TABLE LIST

9 REFERENCES

1. Cecconi, F. & Levine, B. The Role of Autophagy in Mammalian Development. *Dev Cell* **15**, 344-357 (2008).

2. Billmann-Born, S. *et al.* The complex interplay of NOD-like receptors and the autophagy machinery in the pathophysiology of Crohn disease. *Eur J Cell Biol* (2010).doi:10.1016/j.ejcb.2010.10.015

3. Eskelinen, E.-L. & Saftig, P. Autophagy: a lysosomal degradation pathway with a central role in health and disease. *Biochim. Biophys. Acta* **1793**, 664-673 (2009).

4. Levine, B. & Kroemer, G. Autophagy in the pathogenesis of disease. *Cell* **132**, 27-42 (2008).

5. Virgin, H. W. & Levine, B. Autophagy genes in immunity. *Nat. Immunol* **10**, 461-470 (2009).

6. Yorimitsu, T. & Klionsky, D. J. Autophagy: molecular machinery for self-eating. *Cell Death Differ* **12 Suppl 2**, 1542-1552 (2005).

7. Klionsky, D. J. The molecular machinery of autophagy: unanswered questions. *J. Cell. Sci* **118**, 7-18 (2005).

8. Kunz, J. B., Schwarz, H. & Mayer, A. Determination of four sequential stages during microautophagy in vitro. *J. Biol. Chem* **279**, 9987-9996 (2004).

9. Majeski, A. E. & Dice, J. F. Mechanisms of chaperone-mediated autophagy. *Int. J. Biochem. Cell Biol* **36**, 2435-2444 (2004).

10. Schmid, D. & Münz, C. Innate and Adaptive Immunity through Autophagy. *Immunity* **27**, 11-21 (2007).

11. Noda, T., Suzuki, K. & Ohsumi, Y. Yeast autophagosomes: de novo formation of a membrane structure. *Trends Cell Biol* **12**, 231-235 (2002).

12. Ohsumi, Y. Molecular dissection of autophagy: two ubiquitin-like systems. *Nat Rev Mol Cell Biol* **2**, 211-216 (2001).

13. Kraft, C., Peter, M. & Hofmann, K. Selective autophagy: ubiquitin-mediated recognition and beyond. *Nat Cell Biol* **12**, 836-841 (2010).

14. Sakai, Y., Koller, A., Rangell, L. K., Keller, G. A. & Subramani, S. Peroxisome degradation by microautophagy in Pichia pastoris: identification of specific steps and morphological intermediates. *J. Cell Biol* **141**, 625-636 (1998).

15. Ogawa, M. *et al.* Escape of intracellular Shigella from autophagy. *Science* **307**, 727-731 (2005).

16. Guan, J. *et al.* Cvt18/Gsa12 is required for cytoplasm-to-vacuole transport, pexophagy, and autophagy in Saccharomyces cerevisiae and Pichia pastoris. *Mol. Biol. Cell* **12**, 3821-3838 (2001).

17. Baba, M., Osumi, M., Scott, S. V., Klionsky, D. J. & Ohsumi, Y. Two distinct pathways for targeting proteins from the cytoplasm to the vacuole/lysosome. *J. Cell Biol* **139**, 1687-1695 (1997).

18. Ogata, M. *et al.* Autophagy Is Activated for Cell Survival after Endoplasmic Reticulum Stress. *Mol Cell Biol* **26**, 9220-9231 (2006).

19. Ding, W.-X. *et al.* Differential effects of endoplasmic reticulum stress-induced autophagy on cell survival. *J. Biol. Chem* **282**, 4702-4710 (2007).

20. Kouroku, Y. *et al.* ER stress (PERK/eIF2alpha phosphorylation) mediates the polyglutamine-induced LC3 conversion, an essential step for autophagy formation. *Cell Death Differ* **14**, 230-239 (2007).

21. Deretic, V. & Levine, B. Autophagy, immunity, and microbial adaptations. *Cell Host Microbe* **5**, 527-549 (2009).

22. Young, A. R. J. *et al.* Autophagy mediates the mitotic senescence transition. *Genes Dev* **23**, 798-803 (2009).

23. Vellai, T., Takács-Vellai, K., Sass, M. & Klionsky, D. J. The regulation of aging: does autophagy underlie longevity? *Trends Cell Biol* **19**, 487-494 (2009).

24. Mizushima, N., Levine, B., Cuervo, A. M. & Klionsky, D. J. Autophagy fights disease through cellular self-digestion. *Nature* **451**, 1069-1075 (2008).

25. Ylä-Anttila, P., Vihinen, H., Jokitalo, E. & Eskelinen, E.-L. 3D tomography reveals connections between the phagophore and endoplasmic reticulum. *autophagy* **5**, 1180-1185 (2009).

26. Hayashi-Nishino, M. *et al.* A subdomain of the endoplasmic reticulum forms a cradle for autophagosome formation. *Nat Cell Biol* **11**, 1433-1437 (2009).

27. Bernales, S., Papa, F. R. & Walter, P. Intracellular signaling by the unfolded protein response. *Annu. Rev. Cell Dev. Biol* **22**, 487-508 (2006).

28. Berridge, M. J. The endoplasmic reticulum: a multifunctional signaling organelle. *Cell Calcium* **32**, 235-249 (2002).

29. Momoi, T. Conformational diseases and ER stress-mediated cell death: apoptotic cell death and autophagic cell death. *Curr. Mol. Med* **6**, 111-118 (2006).

30. He, C. & Klionsky, D. J. Regulation Mechanisms and Signaling Pathways of Autophagy. *Annu. Rev. Genet.* **43**, 67-93 (2009).

31. Verfaillie, T., Salazar, M., Velasco, G. & Agostinis, P. Linking ER Stress to Autophagy: Potential Implications for Cancer Therapy. *Int J Cell Biol* **2010**, 930509 (2010).

32. Yorimitsu, T. & Klionsky, D. J. Endoplasmic reticulum stress: a new pathway to induce autophagy. *Autophagy* **3**, 160-162 (2007).

33. Yorimitsu, T., Nair, U., Yang, Z. & Klionsky, D. J. Endoplasmic reticulum stress triggers autophagy. *J. Biol. Chem* **281**, 30299-30304 (2006).

34. Rouschop, K. M. A. *et al.* The unfolded protein response protects human tumor cells during hypoxia through regulation of the autophagy genes MAP1LC3B and ATG5. *J. Clin. Invest* **120**, 127-141 (2010).

35. Urano, F. *et al.* Coupling of stress in the ER to activation of JNK protein kinases by transmembrane protein kinase IRE1. *Science* **287**, 664-666 (2000).

36. Ding, W.-X. *et al.* Linking of autophagy to ubiquitin-proteasome system is important for the regulation of endoplasmic reticulum stress and cell viability. *Am. J. Pathol* **171**, 513-524 (2007).

37. Ogata, M. *et al.* Autophagy Is Activated for Cell Survival after Endoplasmic Reticulum Stress. *Mol Cell Biol* **26**, 9220-9231 (2006).

38. Kaser, A. *et al.* XBP1 Links ER Stress to Intestinal Inflammation and Confers Genetic Risk for Human Inflammatory Bowel Disease. *Cell* **134**, 743-756 (2008).

39. Yang, L., Li, P., Fu, S., Calay, E. S. & Hotamisligil, G. S. Defective hepatic autophagy in obesity promotes ER stress and causes insulin resistance. *Cell Metab* **11**, 467-478 (2010).

40. Ozcan, U. *et al.* Endoplasmic reticulum stress links obesity, insulin action, and type 2 diabetes. *Science* **306**, 457-461 (2004).

41. Kimura, S., Maruyama, J., Kikuma, T., Arioka, M. & Kitamoto, K. Autophagy delivers misfolded secretory proteins accumulated in endoplasmic reticulum to vacuoles in the filamentous fungus Aspergillus oryzae. *Biochemical and Biophysical Research Communications* **406**, 464-470 (2011).

42. Mizushima, N. *et al.* Mouse Apg16L, a novel WD-repeat protein, targets to the autophagic isolation membrane with the Apg12-Apg5 conjugate. *J Cell Sci* **116**, 1679-1688 (2003).

43. Komatsu, M. *et al.* Impairment of starvation-induced and constitutive autophagy in Atg7-deficient mice. *J Cell Biol* **169**, 425-434 (2005).

44. Saitoh, T. *et al.* Loss of the autophagy protein Atg16L1 enhances endotoxin-induced IL-1[bgr] production. *Nature* **456**, 264-268 (2008).

45. Kuma, A. *et al.* The role of autophagy during the early neonatal starvation period. *Nature* **432**, 1032-1036 (2004).

46. Smith, T. F. Diversity of WD-repeat proteins. *Subcell. Biochem* **48**, 20-30 (2008).

47. Fujita, N. *et al.* The Atg16L Complex Specifies the Site of LC3 Lipidation for Membrane Biogenesis in Autophagy. *Mol Biol Cell* **19**, 2092-2100 (2008).

48. Kuballa, P., Huett, A., Rioux, J. D., Daly, M. J. & Xavier, R. J. Impaired Autophagy of an Intracellular Pathogen Induced by a Crohn's Disease Associated ATG16L1 Variant. *PLoS ONE* **3**, e3391 (2008).

49. Travassos, L. H. *et al.* Nod1 and Nod2 direct autophagy by recruiting ATG16L1 to the plasma membrane at the site of bacterial entry. *Nat Immunol* **11**, 55-62 (2010).

50. Mukherjee, S., Vaishnava, S. & Hooper, L. V. Multi-layered regulation of intestinal antimicrobial defense. *Cell. Mol. Life Sci* **65**, 3019-3027 (2008).

51. Selsted, M. E. & Ouellette, A. J. Mammalian defensins in the antimicrobial immune response. *Nat. Immunol* **6**, 551-557 (2005).

52. Ouellette, A. J. Paneth cells and innate immunity in the crypt microenvironment. *Gastroenterology* **113**, 1779-1784 (1997).

53. Wiesner, J. & Vilcinskas, A. Antimicrobial peptides: the ancient arm of the human immune system. *Virulence* **1**, 440-464 (2010).

54. Salzman, N. H., Ghosh, D., Huttner, K. M., Paterson, Y. & Bevins, C. L. Protection against enteric salmonellosis in transgenic mice expressing a human intestinal defensin. *Nature* **422**, 522-526 (2003).

55. Tan, X., Hsueh, W. & Gonzalez-Crussi, F. Cellular localization of tumor necrosis factor (TNF)-alpha transcripts in normal bowel and in necrotizing enterocolitis. TNF gene expression by Paneth cells, intestinal eosinophils, and macrophages. *Am. J. Pathol* **142**, 1858-1865 (1993).

56. Takahashi, N. *et al.* IL-17 produced by Paneth cells drives TNF-induced shock. *J. Exp. Med* **205**, 1755-1761 (2008).

57. Dvorak, A. M. Electron microscopy of Paneth cells in Crohn's disease. *Arch. Pathol. Lab. Med* **104**, 393-394 (1980).

58. Cadwell, K. *et al.* A key role for autophagy and the autophagy gene Atg16l1 in mouse and human intestinal Paneth cells. *Nature* (2008).doi:10.1038/nature07416

59. Cadwell, K. *et al.* Virus-Plus-Susceptibility Gene Interaction Determines Crohn's Disease Gene Atg16L1 Phenotypes in Intestine. *Cell* **141**, 1135-1145 (2010).

60. Auernhammer, C.-J. *et al.* Role of the intracellular receptor domain of gp130 (exon 17) in human inflammatory bowel disease. *World J. Gastroenterol* **11**, 1196-1199 (2005).

61. Cho, J. H. & Weaver, C. T. The genetics of inflammatory bowel disease. *Gastroenterology* **133**, 1327-1339 (2007).

62. Xavier, R. J. & Podolsky, D. K. Unravelling the pathogenesis of inflammatory bowel disease. *Nature* **448**, 427-434 (2007).

63. Schreiber, S., Rosenstiel, P., Albrecht, M., Hampe, J. & Krawczak, M. Genetics of Crohn disease, an archetypal inflammatory barrier disease. *Nat Rev Genet* **6**, 376-388 (2005).

64. Hampe, J. *et al.* A genome-wide association scan of nonsynonymous SNPs identifies a susceptibility variant for Crohn disease in ATG16L1. *Nat Genet* **39**, 207-211 (2006).

65. McCarroll, S. A. *et al.* Deletion polymorphism upstream of IRGM associated with altered IRGM expression and Crohn's disease. *Nat. Genet* **40**, 1107-1112 (2008).

66. Barrett, J. C. *et al.* Genome-wide association defines more than 30 distinct susceptibility loci for Crohn's disease. *Nat. Genet* **40**, 955-962 (2008).

67. Parkes, M. *et al.* Sequence variants in the autophagy gene IRGM and multiple other replicating loci contribute to Crohn's disease susceptibility. *Nat. Genet* **39**, 830-832 (2007).

68. Rioux, J. D. *et al.* Genome-wide association study identifies new susceptibility loci for Crohn disease and implicates autophagy in disease pathogenesis. *Nat. Genet* **39**, 596-604 (2007).

69. Plowey, E. D., Cherra, S. J., 3rd, Liu, Y.-J. & Chu, C. T. Role of autophagy in G2019S-LRRK2-associated neurite shortening in differentiated SH-SY5Y cells. *J. Neurochem* **105**, 1048-1056 (2008).

70. Hugot, J. P. *et al.* Association of NOD2 leucine-rich repeat variants with susceptibility to Crohn's disease. *Nature* **411**, 599-603 (2001).

71. Ogura, Y. *et al.* A frameshift mutation in NOD2 associated with susceptibility to Crohn's disease. *Nature* **411**, 603-606 (2001).

72. Kanneganti, T.-D., Lamkanfi, M. & Núñez, G. Intracellular NOD-like receptors in host defense and disease. *Immunity* **27**, 549-559 (2007).

73. Fisher, S. A. *et al.* Genetic determinants of ulcerative colitis include the ECM1 locus and five loci implicated in Crohn's disease. *Nat. Genet* **40**, 710-712 (2008).

74. Cooney, R. *et al.* NOD2 stimulation induces autophagy in dendritic cells influencing bacterial handling and antigen presentation. *Nat Med* **16**, 90-97 (2010).

75. Homer, C. R., Richmond, A. L., Rebert, N. A., Achkar, J.-P. & McDonald, C. ATG16L1 and NOD2 interact in an autophagy-dependent antibacterial pathway implicated in Crohn's disease pathogenesis. *Gastroenterology* **139**, 1630-1641, 1641.e1-2 (2010).

76. Lapaquette, P. & Darfeuille-Michaud, A. Abnormalities in the Handling of Intracellular Bacteria in Crohn's Disease. *Journal of Clinical Gastroenterology* 1 (2010).doi:10.1097/MCG.0b013e3181dd4fa5

77. Cheng, J.-F., Ning, Y.-J., Zhang, W., Lu, Z.-H. & Lin, L. T300A polymorphism of ATG16L1 and susceptibility to inflammatory bowel diseases: A meta-analysis. *World J Gastroenterol* **16**, 1258-1266 (2010).

78. Barnich, N. & Darfeuille-Michaud, A. Adherent-invasive Escherichia coli and Crohn's disease. *Curr. Opin. Gastroenterol* **23**, 16-20 (2007).

79. Fujita, N. *et al.* Differential Involvement of Atg16L1 in Crohn Disease and Canonical Autophagy. *Journal of Biological Chemistry* **284**, 32602 -32609 (2009).

80. Al-Sadi, R. M. & Ma, T. Y. IL-1β Causes an Increase in Intestinal Epithelial Tight Junction Permeability. *The Journal of Immunology* **178**, 4641 -4649 (2007).

81. Plantinga, T. S. *et al.* Crohn's disease-associated ATG16L1 polymorphism modulates pro-inflammatory cytokine responses selectively upon activation of NOD2. *Gut* (2011).doi:10.1136/gut.2010.228908

82. Schreiber, S. *et al.* Increased activation of isolated intestinal lamina propria mononuclear cells in inflammatory bowel disease. *Gastroenterology* **101**, 1020-1030 (1991).

83. Schreiber, S. *et al.* Tumour necrosis factor alpha and interleukin 1beta in relapse of Crohn's disease. *Lancet* **353**, 459-461 (1999).

84. Parronchi, P. *et al.* Type 1 T-helper cell predominance and interleukin-12 expression in the gut of patients with Crohn's disease. *Am. J. Pathol* **150**, 823-832 (1997).

85. Nikolaus, S. *et al.* Increased secretion of pro-inflammatory cytokines by circulating polymorphonuclear neutrophils and regulation by interleukin 10 during intestinal inflammation. *Gut* **42**, 470-476 (1998).

86. Sanchez-Munoz, F., Dominguez-Lopez, A. & Yamamoto-Furusho, J.-K. Role of cytokines in inflammatory bowel disease. *World J. Gastroenterol* **14**, 4280-4288 (2008).

87. Sartor, R. B. Cytokines in intestinal inflammation: pathophysiological and clinical considerations. *Gastroenterology* **106**, 533-539 (1994).

88. Podolsky, D. K. Inflammatory bowel disease. *N. Engl. J. Med* **347**, 417-429 (2002).

89. Kucharzik, T. *et al.* Recent understanding of IBD pathogenesis: implications for future therapies. *Inflamm. Bowel Dis* **12**, 1068-1083 (2006).

90. Nedjic, J., Aichinger, M., Emmerich, J., Mizushima, N. & Klein, L. Autophagy in thymic epithelium shapes the T-cell repertoire and is essential for tolerance. *Nature* **455**, 396-400 (2008).

91. Huett, A. & Xavier, R. J. Autophagy at the gut interface: mucosal responses to stress and the consequences for inflammatory bowel diseases. *Inflamm. Bowel Dis* **16**, 152-174 (2010).

92. Lupp, C. *et al.* Host-mediated inflammation disrupts the intestinal microbiota and promotes the overgrowth of Enterobacteriaceae. *Cell Host Microbe* **2**, 119-129 (2007).

93. Frank, D. N. *et al.* Molecular-phylogenetic characterization of microbial community imbalances in human inflammatory bowel diseases. *Proc. Natl. Acad. Sci. U.S.A* **104**, 13780-13785 (2007).

94. Korzenik, J. R. Is Crohn's disease due to defective immunity? *Gut* **56**, 2-5 (2007).

95. Sartor, R. B. Microbial Influences in Inflammatory Bowel Diseases. *Gastroenterology* **134**, 577-594 (2008).

96. Wehkamp, J. *et al.* Reduced Paneth cell alpha-defensins in ileal Crohn's disease. *Proc. Natl. Acad. Sci. U.S.A* **102**, 18129-18134 (2005).

97. Fellermann, K. *et al.* A chromosome 8 gene-cluster polymorphism with low human beta-defensin 2 gene copy number predisposes to Crohn disease of the colon. *Am. J. Hum. Genet* **79**, 439-448 (2006).

98. Kobayashi, K. S. *et al.* Nod2-dependent regulation of innate and adaptive immunity in the intestinal tract. *Science* **307**, 731-734 (2005).

99. Packey, C. D. & Sartor, R. B. Commensal Bacteria, Traditional and Opportunistic Pathogens, Dysbiosis and Bacterial Killing in Inflammatory Bowel Diseases. *Curr Opin Infect Dis* **22**, 292-301 (2009).

100. Wirtz, S., Neufert, C., Weigmann, B. & Neurath, M. F. Chemically induced mouse models of intestinal inflammation. *Nat Protoc* **2**, 541-546 (2007).

101. Okayasu, I. *et al.* A novel method in the induction of reliable experimental acute and chronic ulcerative colitis in mice. *Gastroenterology* **98**, 694-702 (1990).

102. Dieleman, L. A. *et al.* Dextran sulfate sodium-induced colitis occurs in severe combined immunodeficient mice. *Gastroenterology* **107**, 1643-1652 (1994).

103. Fujioka, Y., Noda, N. N., Nakatogawa, H., Ohsumi, Y. & Inagaki, F. Dimeric Coiled-coil Structure of Saccharomyces cerevisiae Atg16 and Its Functional Significance in Autophagy. *Journal of Biological Chemistry* **285**, 1508 -1515 (2010).

104. Laemmli, U. K. Cleavage of structural proteins during the assembly of the head of bacteriophage T4. *Nature* **227**, 680-685 (1970).

105. Siegmund, B., Lehr, H. A., Fantuzzi, G. & Dinarello, C. A. IL-1 beta -converting enzyme (caspase-1) in intestinal inflammation. *Proc. Natl. Acad. Sci. U.S.A* **98**, 13249-13254 (2001).

106. Siegmund, B. *et al.* Adenosine kinase inhibitor GP515 improves experimental colitis in mice. *J. Pharmacol. Exp. Ther* **296**, 99-105 (2001).

107. Atreya, R. *et al.* Blockade of interleukin 6 trans signaling suppresses T-cell resistance against apoptosis in chronic intestinal inflammation: evidence in crohn disease and experimental colitis in vivo. *Nat. Med* **6**, 583-588 (2000).

108. Reinecke, K. *et al.* Angiotensin II accelerates functional recovery in the rat sciatic nerve in vivo: role of the AT2 receptor and the transcription factor NF-κB. *The FASEB Journal* (2003).doi:10.1096/fj.02-1193fje

109. Schmidt, H. *et al.* Enrichment and analysis of secretory lysosomes from lymphocyte populations. *BMC Immunol* **10**, 41 (2009).

110. Hampe, J. *et al.* A genome-wide association scan of nonsynonymous SNPs identifies a susceptibility variant for Crohn disease in ATG16L1. *Nat Genet* **2**, 207-211 (2006).

111. Wirtz, S., Neufert, C., Weigmann, B. & Neurath, M. F. Chemically induced mouse models of intestinal inflammation. *Nat Protoc* **2**, 541-546 (2007).

112. Okayasu, I. *et al.* A novel method in the induction of reliable experimental acute and chronic ulcerative colitis in mice. *Gastroenterology* **98**, 694-702 (1990).

113. Yoshikawa, H., Takada, K. & Muranishi, S. Molecular weight dependence of permselectivity to rat small intestinal blood-lymph barrier for exogenous macromolecules absorbed from lumen. *J. Pharmacobio-dyn* **7**, 1-6 (1984).

114. Zhao, F. *et al.* Disruption of Paneth and goblet cell homeostasis and increased endoplasmic reticulum stress in Agr2−/− mice. *Dev Biol* **338**, 270-279 (2010).

115. Kabeya, Y. *et al.* LC3, a mammalian homologue of yeast Apg8p, is localized in autophagosome membranes after processing. *EMBO J* **19**, 5720-5728 (2000).

116. Kuma, A., Matsui, M. & Mizushima, N. LC3, an autophagosome marker, can be incorporated into protein aggregates independent of autophagy: caution in the interpretation of LC3 localization. *Autophagy* **3**, 323-328 (2007).

117. Takeuchi, H. *et al.* Synergistic Augmentation of Rapamycin-Induced Autophagy in Malignant Glioma Cells by Phosphatidylinositol 3-Kinase/Protein Kinase B Inhibitors. *Cancer Research* **65**, 3336 -3346 (2005).

118. Papadopoulos, T. & Pfeifer, U. Regression of rat liver autophagic vacuoles by locally applied cycloheximide. *Lab. Invest* **54**, 100-107 (1986).

119. Crider, B. P., Xie, X. S. & Stone, D. K. Bafilomycin inhibits proton flow through the H+ channel of vacuolar proton pumps. *J. Biol. Chem* **269**, 17379-17381 (1994).

120. Porter, E. M., Bevins, C. L., Ghosh, D. & Ganz, T. The multifaceted Paneth cell. *Cell. Mol. Life Sci* **59**, 156-170 (2002).

121. Stappenbeck, T. S. Paneth cell development, differentiation, and function: new molecular cues. *Gastroenterology* **137**, 30-33 (2009).

122. Territo, M. C., Ganz, T., Selsted, M. E. & Lehrer, R. Monocyte-chemotactic activity of defensins from human neutrophils. *J. Clin. Invest* **84**, 2017-2020 (1989).

123. Hoover, D. M. *et al.* The structure of human macrophage inflammatory protein-3alpha /CCL20. Linking antimicrobial and CC chemokine receptor-6-binding activities with human beta-defensins. *J. Biol. Chem* **277**, 37647-37654 (2002).

124. Ouellette, A. J. Paneth cells and innate mucosal immunity. *Curr. Opin. Gastroenterol* **26**, 547-553 (2010).

125. Kaser, A., Martínez-Naves, E. & Blumberg, R. S. Endoplasmic reticulum stress: implications for inflammatory bowel disease pathogenesis. *Current Opinion in Gastroenterology* **26**, 318-326 (2010).

126. Elbein, A. D. Inhibitors of the Biosynthesis and Processing of N-Linked Oligosaccharide Chains. *Annu. Rev. Biochem.* **56**, 497-534 (1987).

127. Ajit Varki, R. C. Natural and Synthetic Inhibitors of Glycosylation. (1999).at <http://www.ncbi.nlm.nih.gov/books/NBK20704/>

128. Bilsborough, J. & Viney, J. L. Gastrointestinal dendritic cells play a role in immunity, tolerance, and disease. *Gastroenterology* **127**, 300-309 (2004).

129. Izcue, A., Coombes, J. L. & Powrie, F. Regulatory T cells suppress systemic and mucosal immune activation to control intestinal inflammation. *Immunol. Rev* **212**, 256-271 (2006).

130. Dieleman, L. A. *et al.* Dextran sulfate sodium-induced colitis occurs in severe combined immunodeficient mice. *Gastroenterology* **107**, 1643-1652 (1994).

131. Tlaskalová-Hogenová, H. *et al.* Involvement of innate immunity in the development of inflammatory and autoimmune diseases. *Ann. N. Y. Acad. Sci* **1051**, 787-798 (2005).

132. Cario, E. Heads up! How the intestinal epithelium safeguards mucosal barrier immunity through the inflammasome and beyond. *Curr Opin Gastroenterol* (2010).doi:10.1097/MOG.0b013e32833d4b88

133. Mizushima, N., Yamamoto, A., Matsui, M., Yoshimori, T. & Ohsumi, Y. In vivo analysis of autophagy in response to nutrient starvation using transgenic mice expressing a fluorescent autophagosome marker. *Mol. Biol. Cell* **15**, 1101-1111 (2004).

134. Kimura, S., Noda, T. & Yoshimori, T. Dissection of the autophagosome maturation process by a novel reporter protein, tandem fluorescent-tagged LC3. *Autophagy* **3**, 452-460 (2007).

135. Tanida, I., Ueno, T. & Kominami, E. LC3 and Autophagy. *Methods Mol. Biol* **445**, 77-88 (2008).

136. Bowman, B. J. & Bowman, E. J. Mutations in subunit C of the vacuolar ATPase confer resistance to bafilomycin and identify a conserved antibiotic binding site. *J. Biol. Chem* **277**, 3965-3972 (2002).

137. Forgac, M. Vacuolar ATPases: rotary proton pumps in physiology and pathophysiology. *Nat. Rev. Mol. Cell Biol* **8**, 917-929 (2007).

138. Wang, Y., Inoue, T. & Forgac, M. Subunit a of the yeast V-ATPase participates in binding of bafilomycin. *J. Biol. Chem* **280**, 40481-40488 (2005).

139. Bowman, E. J., Siebers, A. & Altendorf, K. Bafilomycins: a class of inhibitors of membrane ATPases from microorganisms, animal cells, and plant cells. *Proc. Natl. Acad. Sci. U.S.A* **85**, 7972-7976 (1988).

140. Dröse, S. *et al.* Inhibitory effect of modified bafilomycins and concanamycins on P- and V-type adenosinetriphosphatases. *Biochemistry* **32**, 3902-3906 (1993).

141. Schoonderwoert, V. T., Holthuis, J. C., Tanaka, S., Tooze, S. A. & Martens, G. J. Inhibition of the vacuolar H+-ATPase perturbs the transport, sorting, processing and release of regulated secretory proteins. *Eur. J. Biochem* **267**, 5646-5654 (2000).

142. Taupenot, L., Harper, K. L. & O'Connor, D. T. Role of H+-ATPase-mediated acidification in sorting and release of the regulated secretory protein chromogranin A: evidence for a vesiculogenic function. *J. Biol. Chem* **280**, 3885-3897 (2005).

143. Klionsky, D. J., Elazar, Z., Seglen, P. O. & Rubinsztein, D. C. Does bafilomycin A1 block the fusion of autophagosomes with lysosomes? *Autophagy* **4**, 849-950 (2008).

144. Sobota, J. A., Bäck, N., Eipper, B. A. & Mains, R. E. Inhibitors of the V0 subunit of the vacuolar H+-ATPase prevent segregation of lysosomal- and secretory-pathway proteins. *J. Cell. Sci* **122**, 3542-3553 (2009).

145. Bloushtain-Qimron, N., Yao, J., Shipitsin, M., Maruyama, R. & Polyak, K. Epigenetic patterns of embryonic and adult stem cells. *Cell Cycle* **8**, 809-817 (2009).

146. Bruce Alberts, A. J. Molecular Biology of the Cell. (2002).at <http://www.ncbi.nlm.nih.gov/books/NBK21054/>

147. Podolsky, D. K., Gerken, G., Eyking, A. & Cario, E. Colitis-associated variant of TLR2 causes impaired mucosal repair because of TFF3 deficiency. *Gastroenterology* **137**, 209-220 (2009).

148. Perreault, N. & Jean-François, B. Use of the dissociating enzyme thermolysin to generate viable human normal intestinal epithelial cell cultures. *Exp. Cell Res* **224**, 354-364 (1996).

149. Podolsky, D. K. Regulation of intestinal epithelial proliferation: a few answers, many questions. *Am. J. Physiol* **264**, G179-186 (1993).

150. Evans, G. S., Flint, N. & Potten, C. S. Primary cultures for studies of cell regulation and physiology in intestinal epithelium. *Annu. Rev. Physiol* **56**, 399-417 (1994).

151. Rousset, M. The human colon carcinoma cell lines HT-29 and Caco-2: two in vitro models for the study of intestinal differentiation. *Biochimie* **68**, 1035-1040 (1986).

152. Kaeffer, B. Mammalian intestinal epithelial cells in primary culture: a mini-review. *In Vitro Cell. Dev. Biol. Anim* **38**, 123-134 (2002).

153. Evans, G. S., Flint, N., Somers, A. S., Eyden, B. & Potten, C. S. The development of a method for the preparation of rat intestinal epithelial cell primary cultures. *J. Cell. Sci* **101 (Pt 1)**, 219-231 (1992).

154. Sato, T. *et al.* Paneth cells constitute the niche for Lgr5 stem cells in intestinal crypts. *Nature* **469**, 415-418 (2011).

155. Beaulieu, J. F. & Vachon, P. H. Reciprocal expression of laminin A-chain isoforms along the crypt-villus axis in the human small intestine. *Gastroenterology* **106**, 829-839 (1994).

156. Potten, C. S. & Loeffler, M. Stem cells: attributes, cycles, spirals, pitfalls and uncertainties. Lessons for and from the crypt. *Development* **110**, 1001-1020 (1990).

157. Li, Y. Q., Roberts, S. A., Paulus, U., Loeffler, M. & Potten, C. S. The crypt cycle in mouse small intestinal epithelium. *J. Cell. Sci* **107 (Pt 12)**, 3271-3279 (1994).

158. Davies, J. Q. & Gordon, S. Isolation and Culture of Murine Macrophages. *Basic Cell Culture Protocols* **290**, 091-104 (2004).

159. Gordon, S. Alternative activation of macrophages. *Nat. Rev. Immunol* **3**, 23-35 (2003).

160. Tomida, M., Yamamoto-Yamaguchi, Y. & Hozumi, M. Purification of a factor inducing differentiation of mouse myeloid leukemic M1 cells from conditioned medium of mouse fibroblast L929 cells. *J. Biol. Chem* **259**, 10978-10982 (1984).

161. Cadwell, K., Patel, K. K., Komatsu, M., Virgin, H. W. & Stappenbeck, T. S. A common role for Atg16L1, Atg5, and Atg7 in small intestinal Paneth cells and Crohn's disease. *Autophagy* **5**, 250-252 (2009).

162. Elsbach, P. & Weiss, J. Oxygen-dependent and oxygen-independent mechanisms of microbicidal activity of neutrophils. *Immunol. Lett* **11**, 159-163 (1985).

163. Zhao, Z. *et al.* Autophagosome-independent essential function for the autophagy protein Atg5 in cellular immunity to intracellular pathogens. *Cell Host Microbe* **4**, 458-469 (2008).

164. Fahlgren, A., Hammarström, S., Danielsson, A. & Hammarström, M.-L. Increased expression of antimicrobial peptides and lysozyme in colonic epithelial cells of patients with ulcerative colitis. *Clin. Exp. Immunol* **131**, 90-101 (2003).

165. Porter, E. M., Liu, L., Oren, A., Anton, P. A. & Ganz, T. Localization of human intestinal defensin 5 in Paneth cell granules. *Infect. Immun* **65**, 2389-2395 (1997).

166. Wehkamp, J. *et al.* Reduced Paneth cell alpha-defensins in ileal Crohn's disease. *Proc. Natl. Acad. Sci. U.S.A* **102**, 18129-18134 (2005).

167. Wilson, C. L. *et al.* Regulation of intestinal alpha-defensin activation by the metalloproteinase matrilysin in innate host defense. *Science* **286**, 113-117 (1999).

168. Ramasundara, M., Leach, S. T., Lemberg, D. A. & Day, A. S. Defensins and inflammation: the role of defensins in inflammatory bowel disease. *J. Gastroenterol. Hepatol* **24**, 202-208 (2009).

169. Shi, J. *et al.* A novel role for defensins in intestinal homeostasis: regulation of IL-1beta secretion. *J. Immunol* **179**, 1245-1253 (2007).

170. Wehkamp, J. *et al.* NOD2 (CARD15) mutations in Crohn's disease are associated with diminished mucosal alpha-defensin expression. *Gut* **53**, 1658-1664 (2004).

171. Ogura, Y. *et al.* Expression of NOD2 in Paneth cells: a possible link to Crohn's ileitis. *Gut* **52**, 1591-1597 (2003).

172. Abraham, C. & Cho, J. H. Functional consequences of NOD2 (CARD15) mutations. *Inflamm. Bowel Dis* **12**, 641-650 (2006).

173. Lala, S. *et al.* Crohn's disease and the NOD2 gene: a role for paneth cells. *Gastroenterology* **125**, 47-57 (2003).

174. Gutierrez, M. G. *et al.* Autophagy is a defense mechanism inhibiting BCG and Mycobacterium tuberculosis survival in infected macrophages. *Cell* **119**, 753-766 (2004).

175. Paludan, C. *et al.* Endogenous MHC class II processing of a viral nuclear antigen after autophagy. *Science* **307**, 593-596 (2005).

176. Dengjel, J. *et al.* Autophagy promotes MHC class II presentation of peptides from intracellular source proteins. *Proc. Natl. Acad. Sci. U.S.A* **102**, 7922-7927 (2005).

177. Huang, J. *et al.* Antibacterial autophagy occurs at PtdIns(3)P-enriched domains of the endoplasmic reticulum and requires Rab1 GTPase. *Autophagy* **7**, 17-26 (2011).

178. Amodio, G. *et al.* Endoplasmic reticulum stress reduces the export from the ER and alters the architecture of post-ER compartments. *The International Journal of Biochemistry & Cell Biology* **41**, 2511-2521 (2009).

179. Axe, E. L. *et al.* Autophagosome formation from membrane compartments enriched in phosphatidylinositol 3-phosphate and dynamically connected to the endoplasmic reticulum. *J. Cell Biol* **182**, 685-701 (2008).

180. Matsunaga, K. *et al.* Autophagy requires endoplasmic reticulum targeting of the PI3-kinase complex via Atg14L. *J. Cell Biol* **190**, 511-521 (2010).

10 APPENDIX

10.1 Abbreviations

Table 7: Abbreviations

µg	Microgram
µl	Microliter
A	Adenine
Aa	Amino Acid
Ab	Antibody
APS	Ammonium Persulfate
ATF	Activating Transcription Factor
ATG	AuTophaGy related
ATP	Adenosine 5'-Triphosphate
Baf	Bafilomycin
BMDM	Bone Marrow Derived Macrophage
Bp	Base Pairs
BrdU	5-Bromo-2-Deoxyuridine
BSA	Bovine Serum Albumin
C	Carboxy
CC	Coiled Coil
CD	Crohn Disease
cDNA	Complementary DNA
Cvt vesicle	Cytoplasm-To-Vacuole Transport Vesicle
d	Day
DAI	Disease Activity Index
DAPI	4,6-Diamino-2-Phenylindole Dihydrochloride
DEPC	Diethylpyrocarbonate
DMEM	Dulbecco's Minimal Essential Medium
DMSO	Dimethyl sulfoxide
DNA	Deoxyribonucleic Acid
dNTP	2`-Desoxyribonucleotide-5´-Triphosphate
DSS	Dextran Sodium Sulfate
DTT	Dithithreitol
E	Enzyme
ECL	Electrochemiluminescence
EDTA	Ethylenediaminetetraacetic Acid
eIF2α	Eukaryotic Initiation Factor 2α
ER	Endoplasmic Reticulum
FCS	Fetal Calf Serum
FITC	Fluorescein isothiocyanate
g	gram
G3PDH	Glyceraldehyde-3-Phosphate Dehydrogenase
GTP	Guanosine Triphosphate
GWAS	Genome Wide Association Studies

h	Hour
HBSS	Hank's Balanced Salts
HE	Hematoxylin-Eosin
Hepes	(4-(2-Hydroxyethyl)-1-Piperazineethanesulfonic Acid
HRP	Horseradish Peroxidase
IBD	Inflammatory Bowel Disease
IEC	Intestinal Epithelial Cell
IgG	Immunoglobulin G
IL	Interleukin
IRE1	Inositol Requiring Enzyme
kg	Kilogram
L	Liter
LB	Lysogeny Broth
LC3	Microtubule-Associated Protein 1 Light Chain 3
LIR	LC3-Interacting Region
LPS	Lipopolysaccharide
Lyz	Lysozyme
MDP	Muramyldipeptide
MEF	Mouse Embryonic Fibroblast
MEM	Minimal Essential Medium
mg	Milligram
MHC II	Major Histocompatibility Complex (Class II)
min	Minute
ml	Milliliter
mM	Millimolar
MMM	Mouse Macrophage Medium
MOI	Multiplicity Of Infection
mRNA	Messenger RNA
mTOR	Mammalian Target Of Rapamycin
N	Amino/NH_2
NLR	NOD-Like Receptor
nm	Nanometer
NOD	Nucleotide-Binding Oligomerization Domain
PAS	Periodic Acid-Schiff
PBS	Phosphate Buffered Saline
PCR	Polymerase Chain Reaction
PDI	Protein Disulphide Isomerase
PE	Phosphatidyl ethanolamine
PERK	Protein Kinase RNA-Like Endoplasmic Reticulum Kinase
PI3K	Phosphatodylinositol-3-Kinase 1
PVDF	Polyvinylidene Fluoride
Rm M-CSF	Recombinant Mouse Macrophage Colony-Stimulating Factor
RNA	Ribonucleic Acid

SD	Standard Deviation
SDS	Sodium Dodecyl Sulfate
T	Threonine
TEMED	N,N,N',N'-Tetramethylethylenediamine
TLR	Toll Like Receptor
TNBS	Trinitro Benzene Sulfonic Acid
TNF	Tumor Necrosis Factor
TNG	Trans-Golgi Network
Tun	Tunicamycin
UC	Ulcerative Colitis
UPR	Unfolded Protein Response
UV	Ultra Violet
V	Volt
WT	Wildtype

10.2 Publications

NOD2-C2 - a novel NOD2 isoform activating NF-kappaB in a muramyl dipeptide-independent manner.

Kramer M, **Boeck J**, Reichenbach D, Kaether C, Schreiber S, Platzer M, Rosenstiel P, Huse K.

BMC Res Notes. August 2010; 3: 224.

Molecular signatures of a disturbed nasal barrier function in the primary tissue of Wegener's granulomatosis.

Laudien M, Häsler R, Wohlers J, **Böck J**, Lipinski S, Bremer L, Podschun R, Ambrosch P, Lamprecht P, Rosenstiel P, Till A.

Mucosal Immunol. 2011 Mar 16

The complex interplay of NOD-like receptors and the autophagy machinery in the pathophysiology of Crohn disease.

Billmann-Born S, Lipinski S, **Böck J**, Till A, Rosenstiel P, Schreiber S.

European Journal of Cell Biology, Volume 90, Issues 6-7, June-July 2011, Pages 593-602, SFB 415: Specificity and Pathophysiology of Signal Transduction Pathways

10.3 Curriculum vitae

Lebenslauf

Persönliche Daten

Name:	Dipl. Biol. Janne Böck (geb. Wessel)
Anschrift:	Hansastraße 72, 24118 Kiel,
	Tel. privat: 0431-3868822
	e-Mail: j-boeck@web.de
Geburtstag:	26.02.1981 in Kiel
Familienstand:	verheiratet, 1Kind (geb. am 22.09.2011)

Schulbildung

1987 – 1991	Claus-Rixen-Grundschule in Altenholz
1991 – 2000	Gymnasium Altenholz, Abitur 2000
	(Leistungskurse Deutsch und Biologie)

Wissenschaftlicher Werdegang

09/2011 – 09/2012	Elternzeit
04/2008 – 08/2011	Promotion (rer. nat) am Institut für klinische Molekularbiologie Kiel (Direktor: Prof. Dr. Stefan Schreiber) Arbeitsthema: The role of ATG16L1 in chronic inflammatory bowel disease
09/2007 – 03/2008	Diplomarbeit im Fach Zellbiologie am Forschungszentrum Borstel (Abteilung Biochemische Immunologie), „Aktivierung humaner Leukozyten durch Varianten des CXC-Chemokins Plättchenfaktor 4“, Betreuer: PD Dr. Frank

	Petersen, Prof. Dr. Sylvia Bulfone Paus (Note: sehr gut)
07/2007 – 08/2007	Praktikum im Forschungszentrum Borstel (Abteilung Biochemische Immunologie, PD Dr. Frank Petersen)
10/2002 – 03/2008	Studium der Biologie an der Christian-Albrechts-Universität zu Kiel mit dem Hauptfach Zellbiologie (Note 1,0), dem biol. Nebenfach Mikrobiologie (Note 1,3) und dem nicht-biol. Nebenfach Rechtsmedizin (Note 1,7), Abschluss: Diplom

10.4 Acknowledgement

Danksagung

Sehr herzlich bedanken möchte ich mich bei Herrn Prof. Dr. med. Stefan Schreiber für die Möglichkeit, meine Doktorarbeit im Institut für Klinische Molekularbiologie in Kiel anfertigen zu können.

Mein besonderer Dank gilt Herrn Prof. Dr. Philip Rosenstiel, der mich fachlich und auch persönlich sehr unterstützt und gefördert hat. Durch das spannende Thema und die interessanten und hilfreichen Diskussionen, hat er mich stets motiviert und mein effektives, wissenschaftliches Arbeiten gefördert.

Bei Frau Dr. Susanne Billmann-Born möchte ich mich ganz herzlich für die gute fachliche Betreuung bedanken. Ihre wertvollen Ideen und die Anregung zum eigenständigen Arbeiten haben wesentlich zum Erfolg dieser Arbeit beigetragen. Auch ihr offenes Ohr für alle Lebenslagen war mir eine große Hilfe.

Frau Dr. Olga Gavrilova danke ich für die Unterstützung bei der Durchführung der Maus-Experimente.

Ein großes Dankeschön geht an alle Mitarbeiter des Instituts für Klinische Molekularbiologie, insbesondere an meine Kollegen in der Zellbiologie. Die angenehme und freundschaftliche Atmosphäre hat mich bei experimentellen Rückschlägen stets aufgemuntert. Bei dieser Gelegenheit möchte ich besonders Alina Gräff und Maren Reffelmann wegen ihrer experimentellen Unterstützung danken.

Ganz besonders danke ich meiner Familie, die immer hinter mir steht und mich in allen Lebenslagen unterstützt. Ohne Euch wäre ich nicht da, wo ich jetzt bin.

Vor allem aber möchte ich mich bei Steffen Böck bedanken. Danke Steffen, für deinen Glauben an mich.

10.5 Eidesstattliche Erklärung

Hiermit versichere ich, Janne Böck, an Eides statt, dass ich die vorliegende Arbeit selbstständig und nur mit Hilfe der angegebenen Hilfsmittel und Quellen unter Anleitung meiner akademischen Lehrer angefertigt habe.

Diese Dissertation wurde bisher an keiner anderen Fakultät vorgelegt. Ich erkläre, kein anderes Promotionsverfahren ohne Erfolg beendet zu haben, und dass keine Aberkennung eines bereits erworbenen Doktorgrades vorliegt.

Ich erkläre, dass die Arbeit unter Einhaltung der Regeln guter wissenschaftlicher Praxis der Deutschen Forschungsgemeindschaft entstanden ist.

Kiel, den 10.02.2012
Janne Böck